Turun yliopisto
University of Turku

MONOOXYGENASE DIVERSITY AND OXYGEN ACTIVATION WITHIN POLYKETIDE ANTIBIOTIC BIOSYNTHESIS

Thadée Remy Pierre Grocholski

TURUN YLIOPISTON JULKAISUJA – ANNALES UNIVERSITATIS TURKUENSIS
Sarja - ser. AI osa - tom. 535 | Astronomica - Chemica - Physica - Mathematica | Turku 2016

University of Turku

Faculty of Mathematics and Natural Sciences
Department of Biochemistry
Biochemistry
Doctoral Programme in Molecular Life Sciences

Supervised by

Docent Mikko Metsä-Ketelä, Ph.D.
Department of Biochemistry
University of Turku

Docent Jarmo Niemi, Ph.D.
Department of Biochemistry
University of Turku

Reviewed by

Nina Hakulinen, Ph.D. (Academy Research Fellow)
Department of Chemistry
University of Eastern Finland
Joensuu, Finland

Robert Schnell, Ph.D. (senior researcher)
Department of Medical Biochemistry
and Biophysics
Karolinska Institutet, MBB,
Stockholm, Sweden

Opponent

Professor Timothy Bugg, Ph.D.
Department of Chemistry
University of Warwick
Coventry, UK

ISBN 978-951-29-6421-5 (PRINT)
ISBN 978-951-29-6422-2 (PDF)
ISSN 0082-7002 (Print)
ISSN 2343-3175 (Online)
Painosalama Oy - Turku, Finland 2016

CONTENTS

LIST OF ORIGINAL PUBLICATIONS

This thesis is based on the following original publications, referred to as roman numerals I-IV in the text.

I Koskiniemi, H. *, Grocholski, T. *, Schneider, G. & Niemi, J. (2009) Expression, purification and crystallization of the cofactor-independent monooxygenase SnoaB from the nogalamycin biosynthetic pathway. *Acta Crystallogr. Sect. F Struct. Biol. Cryst. Commun., 65*(Pt 3), 256-9. *Equal contribution.

II Grocholski, T.*, Koskiniemi, H. *, Lindqvist, Y., Mäntsälä, P., Niemi, J. & Schneider, G. (2010) Crystal structure of the cofactor-independent monooxygenase SnoaB from Streptomyces nogalater: implications for the reaction mechanism. *Biochemistry., 49*(5), 934-44. *Equal contribution.

III Grocholski, T.*, Oja, T.*, Humphrey, L., Mäntsälä, P., Niemi, J. & Metsä-Ketelä, M. (2012) Characterization of the two-component monooxygenase system AlnT/AlnH reveals early timing of quinone formation in alnumycin biosynthesis. *J Bacteriol., 194*(11), 2829-36.*Equal contribution.

IV Grocholski, T., Dinis, P., Niiranen, L., Niemi, J. & Metsä-Ketelä M (2015) Divergent evolution of an atypical S-adenosyl-l-methionine-dependent monooxygenase involved in anthracycline biosynthesis. *Proc. Natl. Acad. Sci. USA*., *112*(32), 9866-71.

ABSTRACT

Molecular oxygen (O_2) is a key component in cellular respiration and aerobic life. Through the redox potential of O_2, the amount of free energy available to organisms that utilize it is greatly increased. Yet, due to the nature of the O_2 electron configuration, it is non-reactive to most organic molecules in the ground state. For O_2 to react with most organic compounds it must be activated. By activating O_2, oxygenases can catalyze reactions involving oxygen incorporation into organic compounds. The oxygen activation mechanisms employed by many oxygenases to have been studied, and they often include transition metals and selected organic compounds.

Despite the diversity of mechanisms for O_2 activation explored in this thesis, all of the monooxygenases studied in the experimental part activate O_2 through a transient carbanion intermediate.

One of these enzymes is the small cofactorless monooxygenase SnoaB. Cofactorless monooxygenases are unusual oxygenases that require neither transition metals nor cofactors to activate oxygen. Based on our biochemical characterization and the crystal structure of this enzyme, the mechanism most likely employed by SnoaB relies on a carbanion intermediate to activate oxygen, which is consistent with the proposed substrate-assisted mechanism for this family of enzymes.

From the studies conducted on the two-component system AlnT and AlnH, both the functions of the NADH-dependent flavin reductase, AlnH, and the reduced flavin dependent monooxygenase, AlnT, were confirmed. The unusual regiochemistry proposed for AlnT was also confirmed on the basis of the structure of a reaction product. The mechanism of AlnT, as with other flavin-dependent monooxygenases, is likely to involve a caged radical pair consisting of a superoxide anion and a neutral flavin radical formed from an initial carbanion intermediate.

In the studies concerning the engineering of the S-adenosyl-L-methionine (SAM) dependent 4-O-methylase DnrK and the homologous atypical 10-hydroxylase RdmB, our data suggest that an initial decarboxylation of the substrate is catalyzed by both of these enzymes, which results in the generation of a carbanion intermediate. This intermediate is not essential for the 4-O-methylation reaction, but it is important for the 10-hydroxylation reaction, since it enables substrate-assisted activation of molecular oxygen involving a single electron transfer to O_2 from a carbanion intermediate. The only role for SAM in the hydroxylation reaction is likely to be stabilization of the carbanion through the positive charge of the cofactor. Based on the DnrK variant crystal structure and the characterizations of several DnrK variants, the insertion of a single amino acid in DnrK (S297) is sufficient for gaining a hydroxylation function, which is likely caused by carbanion stabilization through active site solvent restriction.

Despite large differences in the three-dimensional structures of the oxygenases and the potential for multiple oxygen activation mechanisms, all the enzymes in my studies rely on carbanion intermediates to activate oxygen from either flavins or their substrates. This thesis provides interesting examples of divergent evolution and the prevalence of carbanion intermediates within polyketide biosynthesis. This mechanism appears to be recurrent in aromatic polyketide biosynthesis and may reflect the acidic nature of these compounds, propensity towards hydrogen bonding and their ability to delocalize π-electrons.

TIIVISTELMÄ

Molekulaarinen happi on soluhengityksen ja aerobisen elämän avaintekijä. Sen korkeasta hapetus-pelkistyspotentiaalista johtuen sitä hapettimena käyttävillä organismeilla on erityisen paljon vapaata energiaa käytettävissään. Tästä huolimatta happimolekyylin elektronirakenne aiheuttaa sen, että se ei reagoi useimpien orgaanisten molekyylien kanssa perustilassa. Jotta O_2 reagoisi orgaanisten molekyylien kanssa, se täytyy aktivoida. Oksigenaasientsyymit pystyvät aktivoimaan O_2:n niin että se pystyy reagoimaan. Useiden oksigenaasien aktivointimekanismeja on tutkittu, ja ne perustuvat usein siirtymämetallien tai tiettyjen orgaanisten molekyylien käyttöön.

Tässä väitöskirjassa käsitellään lukuisia hapen aktivointimekanismeja, mutta kaikki kokeellisessa osassa käsitellyt mono-oksigenaasit käyttävät karbanionimekanismia.

Yksi näistä entsyymeistä on pieni kofaktoriton mono-oksigenaasi SnoaB. Kofaktorittomat mono-oksigenaasit ovat epätavallisia oksigenaaseja, jotka eivät tarvitse siirtymämetalleja tai orgaanisia kofaktoreita hapen aktivoimiseen. Biokemialliset kokeet ja entsyymin rakenne osoittavat todennäköisimmäksi reaktiomekanismiksi karbanionivälituotteen, kuten muillakin substraattiavusteisilla, kofaktorittomilla mono-oksigenaaseilla.

Kaksikomponenttinen mono-oksigenaasi AlnT-AlnH koostuu NADH-riippuvaisesta flaviini-reduktaasista AlnH ja pelkistyneestä flaviinista riippuvaisesta mono-oksigenaasista AlnT; molempien funktiot osoitettiin kokeellisesti. AlnT:n epätavallinen reagointikohta varmistettiin analysoimalla reaktiotuotteen rakenne. AlnT:n reaktiomekanismi perustuu kaikkien flaviini-mono-oksigenaasien tavoin siihen, että karbanionivälituotteesta syntyy superoksidianionista ja neutraalista flaviiniradikaalista koostuva sidottu radikaalipari.

Vertailtaessa S-adenosyylimetioniini(SAM)-riippuvaista 4-O-metylaasia DnrK ja sen kanssa homologista epätyypillistä 10-hydroksylaasia RdmB totesimme molempien entsyymien katalysoivan substraatin dekarboksylaatiota, jolloin syntyy karbanionivälituote. Tämä välituote ei ole tarpeellinen 4-O-metylaatioreaktion kannalta, mutta on välttämätön 10-hydroksylaatiolle, koska se mahdollistaa substraattiavusteisen hapen aktivoinnin yhden elektronin siirrolla. SAM:in funktiona hydroksylaatiossa on ilmeisesti karbanionin stabilointi kofaktorin positiivisen varauksen avulla. Yhden DnrK-variantin rakenne ja useiden DnrK-varianttien biokemialliset ominaisuudet osoittavat, että yhden aminohapon (seriini 297) lisääminen molekyyliin mahdollistaa hydroksylaatioreaktion estämällä karbanionin neutralisoitumista.

Huolimatta tutkittujen oksigenaasien rakenteiden erilaisuudesta, ja lukuisista periaatteellisesti mahdollisista hapen aktivointimekanismeista, kaikki tutkimani entsyymit käyttävät karbanioni-välituotetta, joka muodostuu joko substraatista tai flaviinista, hapen aktivointiin. Tässä väitöskirjassa esitetään mielenkiintoisia esimerkkejä divergentistä evoluutiosta, ja karbanioni-mekanismin yleisyydestä polyketidien biosynteesissä. Tämä mekanismi näyttää toistuvan aromaattisten polyketidien biosynteesissä johtuen niiden happamista ominaisuuksista, kyvystä muodostaa vetysidoksia, ja π-elektronien delokalisaatiosta molekyylissä.

ABBREVIATIONS

αKG	α-Ketoglutarate
BLAST	Basic Local Alignment Search Tool
CYP	cytochrome P450
EPR	electroparamagnetic resonance
EDTA	ethylenediaminetetraacetic acid
FAD	flavin adenine dinucleotide
FMN	flavin mononucleotide
HOD	1 H-3-Hydroxy-4-oxoquinaldine 2,4-dioxygenase
HPLC	high pressure liquid chromatography
Hc	hemocyanin
IDO	intradiol dioxygenase
LC-MS	liquid chromatography–mass spectrometry
MMOH	methane monooxygenase hydroxylase
MMOR	methane monooxygenase NADH dependent reductase
MMOB	methane monooxygenase regulatory protein
NMR	nuclear magnetic resonance
PHM	peptidylglycine α-hydroxylating monooxygenase
PheH	phenylalanine hydroxylase
SAH	S-adenosyl-L-homocysteine
SAM	S-adenosyl-L-methionine
sMMO	soluble methane monooxygenase
ROS	reactive oxygen species
TcmF1	tetracenomycin F1 monooxygenase
TβM	tyramine β- monooxygenase
TrpH	tryptophan hydroxylase
Ty	tyrosinase
TyrH	tyrosine hydroxylase
BH4	tetrahydrobiopterin
Co	catechol oxidases
DβM	dopamine β- monooxygenase

1. INTRODUCTION

1.1. Dioxygen and Oxygen Activation

1.1.1. Origins of Dioxygen in the Atmosphere

Within our galaxy, oxygen is the third most abundant element by mass, after hydrogen and helium. On Earth, oxygen is the most abundant element, after iron, representing some 30 % of the Earth's mass and constituting almost 50 % of the Earth's crust (Morgan & Anders, 1980; Clennan & Pace, 2005). Despite representing a large percentage of the earth's mass, molecular oxygen or dioxygen (O_2) has only been present in significant concentrations since the Paleoproterozoic eon between 3.0 and 2.3 billion years ago (Crowe *et al.*, 2013; Hamdane *et al.,* 2008). Prior to this period, although O_2 producing photosynthesizing cyanobacteria existed (fossils have indicated that cyanobacteria were present as early as 3.5 billion years ago (Fenchel & Finlay, 2008)), atmospheric compositions of dioxygen were globally low for hundreds of millions of years (Johnston *et al.,* 2005; Holland, 2009; Crowe *et al.*, 2013). Prior to the Paleoproterozoic eon, iron and inorganic as well as organic matter, dissolved within the earth's oceans, chemically captured the release of any dioxygen. As these oxygen sinks became saturated, atmospheric oxygen levels multiplied (Holland, 2009). Even though this event occurred over several hundreds of millions of years, it marked one of the most significant periods of life on Earth. It resulted not only in the first mass extinction of global anaerobic lifeforms of the time but also led to the rise of novel geochemistry and geology (Sawyer, 1991; Holland, 2006; Holland, 2009; Crowe *et al.*, 2013; Canfield *et al.*, 2013). This event, referred to as the great oxygenation event, was the root of a new biodiversity and coincided with the development of multicellular organisms.

1.1.2. Photoprotective Role of Dioxygen to Surface-Dwelling Life

Currently, molecular oxygen in our atmosphere plays a key role in sustaining life. By absorbing ultraviolet (UV) radiation produced by the sun, molecular oxygen is split, resulting in two free oxygen atoms (O·). This highly reactive atomic oxygen reacts with molecular oxygen to form ozone (O_3). Ozone can subsequently be split when hit by UV radiation, which once again forms molecular oxygen and atomic oxygen. This continuing cycle (also known as the Chapman cycle) occurs mostly in the stratosphere (10 to 50 km above sea level), but also partly in the mesosphere (50 km to 85 km above sea level). Molecular oxygen and ozone contained within these layers absorb almost all UV-c radiation (100–280 nm) as well as most UV-b radiation (280–315 nm). Without the ozone layer absorbing this UV radiation, life on the surface would be impossible due to the generation of reactive oxygen by UV light or photo-induced reactions of complex organic molecules (see section 1.1.3.) (Pattison & Davies, 2006). Since the early 20th century, UV light has thus been used extensively in biology laboratories and medical facilities for sterilization and disinfection purposes.

1.1.3. Dioxygen within Biological Reactions

Levels of molecular oxygen in the atmosphere are currently maintained through the photosynthesis by cyanobacteria, algae and plants. By absorbing energy from light, a succession of proteins and small molecules can oxidize water to dioxygen. The simplified reaction is illustrated below:

$$6\ H_2O + 6\ CO_2 + \text{light} \rightarrow C_6H_{12}O_6 + 6\ O_2 \quad (1)$$

Cellular respiration is, essentially, the reverse reaction:

$$C_6H_{12}O_6 + 6\ O_2 \rightarrow 6\ H_2O + 6\ CO_2 \quad (2)$$

Molecular oxygen is reduced to water through a series of reactions. The energy from this reaction is used to synthesize ATP, which can be used by cells as an energy source (Sawyer, 1991). Despite the importance of molecular oxygen for cellular respiration and aerobic life, dioxygen is toxic to cells at high partial pressures. In addition, given enough time,

oxygen is able to oxidize most atoms. Yet, molecular oxygen is in itself relatively non-reactive. Only the reduction of dioxygen results in highly reactive oxygen species (ROS) such as hydrogen peroxide (H_2O_2) and superoxide (O_2^-). It is these highly reactive and dangerous by-products of oxygen in organisms that have been traditionally linked to cellular damage and cancer (Simic and Jovanovic, 1989). To avert cellular damage and ultimately cell death, cells have evolved a battery of compounds and enzymes to deal with these ROSs and exploit them within cellular functions (Panieri & Santoro, 2015). These include antioxidants such as glutathione, vitamin C, vitamin E and even uric acid (Simic & Jovanovic, 1989). Radical scavenging enzymes such as superoxide dismutase, peroxidases and catalases are also used by cells to deal with ROSs. Despite the dangers of ROSs for aerobic biological organisms, the amount of free energy available to organisms through the use of molecular oxygen is greatly increased compared to other possible oxidants. It is this double-edged sword that makes the study of oxygen in biological systems so appealing.

1.1.4. Spin Barrier

Most organic molecules generally contain electron pairs with molecular orbitals in directionally opposing spins (+½ and - ½). Counterbalanced spins are favored as they equate to lowered energy minima. In addition, a molecule with overall molecular orbital spins, or spin angular momentum, of 0 (S =+½ - ½= 0) has no magnetic properties. This electron state is referred to as a *singlet state.* Oxygen has two valencies, and thus one would expect dioxygen to have a spin angular moment of 0. However, dioxygen has paramagnetic properties, indicating that the two electrons in the outermost orbital have an overall spin angular momentum different from zero. In fact, the overall spin angular moment of dioxygen is S= +½+½ = 1: a *triplet state*. The triplet state or *ground state* ($^3O_2$) of dioxygen actually contains two unpaired electrons in two antibonding π* electron orbitals (Hamilton, 1990; Bugg, 2003), which is illustrated in Scheme 1 below. This electron orbital configuration is why the dioxygen molecule is referred to as “biradical” by nature, as it contains two unpaired electrons.

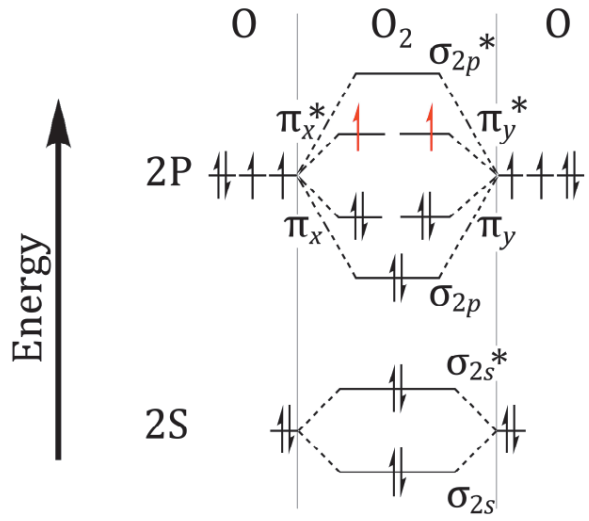

Scheme 1: The energy diagram of the molecular orbital diagram for O_2 with 12 valence electrons, following Hund's rule. The last two electrons (in red) occupy the 2P π* antibonding orbitals as singly unpaired electrons resembling molecule containing radicals.

According to Pauli's Exclusion Principle, it is impossible for two electrons to reside in the same molecular orbital if they do not have opposite spin states. Therefore, a direct reaction between most organic molecules found in singlet state and dioxygen, in triplet state, is impossible (Malmström, 1982; Sawyer, 1991). This property of dioxygen explains why it is non-reactive to most organic compounds despite these reactions being strongly thermodynamically favorable. A spin barrier, or activation barrier, exists between dioxygen (S = 1) and most organic molecules (S = 0); in order to react, oxygen must be "activated".

1.1.5. Oxygen Activation

As stated earlier, dioxygen in the ground state is relatively unreactive with most organic compounds. For $^3O_2$ to react with most organic compounds (in singlet state), it must be activated. Generally, activation can occur by two different mechanisms: absorption of energy or monovalent reduction.

Through absorption of energy, the spin state of one of the unpaired electrons in π* orbital can be reversed, resulting in singlet state dioxygen with two electrons in the π* orbital with opposite spins. This change in electron orbital has traditionally been studied in chemistry through the use of light (Kautsky & de Bruijn, 1931), although if high energy UV radiation is used, the triplet dioxygen bond can be cleaved (see section 1.1.2.).

In the singlet state, reactions with dioxygen and most organic compounds are very favorable and exothermic. Reactions with dioxygen in a singlet state can even involve a simultaneous reduction of both oxygen atoms. However, the transition from triplet to singlet dioxygen is endothermic and requires about 22.5 Kcal/mol (Clennan, 2005).

The second mechanism by which $^3O_2$ can be activated involves stepwise reduction of one of the two oxygen atoms; this is called a monovalent reduction. This reduction is also endothermic but requires significantly less energy (estimated to be between 3.7 to 7.5 kcal/mol). The monovalent reduction of oxygen results in the formation of superoxide (O_2^-), which is essentially a singlet state dioxygen with an

additional electron. Traditionally, three types of monovalent reductions of $^3O_2$ have been observed in biological systems. These include coupling with stabilized free radicals, electron transfers, or complexing with metal ions (Hamilton, 1990). Subsequent reactions with superoxide can involve either reductions, for example with metal ions, or oxidations, for example with organic compounds such as ascorbic acid (Nishikimi, 1975). These reactions are exothermic, resulting in compounds such as hydrogen peroxide, hydroxyl radicals, or water.

In Figure 1, the activation energy required for the transition from ground state dioxygen to singlet oxygen or superoxide is illustrated with subsequent exothermic reductions to hydrogen peroxide, hydroxyl radical, and water. With enzymes, monovalent reductions are more likely to occur than a transition from a triplet to singlet state dioxygen as they are thermodynamically more favorable. To overcome the spin barrier, transition metals and select organic compounds are extensively used in the monovalent reduction of triplet dioxygen. The types of mechanisms by which enzymes activate dioxygen will be examined further in the sections below.

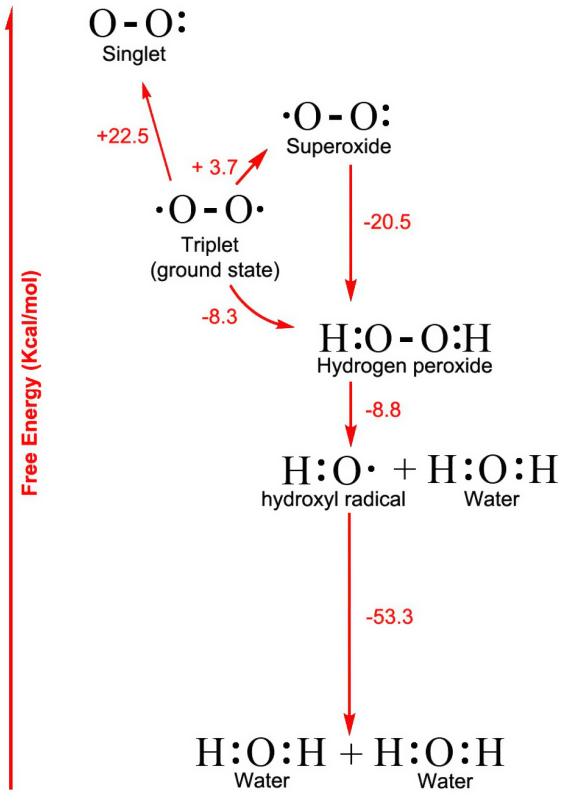

Figure 1: Simplified illustration of the various states of oxygen as Lewis structures with bond dissociation energies (in Kcal/mol). An energy barrier exists between the ground state of oxygen and the singlet state or superoxide state. As a singlet state O_2 or superoxide, O_2 is reactive to most organic compounds. Due to the large energy barrier, the monovalent reduction of triplet oxygen is more likely to occur in biological systems than a transition from triplet to singlet state dioxygen. In either case, a catalyst is required to make the transition away from a triplet state.

(Values calculated from Latimer diagram for O_2 from Sawyer, 1991)

1.2. Oxygenases

In 1955, two papers by Mason and Hayaishi altered our understanding of enzymatic reactions with molecular oxygen. Prior to this period, enzymatically catalyzed oxygen incorporation into substrates was deemed possible only if the oxygen atom came from water (Hayashi, 1974). However, both researchers proved, with $^{18}O_2$ oxygen isotopes, that direct incorporation of oxygen into organic compounds occurred. For Mason, this reaction was observed through the tyrosinase reaction where the incorporation of one oxygen atom from O_2 into phenol resulted in

diphenol (Mason *et al.*, 1955; Solomon *et al.*, 2014). For Hayaishi, oxygen incorporation into the substrate was observed by a catechol oxygenase reaction where both oxygen atoms from O_2 were incorporated into catechol, resulting in ring cleavage to obtain musconic acid (Hayaishi *et al.*, 1955). These enzymes, originally referred to as oxygen transferases, are today referred to as *oxygenases*. Hayaishi later coined the terms monooxygenase (Equation 3) and dioxygenase (Equation 4) to distinguish between the two types of oxygenation reactions. The overall equations for these types of enzymes are illustrated below:

$$S + AH_2 + O_2 \rightarrow SO + A + H_20 \quad (3)$$

$$S + O_2 \rightarrow SO_2 \quad (4)$$

Equations 3 & 4: General reaction for monooxygenases (3) and dioxygenases (4), where A is a hydrogen donor and S is the substrate. Monooxygenase reactions (3) result in the incorporation of a single oxygen atom into the substrate, while dioxygenase reactions (4) incorporate two oxygen atoms.

Oxidases, though performing very similar reactions to oxygenases, do not result in oxygen incorporation into the product. Oxidases, which involve oxygen, catalyze a reduction of dioxygen to either H_2O or H_2O_2. These reactions are often coupled with the oxidation of a substrate and typically include proton abstraction (Holm *et al.*, 1996). By definition, only oxygenases are able to incorporate oxygen from molecular oxygen into organic substrates. However, it is worth noting that under non-ideal conditions, the reactions catalyzed by many oxygenases may become *uncoupled*. In these instances, instead of the incorporation of an oxygen into the substrate, the reaction leads to the oxidation of the substrate, while O_2 is usually reduced to peroxide (Newcomb *et al.*, 2003). Thus, a close link between oxygenases and oxidases can been established. Since Mason's and Hayaishi's original publications, a myriad of literature has accumulated on oxygenase enzymes in their various uses (Yamamoto, 2006; Torres Pazmiño *et al.*, 2010). Active sites containing heme, non-heme iron, copper, and manganese are known catalytic centers for these reactions. Select organic compounds such as flavins are also widely used. The mechanisms by which these enzymes are able to incorporate O_2 into organic compounds are remarkable, as the reactions are considered challenging when using traditional chemistry (Bugg, 2003 and 2014). In the sections below, selected examples of the mechanisms by which oxygenases are able to activate oxygen are explored in greater detail, focusing specifically on monooxygenases.

1.2.1. Heme-Dependent Monooxygenases

Many enzymes contain heme (iron protoporphyrin IX), which is an oxygen-binding prosthetic group (Figure 2). The iron found in heme is known to exist in three oxidative states: ferrous (Fe II), ferric (Fe III) and ferrate (Fe IV). The loss of an electron occurs during the transition from ferrate to ferric state as well as from ferric to ferrous state. In addition, both ferrous and ferric states have a low spin state (S=0 and S=1/2, respectively) and a high spin state (S= 2 and S= 5/2, respectively). These spin states reflect their electron orbital configurations and have been comprehensively studied to gain insight into various enzymatic reaction mechanisms (Costas *et al*., 2004; Wong *et al*., 2013; Srnec *et al*., 2014).

In heme, the iron atom is bound to 6 ligands in an octahedral coordination sphere. It is covalently bound to 4 nitrogen atoms and can form two additional bonds (with two axial ligands) on either side of the heme plane (Holm *et al*., 1996). The heme prosthetic group is typically tightly bound, generally non-covalently, to enzymes by the two axial ligands. Various amino acids can act as

axial ligands to the heme iron. These axial ligands include amino acids such as histidine residues (in the case of hemoglobin or myoglobin), cysteine residues (in the case of cytochrome P450 or cytochrome C), or tyrosine residues (such as heme-dependent dehydrogenases), completing the six coordination sites for the iron atom. The significant conjugation within the prosthetic group gives heme the ability to activate oxygen through a one electron transfer step and the formation of a delocalized cation radical. The environment of the heme and the resulting chemical proficiency of the heme enzyme are greatly dependent on which amino acids coordinate the axial ligands (Holm *et al*., 1996). Changes in coordinating residues have a noticeable effect, since the redox potential of iron and its ability to bind oxygen is altered. Both hemoglobin and myoglobin, which are the best studied heme-containing proteins, bind dioxygen reversibly with a ferrous iron. If the histidine residue involved in coordinating the heme is mutated to tyrosine, the redox potential of the iron is modified resulting in hemoglobin M. The iron atom of heme, which is in a ferric state, is unable to bind O_2 due to coordination by negatively charged oxygen atom from the tyrosine side chain (Pulsinelli *et al.,* 1973) However, since hemoglobin and myoglobin are solely utilized as oxygen carriers, they are of little interest to this thesis since they do catalyze oxygenation reactions.

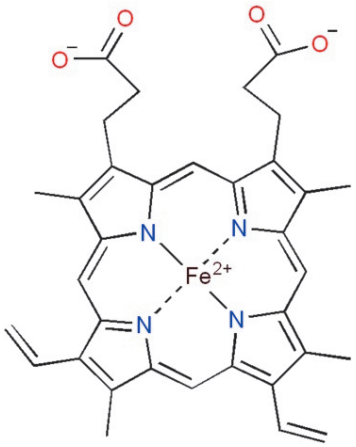

Figure 2: The structure of iron-protoporphyrin IX (heme). It is composed of 4 pyrrole rings covalently linked by methine bridges and an iron atom. Heme can be found in hemoglobin, catalases, peroxidases and cytochrome P450.

Likewise, catalases and peroxidase enzymes, though they require heme for activity, catalyze the decomposition of ROS into water and dioxygen (Frey & Hegeman, 2007) and are thus not relevant to oxygenation reactions. Cytochrome C and cytochrome P450 (CYP), on the other hand, have both been observed to result in the hydroxylation of substrates through the use of molecular oxygen activation (Frey & Hegeman, 2007). However, within the inner membrane of the mitochondrion, cytochrome C acts as a component of the electron transport chain, which is not known to bind oxygen. Of the two enzymes, only CYP is a known monooxygenase.

1.2.2. Cytochrome P450 Monooxygenases

Cytochrome P450 (CYP) enzymes were originally named for their biophysical properties; the characteristic carbonmonoxy-CYP complex of these enzymes has an absorbance maximum at 450 nm. It is one of the most abundant oxygenases in nature and found in all kinds of lifeforms (Nelson *et al*., 1996 and 2004; Hamdane *et al*., 2008). They are heme-dependent monooxygenases that typically catalyze the oxidation of aliphatic and aromatic carbon atoms. CYPs are usually part of a multicomponent electron-transfer chain system known as *P450-containing system*, where the CYPs perform the last reaction, hydroxylation. Over the last 50 years, cytochrome P450 and P450-containing systems have received considerable interest, as they play a key role in the biosynthesis of endogenous compounds (such as steroids),

detoxification and human drug metabolism (Ortiz de Montellano, 2013). CYPs are also of particular interest as many of them are promiscuous and diverse biocatalysts (Hamdane *et al*., 2008). The most common reaction they perform is described below in Equation 5:

$$RH + O_2 + NAD(P)H + H^+ \rightarrow ROH + H_2O + NA(D)P^+ \qquad (5)$$

Equation 5: The general reaction of cytochrome P450 enzymes. An aliphatic- carbon containing substrate (RH), molecular oxygen and NAD(P)H are required for CYP activity. The net result of the monooxygenation reaction is the incorporation of one oxygen atom into RH and water.

Within P450-containing systems, NAD(P)H usually supplies electrons that are required for activity via a redox partner. It is these redox partners that are also used for the classification of CYPs (Hamdane *et al.,* 2008). Class I, found in bacteria and mitochondrial membranes, are ferredoxin redox partners. Class II CYPs are found in endoplasmic reticulum membranes and receive electrons from NADPH-dependent P450 reductases. Class III can be described as the chimeras of CYPs, and their NADPH-dependent reductases are similar to those found in class II. Finally, class IV is capable of accepting electrons directly from NADPH.

The activity of cytochrome P450 enzymes can be traced to the heme cofactors, where the iron atom is coordinated between four nitrogen atoms along with two axial ligands, one of which is a cysteine residue. Oxygen activation is thought to proceed in P450 enzymes in a stepwise fashion, involving both iron and oxygen intermediates. The multiple intermediate species generated within CYPs are illustrated in Figure 3. In the traditional scenario, the resting ferric heme Fe (III) is thought to be in equilibrium between a six-coordinated iron in a low spin state (where water molecules are bound) and a five-coordinated iron in a high spin state (Conner *et al*., 2015) (1, figure 3). As the enzyme binds the substrate, structural changes to CYP shifts this equilibrium towards a high spin state, which leads to the displacement of the water ligand (Ener *et al*., 2010; Krest *et al*., 2013; Conner *et al*., 2015) (2, figure 3). Upon the binding of the substrate, the redox partner can transfer an electron to heme-Fe (III), resulting in a reduced heme-Fe (II) and the initiation of the catalytic cycle of CYP (3, Figure 3). In a reduced high spin state, molecular oxygen can then bind, reversibly, resulting in a superoxide-iron complex (4, Figure 3). After a subsequent reduction, a peroxo-iron species is formed. The protonation of the peroxo-iron species results in a hydroperoxo-iron intermediate (5, Figure 3). Within the catalytic cycle of CYPs, after step (5) the reactions are quick and thus notoriously difficult to follow. Further protonation results in one of two possible outcomes, depending on where protonation occurs. If protonation occurs on the oxygen closest to the iron atom, an iron-complexed hydrogen peroxide is formed (6, Figure 3). If formed, the hydrogen peroxide may dissociate, which results in a shunt reaction. However, if protonation occurs on the distal oxygen farther from the iron atom, an iron-oxo species (7, Figure 3) is formed with the simultaneous loss of a water molecule. Traditionally, it is the iron-oxo species (or ferryl porphyrin radical cation) that is thought to be responsible for the hydroxylation reactions catalyzed by CYPs (Ener *et al*., 2010).

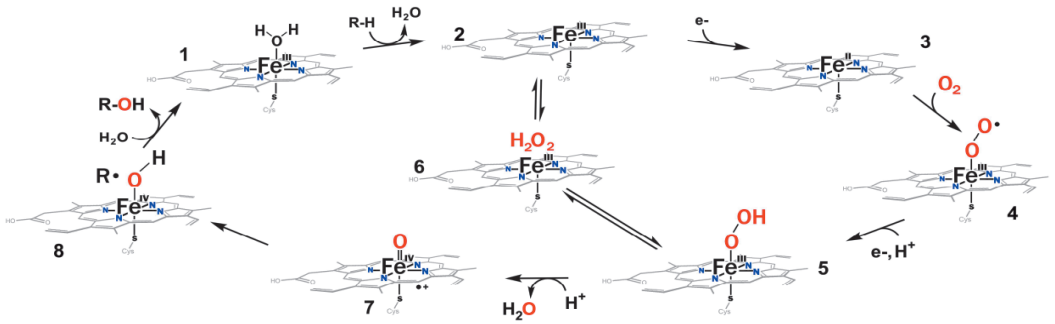

Figure 3: The proposed reaction mechanism for cytochrome P450 (Adapted from Ener et al., 2010)

Since the 90s, the generally accepted molecular mechanism has been the hydrogen abstraction-oxygen rebound mechanism (Figure 4; Kumar *et al*., 2004). In this mechanism, the iron-oxo species (7, Figure 4) abstracts a hydrogen atom from the substrate to generate a radical intermediate (8, Figure 4). This radical then reacts with the iron hydroxide species resulting in the hydroxylation of the substrate (1, Figure 4). The heme-Fe (III) returns to its resting state, and the cycle may begin anew once a new substrate molecule is bound (1).

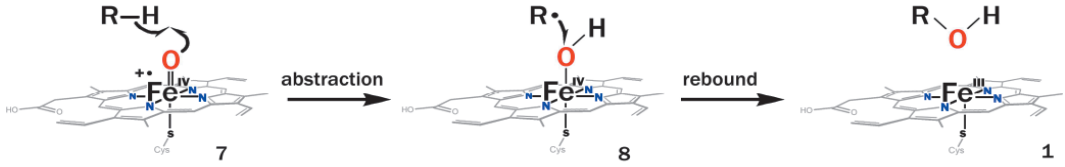

Figure 4: Illustration of the rebound molecular mechanism for cytochrome P450.(Adapted from Newcomb *et al.,* 2003)

Until recently, experimental evidence for the existence of iron-oxo species (7, Figure 3 & 4), also called cytochrome P450 compound I (P450-I), was lacking. In a seminal paper by Rittle and Green, the capture and characterization of P450-I was reported, substantiating the hydrogen abstraction-oxygen rebound mechanism (Rittle & Green, 2010; Krest *et al.*, 2013). Additionally, recent experiments with heme containing a photosensitized non-native cysteine provides evidence for the existence of the radical intermediate (8, figure 3 &4) also known as compound II (Ener *et al*., 2010). In addition to the evidence for P450-I and compound II (7&8, Figure 3 &4), other iron-oxygen species, such as the hydroperoxo-iron species (5, Figure 3), have also been experimentally observed (Davydov *et al.*, 2005), while iron-complexed hydrogen peroxide (6, Figure 3) has been suggested (Newcomb & Chandrasena, 2005). Experiments with radical clock substrate probes that may be used to distinguish between cation and radical mechanisms (Newcomb *et al.*, 2000 and 2003) have also hinted that the CYPs' mechanism for oxidation may not exclusively be based on radicals.

1.2.3. Non-Heme Iron-Dependent Monooxygenases

Many enzymes containing iron atoms in their active site are able to activate oxygen even though they lack a protoporphyrin IX prosthetic group; they are called non-heme iron-dependent enzymes. They can be classified into mononuclear (see section 1.2.4. for an example) or binuclear non-heme iron enzymes, which contain one or two iron atoms in the active centers, respectively. The iron oxidation states, spin states and electron configurations are often comparable to those

of heme-dependent enzymes (Solomon *et al.*, 2000, Srnec *et al.*, 2014). Numerous examples of mononuclear or binuclear non-heme iron enzymes have been characterized, but the reaction mechanism for most of these enzymes is similar and relies on reduced ferrous (Fe II) iron to bind and activate O_2 directly (Buongiorno & Straganz, 2013). Of these, one of the best studied non-heme iron-dependent monooxygenase is the binuclear non-heme iron containing soluble methane monooxygenase (sMMO), which belongs to the family of bacterial multicomponent monooxygenases. Even though copper sMMOs are known to exist, iron-dependent sMMOs are usually expressed in conditions of low copper availability. These enzymes are vital for their hosts, methanotrophs, which are able to utilize methane as their only source of carbon. The reaction of sMMOs is illustrated in Equation 6 below:

$$CH_4 + O_2 + NADH + H^+ \rightarrow CH_3OH + H_2O + NAD^+ \qquad (6)$$

Like CYPs, MMOs are multicomponent systems. They are composed of a monooxygenase, e.g. the methane monooxygenase hydroxylase (MMOH), an NADH-dependent reductase (MMOR) partner, and a third component, which is the regulatory protein (MMOB) required for efficient catalysis and facilitation of electron transfer (Merkx *et al.*, 2001, Tinberg & Lippard, 2011). Similarly to CYPs, MMOHs are promiscuous catalysts and accept, in addition to methane, various types of hydrocarbons, aromatic rings and sulfides as substrates (Solomon *et al.*, 2000, Merkx *et al.*, 2001). Studies have predominantly focused on two MMOHs: the MMOH from *Methylosinus trichosporium* OB3b, and the MMOH from *Methylococcus capsulatus.* The first high resolution crystal structure of MMOH from *M. capsulatus* was described by Rosenzweig *et al.* in 1993. It provided a detailed view into the diiron site and laid the foundations for the study of transient intermediates involved in the activation of dioxygen.

The structure of MMOH is composed of a 251 kDa heart-shaped heterodimer containing α2β2γ2 subunits. The α-subunit contains the diiron center and is responsible for catalyzing the hydroxylation reaction. The two irons of the active site, Fe1 and Fe2, are coordinated by two histidine and four glutamate residues that point inside the four helix bundle structure (Figure 5). Solvent molecules are also present in the active site and complete the octahedral coordination sphere (Tinberg & Lippard, 2011). For the last 30 years, intensive spectroscopic studies, studies into a multitude of other crystal structures in complex with diverse substrates/products, and transient kinetic studies have provided significant insight into the various oxidation states and intermediates of the MMOH reaction cycle (Merkx *et al*., 2001).

Through transient kinetic studies, in addition to the resting state of MMOHox, eight intermediates have been uncovered in the catalytic cycle of MMOH (Banerjee et al., 2015; Figure 6). At the start of the catalytic cycle, both irons are bridged by two hydroxide ligands (MMOHox). The geometry (distorted octahedral) and distances of both irons (about 3.1 Å) have been observed in various structures. In MMOHox, both irons are in ferric state (Fe III) and cannot bind dioxygen (MMOHox, Figure 6). Upon forming a complex with the NADH-dependent MMOR and MMOB, both ferric irons are reduced to the ferrous state (FeII). Unlike with CYP, the reduction of both irons has been observed in the absence of a substrate. When both irons are reduced, the pseudo-octahedral geometry is modified. This results in the displacement of both bridging hydroxide ligands. Glu243, chelated only to Fe2 in MMOHox, assumes an additional bridging role for both Fe1 and Fe2 in MMOHred (Figure 6). The chelation of Glu 243 to Fe1 modifies the distance between the irons and, additionally, enables the site to become more accessible. The binding of dioxygen to MMOHred subsequently occurs, leading to a transient complex (compound O) where oxygen in bound to the MMOH but not directly to the iron ions (Banerjee & Lipscomb, 2013). Compound O then forms a peroxodiiron (III) intermediate (compound P) via

a compound P* intermediate (Lee & Lipscomb 1999; Tinberg & Lippard, 2009; Banerjee et al., 2013). Compound P was formally identified through Mössbauer spectroscopy and UV-vis stopped flow (Tinberg & Lippard, 2011). Compound P decays spontaneously to form compound Q, resulting in the loss of a water molecule. Compound Q has been observed in the absence of any substrate, where it decays over several seconds and has been trapped using several spectroscopic techniques (Banerjee et al., 2015). Banerjee et al. have recently confirmed that both oxygens are derived from O2 in the compound Q intermediate.

The mechanism by which compound Q is able to insert an oxygen into the substrate has been known since 1990 (Ruzicka et al., 1990), and its structure is still controversial (Solomon et al., 2000). Upon forming Q, the substrate subsequently binds (intermediate QS), leading to a hydrogen abstraction and a rebound mechanism similar to that proposed for CYP (intermediate RS).

The rebound mechanism, like with CYP, was originally postulated by several groups (Ruzika *et al.*, 1990; Priestly *et al.*, 1992) for MMOH. Reactions with 1,1-dimethylcyclopropane lead to two different compounds, depending on the mechanism, which indicates that both cation (13 % occurrence) and radical (87 % occurrence) intermediates occur.

This finding, in a manner analogous to the papers concerning the mechanism of CYPs, was reproduced many times with other probes (Liu *et al.*, 1993; Brazeau *et al.*, 2001). For these reasons the molecular mechanism by which the reaction is carried out is still unresolved. After the hydroxylation reaction of the substrate, both the product and the MMOH intermediate, compound T, each contain a single atom from O_2 (Banerjee *et al.*, 2015). After the hydroxylation reaction, both iron atoms are returned to the ferric state. Upon the release of the product and the binding of a water molecule, the MMOH returns to the resting state; $MMOH_{ox}$.

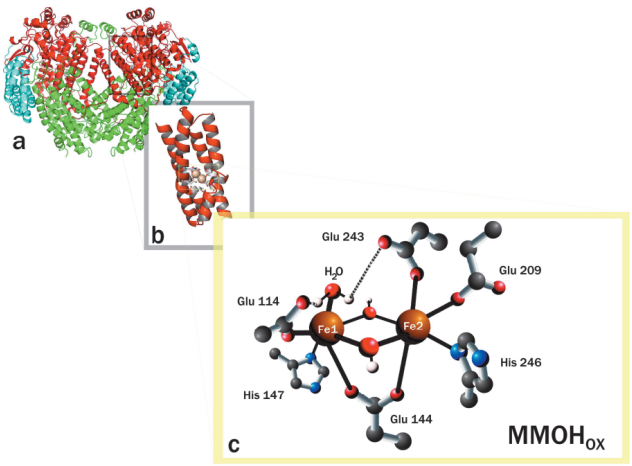

Figure 5: The three structural levels of the MMOH

a. The overall fold of the MMOH. The heterodimer has a vertically twofold symmetry. α subunits: red, β subunits: cyan and the γ subunits: green.
b. The four helix bundle with Glu (E), His (H), and diiron ligands.
c. Ball-and-stick model of the diiron center in $MMOH_{ox}$. The two iron ligands, Fe1 and Fe2, are coordinated by two histidines and four glutamic acids as well as various solvent-derived ligands.

(Adapted from Merkx at al., 2001)

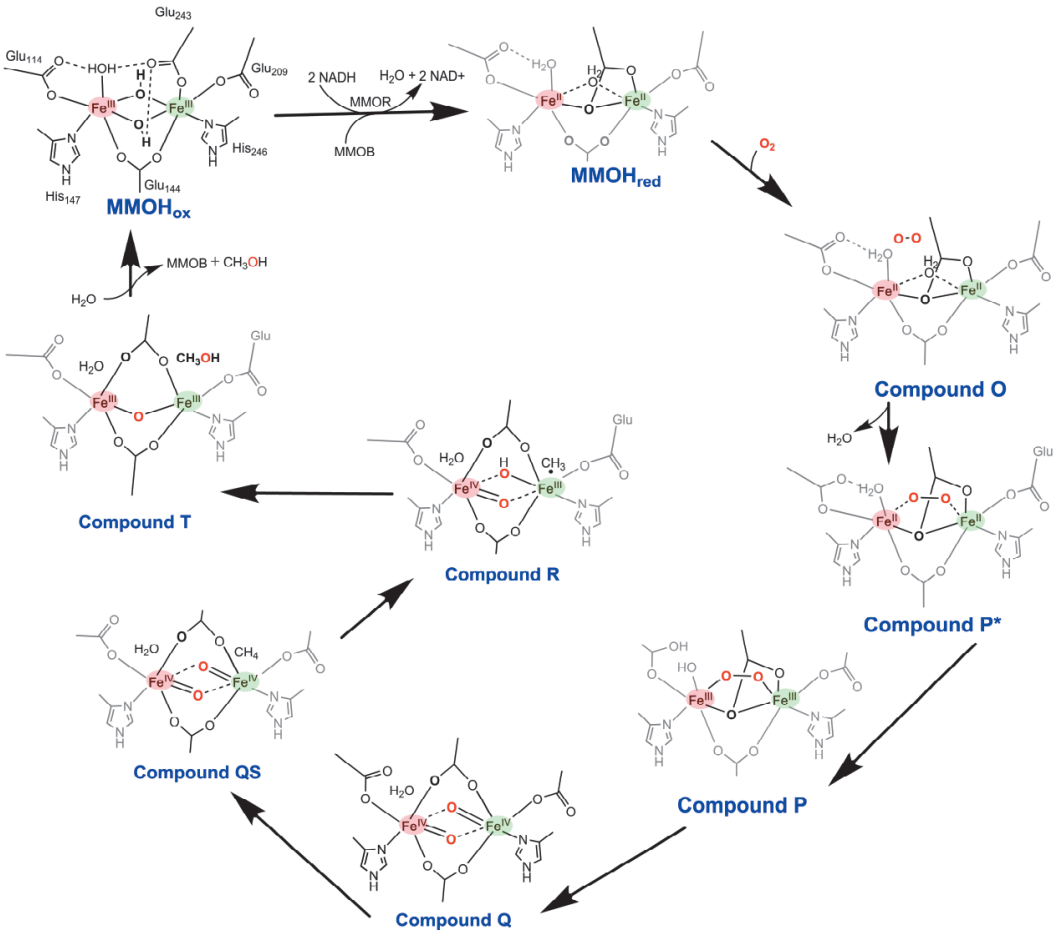

Figure 6: Model for the reaction mechanism for the MMOH from *M. capsulatus* based on the first crystal structure and various identified spectroscopic intermediates. The Fe1 iron is highlighted in red, while the Fe2 iron is highlighted in green. (Adapted from Banerjee *et al*., 2013 & 2015)

1.2.4. α-Ketoglutarate-Dependent Oxygenases

Another prominent group of non-heme iron-dependent oxygenases is the α-ketoglutarate (αKG) dependent oxygenases, also known as 2-oxoglutarate-dependent oxygenases. They were first identified in the early 60s as enzymes involved in collagen biosynthesis, such as lysine-5 hydroxylase or proplyl-4-hydroxylase (Culpepper *et al.*, 2011). Since then, αKG-dependent oxygenases have been observed to catalyze physiologically important processes in animals, such as hypoxic sensing, fatty acid metabolism, DNA repair, and gene expression. They have also been linked to the aging process via a "simple" hydroxylation reaction (McDonough *et al.*, 2010; Loenarz & Schofield, 2010; Cheng *et al.*, 2014; Markolovic *et al.*, 2015; Salminen *et al.*,2015). About 80 αKG-dependent oxygenases have been identified in humans alone (McDonough *et al.*, 2010). In addition, a multitude of primary substrates are known to be recognized by these enzymes, including proteins, methylated nucleotides, lipids, and various small molecules (Hausinger *et al.*, 2004). This diversity in substrates has led some to claim that these enzymes

may have one of the widest ranges of oxidative reactions of any enzyme family (McDonough *et al.*, 2010). The most common reaction they perform is described below in Equation 7:

$$\mathrm{R-H + O_2 + \alpha-ketoglutarate \rightarrow R-OH + CO_2 + succinate} \qquad (7)$$

Equation 7: The general equation for the α-ketoglutarate-dependent oxygenase, where R is the primary substrate.

Based on the equation above, α-ketoglutarate-dependent oxygenases can be considered dioxygenases, since an oxygen atom is incorporated into both the primary substrate as well as the succinate (secondary substrate). Sequence comparison of αKG-dependent oxygenases reveals a highly conserved His1-X-Asp/Glu-Xn-His2 motif. These three amino acid side chains are required for Fe(II) binding. Both histidines are strictly conserved, while the aspartate can be replaced by a glutamate. This sequence motif, also called the *facial triad*, along with beta helix fold is the hallmark of the αKG-dependent oxygenases and reflects the iron atom binding site (McDonough *et al*., 2010). Surprisingly, the model for the mechanisms by which αKG-dependent oxygenases are able to activate oxygen was already proposed in the early 80s (Hanauske-Able & Günzler, 1982) despite no structural information being available for αKG-dependent oxygenases till the late 90s, (Roach *et al.,* 1995; Valegård *et al.,* 1998). A general reaction mechanism for αKG-dependent oxygenases is illustrated in Figure 7:

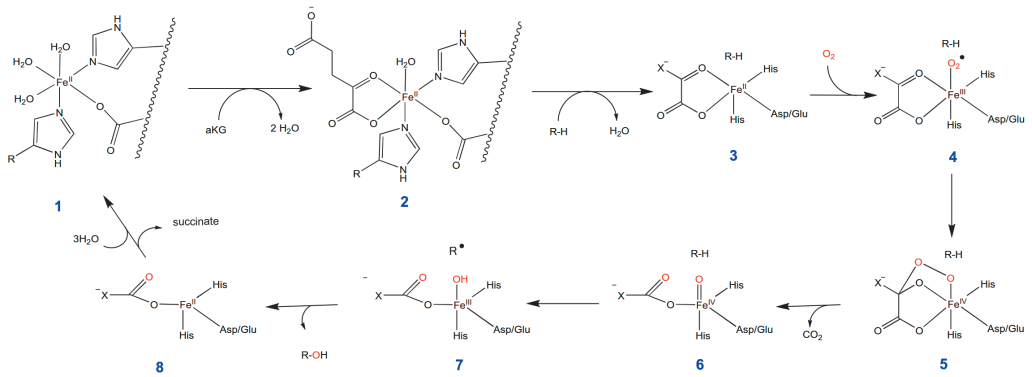

Figure 7: Illustration of the general hydroxylation mechanism of α-ketoglutarate-dependent oxygenases with emphasis on reactive intermediates. R-H is the primary substrate and X is an abbreviated version of α-ketoglutarate (adapted from Casey *et al*., 2013)

The iron atom at the start of the cycle is coordinated by three water molecules and confirmed by multiple crystal structures of αKG-dependent oxygenases free of αKG or substrates (1, Figure 7) (Valegård *et al.,* 1998; Dann *et al.*, 2002). By binding αKG, two water molecules are displaced from the iron (2, Figure 7). Once again several structures are available with αKG chelated to iron (Valegård *et al.*, 2004, Dann *et al.*, 2002, Zhang *et al.*, 2000; Qin *et al.*, 2013; Zhou *et al.*, 2001), confirming the existence of this intermediate. UV-vis stopped flow experiments have also suggested that the binding of αKG induces a conformational change in α-ketoglutarate-dependent oxygenases (Ryle *et al.*, 1999). With the binding of the primary substrate (3, Figure 7), the loss of a water is observed and reflected in the coordination of the iron (Müller *et al.*, 2004; Grzyzka *et al.*, 2010; Casey *et al.*, 2013). Upon reacting with oxygen, an Fe(III) superoxo species is formed (4, Figure 7) which, with subsequent nucleophilic attack on the αKG keto group, results

in an Fe (IV) peroxyhemiketal bicyclic complex (5, Figure 7). Though intermediates 4 and 5 have not been observed (Grzyska *et al.*, 2010), intermediate 6 has been observed (Proshlyakov *et al.,* 2004; Gryska *et al.,* 2010; Casey *et al.*, 2013). The activated oxygen is then able to abstract a hydrogen atom from the primary substrate, forming a substrate radical (7, Figure 7). This radical then reacts with the hydroxyl group in a rebound-like mechanism similar to the one in cytochrome P450. With release of the substrate, the iron returns to its initial ferrous state (8, Figure 7). By releasing the succinate, three water molecules can coordinate the iron ion again and the catalytic cycle can begin anew (1).

As stated above, because α-ketoglutarate-dependent oxygenases have a wide range of oxidative reactions, the reaction mechanism above may not apply to many of the known α-ketoglutarate-dependent oxygenases. Despite being related to the αKG-dependent hydroxylases by sequence and still containing the His1-X-Asp/Glu-Xn-His2 motif, some members of this family catalyze "nonstandard" reactions, such as desaturation, ring expansion, ring formation, or other types of oxidative reactions, such as the well-studied enzyme decetoxycephalosporin C synthase (Tarhonskaya *et al.*,2014; Hausinger *et al.,*2004). Some of these enzymes have even been observed to use an alternative co-substrate (Mcdonough, 2010). As such, a universal mechanism is not applicable to all αKG-dependent oxygenases. Some argued that because the iron site of αKG-dependent oxygenases only has three "fixed" ligands, the reactive oxidizing intermediate is more "flexible", thus granting αKG-dependent oxygenases a wider range of catalysis for oxidative reactions compared to CYPs.

1.2.5. Copper-Dependent Monooxygenase

After iron, copper is the most abundant metal found in oxygenases (Evans *et al.*, 2003). Copper oxygenase reactions are diverse and include peptide hormone and neurotransmitter biosynthesis, melanin biosynthesis, iron homeostasis, and methane oxidation (Rosenzweig and Sazinsky, 2006). Like iron, copper can be found in three biologically relevant oxidative states, Cu(I), Cu(II) and Cu (III), although the last is significantly rarer (Holm *et al.*, 1996; Hemsworth *et al.*, 2013). The *copper centers* found within these enzymes, which can have one or more copper atoms, were historically classified according to their spectroscopic attributes into three types that reflect their d^9 electron shell configuration (Solomon *et al.*, 1996). Type 1 or blue copper enzymes contain a single copper center and absorb at 600 nm due to a bond from a sulphur atom from the protein (Cys or less commonly Met) to the copper atom or atoms (Solomon *et al.*, 1996 and 2014). Type 2 or normal copper proteins have a copper-sulphur bond but lack distinctive features in their optical spectra. These enzymes are generally involved in oxidation and oxygenation reactions (Solomon *et al.*, 1996 and 2014). Type 3 or coupled binuclear coppers contain a pair of copper centers. Type 3 copper centers can be easily identified due to the strong spin pairing (S = 0) of the two copper atoms reflecting their spatial configuration. As a result, they lack a distinct electroparamagnetic resonance (EPR) signal. Type 3 copper proteins also contain oxidases as well as oxygen binding proteins (Solomon *et al.*, 1996 and 2014; Lewis and Tolman, 2004). The section below will focus on the type 2 and type 3 enzymes, which are known copper monooxygenases.

1.2.6. Type 2 Copper Monooxygenases

Three eukaryotic proteins are well known type 2 copper monooxygenases. These are the peptidylglycine α-hydroxylating monooxygenase (PHM), the dopamine β- monooxygenase (DβM), and the recently identified insect tyramine β- monooxygenase (TβM) (Klinman 2006; Hess *et al.*, 2008; Solomon *et al.*, 2014), all of which share a highly conserved mechanism (Osborne *et al.*, 2013). All of these enzymes are involved in the synthesis of neurotransmitters, peptide

hormones or growth factors and are composed of dimeric or tetrameric structures, although TβM has been reported to be functional as a monomer. (Gray *et al.*, 2006). The overall reactions for these enzymes are illustrated in Figure 8.

DβM, PHM and TβM all require two copper atoms for activity. In the structures of these enzymes (Prigge *et al.*, 1997; Solomon *et al.*, 2014) both coppers have a different coordination environment. The Cu_M (or Cu_B) copper is coordinated by two histidines and a methionine, while the Cu_H (or Cu_A) is coordinated by three histidines (Figure 9). The reaction cycle of DβM (similar to PHM or TβM) begins with two reduced copper atoms, which coordinate dopamine, followed by the subsequent binding of O_2. The copper atoms appear to have different functions; Cu_M is thought to be involved in hydroxylation, while Cu_H is involved in electron storage/transfer through solvated water. Surprisingly, both active site copper atoms are solvent-exposed and separated by a large gap of about 11 Å, which is too large for direct electron transfer. Yet, without any bridging ligand, an electron transfer across this gap still occurs, because Cu_H gets oxidized at the end of the reaction, as can be observed from the early EPR studies of DβM (Perry & Hegeman, 2007).

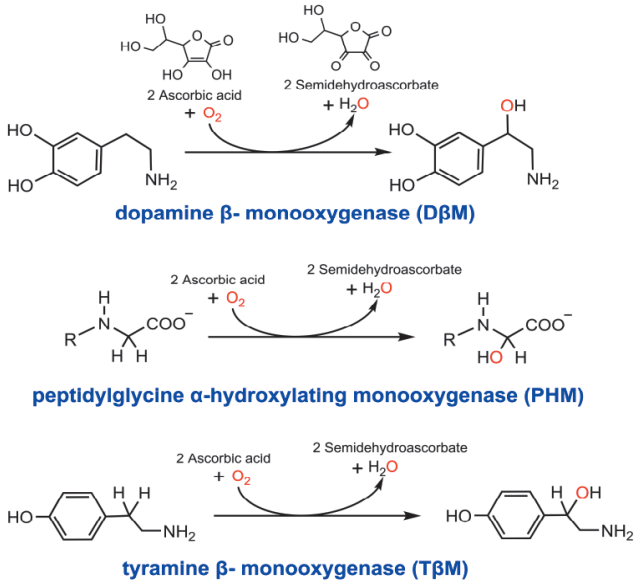

Figure 8: The overall reaction of DβM, PHM and TβM. For the monooxygenation reaction, molecular oxygen and two ascorbates are needed. R is peptides in the PHM reaction.

Based on the comprehensive studies by Klinman *et al.*, the reaction mechanism most likely to occur is illustrated in Figure 9. The basis for this mechanism is inferred from multiple kinetic and isotope effect experiments with both $^{18}O_2$ and a deuterated substrate. Upon substrate and oxygen binding, an electron transfer from reduced Cu_M copper to O_2 results in a superoxo Cu_M^{II} intermediate (Evans *et al.*, 2003; Klinman, 2006; Zhu *et al.*, 2015). Proton abstraction from the substrate by Cu_M^{II} is then thought to occur. This results in substrate C-H bond cleavage leading to a hydroperoxy Cu_M^{II} complex and a substrate radical intermediate. One of the most controversial aspects of the mechanism then occurs. A proposed long range electron transfer occurs from the Cu_H to the Cu_M copper through a solvent-filled cleft between the domains. This proton-coupled electron transfer is likely to be mediated by hydrogen-bonded waters and conserved tyrosine amino acid (Zhu *et al.*, 2015). This electron/proton transfer, resulting in Cu^{II}_H, generates a Cu^{II}_M-O• radical, which reacts with the substrate radical to form a product that is ligated to Cu^{II}_M.

Subsequent reduction of both coppers by ascorbate results in the release of a hydroxylated product and a water, thus enabling the cycle to begin anew.

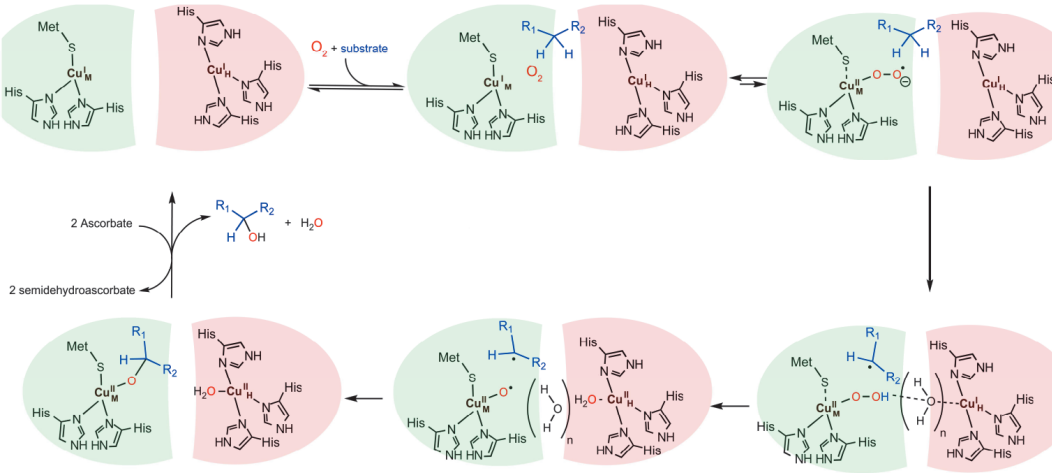

Figure 9: The proposed mechanism for type 2 copper monooxygenases based on the DβM reaction cycle. The copper Cu_M is in green, while the copper Cu_H is in red. The distance between Cu_M and Cu_H is too great for direct electron transfer but involves electron transfer through a water molecule that bridges this cleft. Highlighted in yellow is the proposed mechanism by Klinman (Adapted from Klinman, 2006).

The proposed mechanism is not universally accepted. Though today there is a generally accepted consensus that there is a hydroperoxy complex intermediate, the mechanism by which hydroxylation occurs is debated, as no intermediates have been directly observed. For Chen and Solomon (2004), based on density function theory calculations, the reaction order is different. According to their proposal, when the hydroperoxy Cu_M^{II} complex intermediate is formed, it is the radical substrate, through water-assisted OH transfer, that cleaves the O-O bond resulting in hydroxylation reaction. This reaction occurs prior to the electron/proton transfer from Cu_H. The Cu^{II}_M-O• radical generated from this reaction would then be oxidized by Cu_H via an electron transfer step. Upon the oxidation of ascorbates, both copper atoms return to their reduced state. Meliá *et al.*, (2013) on the other hand, proposed a rebound mechanism through molecular dynamic calculations. According to their reaction model, upon hydrogen abstraction by the Cu^{II}_M atom, the hydroperoxy is transferred to the radical substrate instead. This transfer results in the formation of Cu^{I}_M. Via a long-range electron transfer step from the Cu_H, the dioxygen bond is then cleaved, resulting in a Cu^{II}_M product and a hydroxylated intermediate. The reduction of both copper atoms by the ascorbates would result in the release of the hydroxylated product and a water molecule. Despite differences in alternative mechanisms, all of these mechanisms include a long-range electron transfer from Cu_H via a channel of hydrogen bonds composed of water molecules, which is not fully understood (Klinmam, 2006; Meliá *et al.*, 2013). Due to the chemical nature of certain amino acids, many potential candidates are likely to form hydrogen bonds with water and many not be strictly conserved. Though these amino acids may not be directly involved in the reaction, they many help establish a channel of hydrogen bonds. Due to this complex interaction with water molecules, several mechanisms are possible.

1.2.7. Type 3 Copper Oxygenases

Type 3 copper oxygenases often involve the production of natural phenolic pigment or melanin. The production of melanin is utilized for various purposes from bacteria to plants and animals. These functions include wound healing in plants, such as *Rhus vernicifera* (Hüttermann *et al.*, 2001), immunological responses through reactive quinols in insects (Eleftherianos & Revenis 2011), hardening of new cuticles in arthropods (Burmester 2001), the browning of fruits and plants, UV light protection, and skin/hair color determination in humans, as well as the production of L-DOPA (L-3,4-dihydroxyphenylalanine), an important neurotransmitter precursor (Baron & Suggs, 2014; Decker *et al.*, 2006; Bogdan, 2007; Oetting, 2000; Halaouli *et al.*, 2006). Common type 3 copper proteins include hemocyanin (Hc), catechol oxidases (Co), and tyrosinase (Ty) enzymes (Mason *et al.*, 1955; Solomon *et al.*, 1996 and 2014; Rolff *et al.*, 2011). All of these enzymes contain six histidine residues that coordinate two copper ions, CuA and CuB. Despite similarities in the coordination of copper, these enzymes have different functions (Golfeder, 2014). The main function of Hc is, in anthropods and mollusks, oxygen transport. For Co and Ty, on the other hand, the main function is the oxidization of phenol-like molecules. All type 3 copper proteins have similarities in terms of sequence (Fujimoto *et al.*, 1995; Matoba *et al.*, 2006) as well as structure (Matoba *et al.*, 2006; Solomon *et al.*, 2014) despite a major difference in their functions. Yet, by exposing deeply buried copper atoms in Hc (through proteolytic cleavage or detergents) to a solvent, Hc proteins can be converted to functional Co or Ty enzymes (Decker *et al.*, 2006; Rolff *et al.*, 2010; Li *et al.*, 2009). These observations have prompted suggestions that Hc and Co as well as all type 3 copper proteins share a common ancestor (Halaouli *et al.*, 2006).

Of type 3 copper oxygenases, TY is the only one described as a monooxygenase. Despite its prevalence, the first structure for tyrosinase was only available in 2006 from *Streptomyces castaneoglobisporus* HUT 6202 (Matoba *et al.*, 2006). Ty, unlike other type 3 copper enzymes, can catalyze two separate reactions: the hydroxylation of monophenols and the oxidation of diphenols to form quinones, as illustrated in Figure 10 (Rolff *et al.*, 2011; Solomon *et al.*, 1996 and 2014).

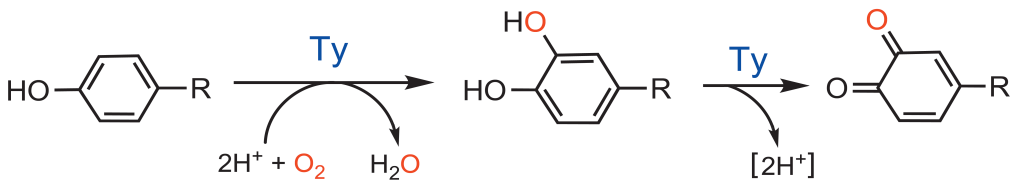

Figure 10: Tyrosinase (TY) monooxygenase reactions can convert phenolic compounds to corresponding quinone compounds via an ortho-diphenol.

The reaction mechanism proposed for tyrosinase (Figure 10) was established prior to any structural data on Ty based on kinetic data and the identification of various spectral intermediates (Solomon *et al.*, 2014). The Deoxy, Oxy and Met reaction intermediates were later confirmed through crystallographic structures (Matoba *et al.*, 2006; Sendovski *et al.*, 2011; Goldfeder *et al.*, 2014) and are the basis for the reaction mechanism (Figure 10).

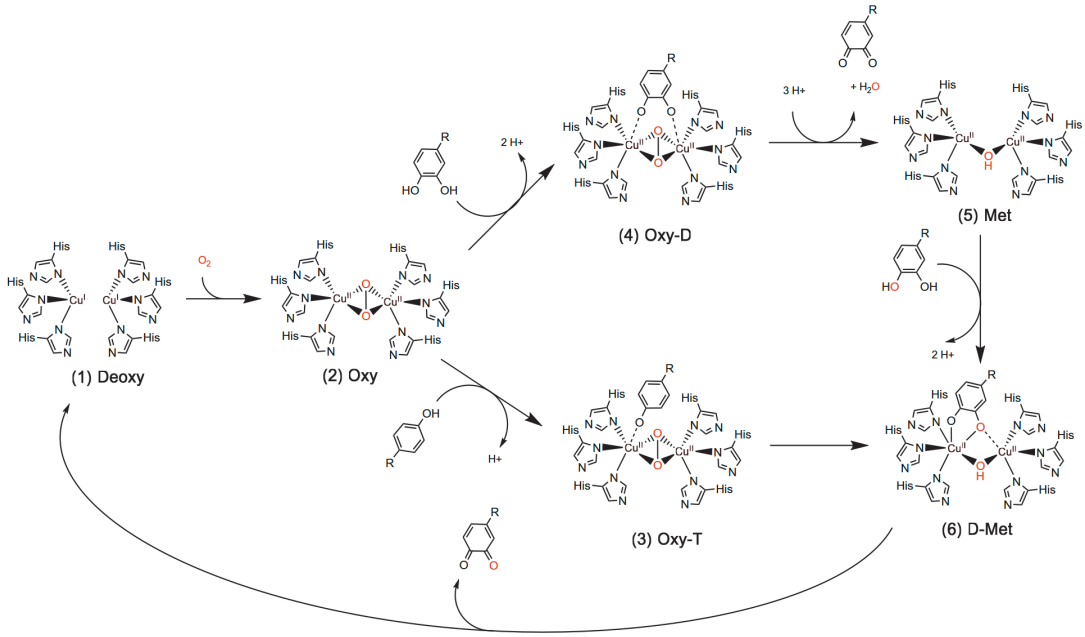

Figure 11: Model for the reaction cycle of tyrosinase. Both interpenetrating cycles, the oxidase reaction cycle (2, 4, 5, and 6) and the hydroxylation cycle (2, 3, 6), are presented. Two substrates are needed to return Ty to Deoxy state, resulting in the reduction of dioxygen to two waters for the oxidase cycle, while the monooxygenase cycle requires only a substrate to return to the deoxy state (adapted from Solomon, 2014)

The cycle starts with the deoxy (1, Figure 11) intermediate, where both copper ions are in the reduced Cu (I) state. Upon binding O_2, both copper ions are oxidized to Cu (II), resulting in the Oxy state (2, Figure 11). Two alternative catalytic cycles can occur, depending on the substrate.

The first possibility is an oxidase cycle. If a diphenol is available, it results in a subsequent Oxy-D state (4, Figure 11), leading to the oxidation of the diphenol and a water. Upon the release of quinone and water, the enzyme transitions to the Met state (5, Figure 11). If an additional diphenol is available, binding will result in the D-Met state (6, Figure 11), which will then result in the oxidation of a quinone. Upon release of the quinone and water, both copper ions are reduced and the cycle can begin anew.

Alternatively, a monooxygenase cycle can occur. If a phenol is available, a shift from the Oxy (2, Figure 11) to Oxy-T (3, Figure 11) is thought to occur. Although Oxy-T (3) has not been observed, mutational studies favor the coordination of the phenol to one copper atom, Cu_A (Solomon *et al.*, 2014). An electrophilic aromatic substitution is credited for the hydroxylation reaction leading to a diphenol intermediate. This intermediate has been observed using borate anion as a trapping agent (Yamazaki & Itoh, 2003). The bound diphenol intermediate then leads to a D-Met state (6, Figure 11). Oxidation of the diphenol then occurs leading to a quinone being formed. Upon release of the quinone, both copper ions are reduced, and the cycle can begin anew.

The interpenetrating cycles of Ty have raised several questions. One concerns the need for and initial deprotonation of the entering substrates. Goldfeder *et al.* (2014) have proposed that the deprotonation is structurally based on a conserved hydroxide/water molecule activated by glutamic acid and asparagine. This finding would explain the solvent isotope effect observed in Ty (Solomon *et al.*, 2014). Another fundamental question is how Ty is able to perform the

hydroxylation of phenol-like compounds when Co is not, despite their similarities. Because the oxidation cycle is the same in Co as in Ty, subtle differences in residues surrounding the substrate-binding pocket are likely to be responsible for the ability of Ty to perform the monooxygenase cycle (Klabunde *et al*., 1998). Several theories have been proposed to explain why Ty is able to catalyze a monooxygenase reaction and Co is not. According to the findings of Goldfeder *et al.* (2014), despite the similar orientation of substrate binding for Co and Ty, Co are not able to perform Ty reactions due to a bulky residue (such as Phenylalanine) providing steric hindrance as well as a thioether Cys-His bond restricting the CuA geometry. Without these two constraints, the substrate rearrangement needed for the hydroxylation of a phenol is possible leading to the monooxygenation reaction of Ty (Goldfeder *et al.*, 2014). However, Co from *Aspergillus oryzae* has neither a Cys-His thioether bond nor a restricting phenylalanine (Hakulinen *et al.*, 2013).

1.2.8. Substrate Activation of Oxygen in Metal-Dependent Oxygenases

As previously mentioned, one of the first oxygenases to be identified was catechol oxygenase (Hayaishi *et al.*, 1955; Fujisawa & Hayaishi, 1968; Brown *et al.*, 2004). Traditionally, these types of dioxygenases have been classed into two families: intradiol dioxygenases (IDOs) and extradiol dioxygenases. This classification is based on reaction products and the type of cleavage these enzymes catalyze, or which carbon atom the oxygen is attached to (Fujisawa & Hayaishi, 1968; Fujisawa *et al.*, 1972; Bugg, 2003; Brown *et al.*, 2004). It is worth noting that, while intradiol and extradiol dioxygenases are not structurally related, they perform similar reactions (Vetting *et al.*, 2004). Furthermore, identical key intermediates have been identified for both types of oxygenases (Knoot *et al.*, 2015), although the dioxygen incorporation event in itself is different. The difference between IDOs and extradiol oxygenases is most evident in the oxidation state of their iron atom. In IDOs, only a ferric state (Fe III) iron is observed throughout the reaction cycle (Solomon *et al.*, 2014; Knoot *et al.*, 2015), whereas in extradiol dioxygenase, the iron oxidation states vary during the reaction cycle (Fe II and Fe III are both observed). The activation of O_2 in IDO does not require the reduction of metal ions. The proposed mechanism for IDOs is in strong contrast with all of the reaction mechanisms described above. Although IDOs are metal-dependent, their reaction mechanisms rely instead on the activation of triplet state O_2 through an organic substrate (Solomon *et al.*, 1996; Brown *et al.*, 2004; Bugg, 2003; Pau *et al.-,* 2007; Knoot *et al.*, 2015). Activation of oxygen through organic molecules exemplifies a fundamental mechanistic difference to the oxygenases mentioned above that require reduced transition metals. Thus, although IDOs are dioxygenases and not monooxygenases, they are worth mentioning as the mechanism for activating oxygen through organic substrates has been well studied.

A well-studied IDO is Protocatecuate 3,4-dioxygenase. Like all IDOs, it is a mononuclear non-heme iron-dependent dioxygenase, which was first discovered in *Pseudomonas putida* (Hayaishi *et al.*, 1968) and was one of the first dioxygenase structures to be solved (Ohlendorf *et al.*, 1988). It comprises of two polypeptide chains (α and β) assembled as a dimer and encoded by two distinct genes. The sequence identity across various species is highly conserved with at least 40 % identity in the α-chain, while the β-chain is even more similar (50% identity), likely due to the iron being coordinated by the β-chain. In the β-chain, the residues involved in iron coordination are strictly conserved and include two histidines and two tyrosines (Figure 12). The iron geometry is essentially trigonal bipyramidal (1) with a solvent molecule, generally a hydroxide, also involved in the coordination (Brown *et al.*, 2004; Knoot *et al.*, 2015).

The reaction mechanism of IDOs has been established (Knoot *et al.*, 2015) with diverse techniques, including the crystal structures of native and mutant enzymes, kinetic studies with

various substrates and inhibitors (Vetting *et al.*, 2000; Horsman *et al.*, 2005), and spectroscopic studies such as EPR (Pau *et al.*, 2007) and x-ray absorption fine structure (Aitken *et al.*, 2004). Recently, some of the key catalytic intermediates were directly observed in crystal structures using a 4-fluorocatechol as a substrate analogue (Knoot *et al.*, 2015).

The proposed mechanism for IDOs is illustrated in Figure 12. From the resting state of IDOs (1, Figure 12), the coordinating tyrosine and hydroxide units are displaced upon substrate binding (2, Figure 12). The attack on the substrate by O_2 is a concerted process where the aromatic substrate is proposed to provide the reducing electrons (Pau *et al.*, 2007) (3, Figure 12). After the initial attack, a 6C-alkylperoxo species is formed (4, Figure 12), which is subsequently rearranged to an oxidation of one oxygen atom (in orange) to a 5C-alkylperoxo species (5, Figure 12). The O-O bond cleavage is thought to be driven by the protonation of the oxygen (6, Figure 12) by either a metal-bound solvent molecule or deprotonation of tyrosine, which leads to the formation of an anhydride intermediate (7, Figure 12). Finally, a nucleophilic attack by the hydroxide group on the anhydride results in the ring cleavage (8, Figure 12) yielding the product of the reaction.

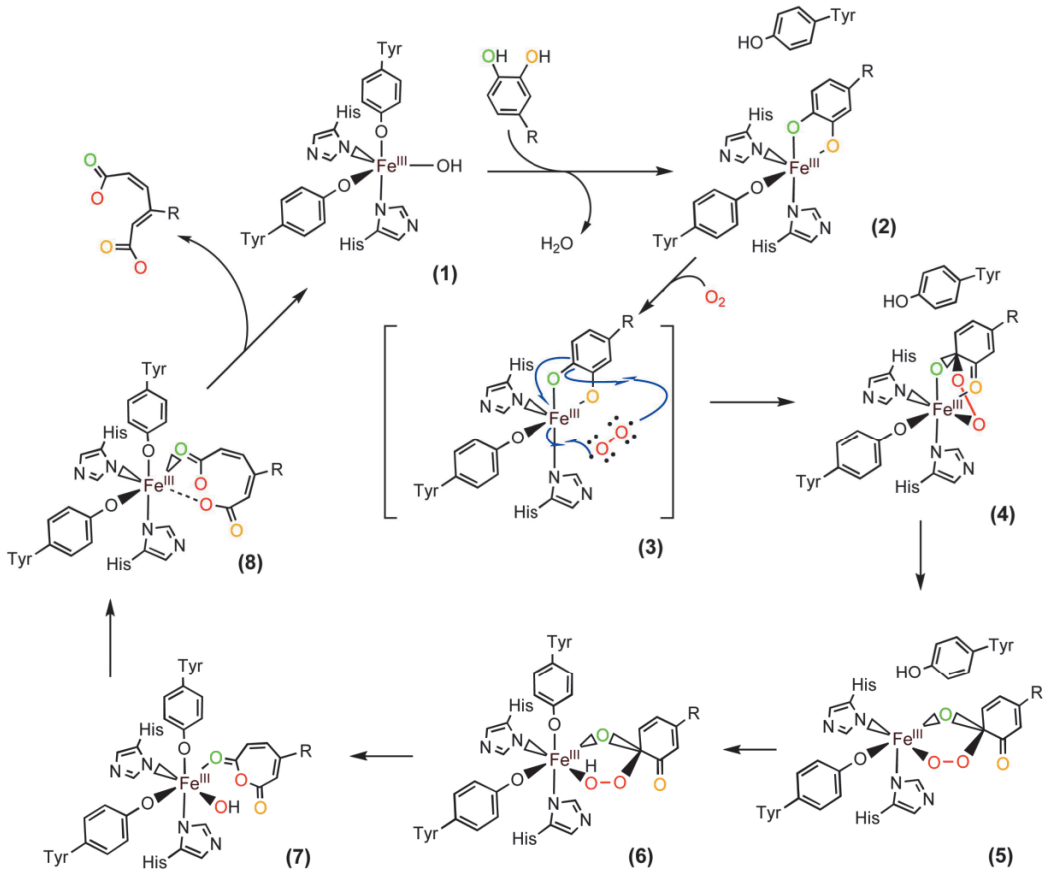

Figure 12: The proposed mechanism for IDOs involving the activation of organic substrates for reactions with O_2 in the triplet state (in red). The oxygens of the substrate are colored in orange and green for visualization purposes. (Adapted from Knoot *et al.,* 2015)

Despite being a metal-dependent enzyme, it is the substrate that drives the reaction and activates triplet oxygen instead of a reduced metal as in the sections above. This same paradigm

has also been observed in certain extradiol dioxygenases, where metal swapping (from Mn to Fe) has no apparent effect on K_M or V_{MAX} (Emerson *et al.*, 2008), which may indicate that the activation dioxygen is substrate-dependent. More examples of organic molecules that are able to "activate" oxygen will be examined below.

1.2.9. Flavoenzymes and Flavin-Dependent Monooxygenases

Flavins are universally found in organisms from bacteria to mammals. The enzymes that utilize this prosthetic group, flavoenzymes, are generally brightly yellow in color due to the presence of flavins (Jenson *et al.*, 2012; Massey, 2000). Despite being vital for a number of cellular functions, higher organisms have lost their ability to synthesize flavins, and the acquisition of the cofactors is wholly dependent on the diet or obtained from bacteria from the intestinal flora (Bacher *et al.*, 2000). Usually flavoenzymes bind flavins noncovalently, but in some cases one or two covalent bonds with flavins have been observed (Mattevi *et al.*, 1997; Alexeev *et al.*, 2007). The most common flavin derivatives used by flavoenzymes are FMN (flavin mononucleotide) and FAD (flavin adenine dinucleotide). Both are derived from riboflavin, also called vitamin B_2, which consists of an isoalloxazine ring with a ribitol-sugar moiety. FMN has an additional phosphate, while FAD has a pyrophosphate and an adenosine moiety (Figure 13). Both the phosphate and adenosine moieties are mainly used to anchor the cofactor to the enzyme.

Flavin-binding proteins are involved in a myriad of reactions in cellular processes, including energy metabolism, protein folding and even apoptosis (Massey, 2000; Senda *et al.*, 2009; Huijbers *et al.*, 2013; Peé, 2012; Colibus & Mattevi, 2006; Joosten & Berkel, 2007). Flavin's ability to accept a pair of hydrogens and electrons enables many oxidative enzymes to use them as prosthetic groups in various roles. They are at the heart of energy metabolism in which they play a key role in the electron transport chain (Massey 2000; Joosten and Berkel 2007; Senda *et al.*, 2009). In addition, their remarkable redox proprieties enable them to be used in diverse reactions such as halogenations (Peé, 2012), Baeyer-Villiger oxidations (Jensen & Berkel 2012), epoxidations (Büch *et al.*,1995), and hydroxylation reactions (Li *et al.*, 2008; Lindqvist *et al.*, 2009; Kallio *et al.*, 2013; Patrikainen *et al.*, 2014). It is the last of these reactions that is of central interest in this thesis, as it involves the splitting of an O-O bond that leads to the incorporation of one oxygen atom into the substrate and the reduction of the other atom to water.

Historically, there were scientific debates as to how the initial spin forbidden reaction between flavin and oxygen occurred (Massey, 2000). Presently, the commonly accepted model (Figure 14) involves the activation of oxygen through an exchange/transfer of one electron from a reduced singlet flavin unit to triplet oxygen (Huijbers *et al.*, 2014). This causes a caged radical pair consisting of a superoxide anion and a neutral flavin radical. The formed radical pair collapses, resulting in spin inversion and the formation of peroxyflavin (or C(4a)-hydroperoxide anion). Upon proton uptake, a neutral flavin-hydroperoxide is formed. This covalent intermediate has been observed spectroscopically in several flavin-dependent monooxygenases (Brosi *et al.*, 2014). In solution, without flavoenzymes, flavin hydroperoxide intermediates are unstable and prone to decay to hydrogen peroxide and oxidized flavin. Within the active sites of flavoenzymes, where the stabilizing micro-environment can be modulated, both flavin-hydroperoxide and peroxyflavin can result in the hydroxylation of the substrate instead of hydrogen peroxide formation (Massey, 1995). Depending on the protonation state, the flavin-hydroperoxide attacks the substrate via an electrophilic or a nucleophilic attack. The distal oxygen is then transferred to the substrate, resulting in a hydroxylated substrate and an oxidized flavin upon release of water (Figure 14). These enzymes are sometimes referred to as *intermolecular dioxygenases*, as one oxygen atom is incorporated into flavin while the other is incorporated into the substrate.

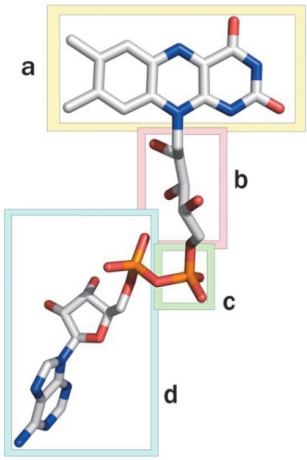

Figure 13: The structure of riboflavin and flavin adenine dinucleotide.

a. the tricyclic isoalloxazine ring from which flavins are derived
b. ribitol-sugar
c. phosphate
d. phosphate and adenosine

Riboflavin (vitamin B_2) consists of the isoalloxazine ring and the ribitol-sugar moiety (a+b), FMN consists of riboflavin and a phosphate moiety (a+b+c), while FAD consist of riboflavin, a pyrophosphate and an adenosine moiety (a+b+c+d).

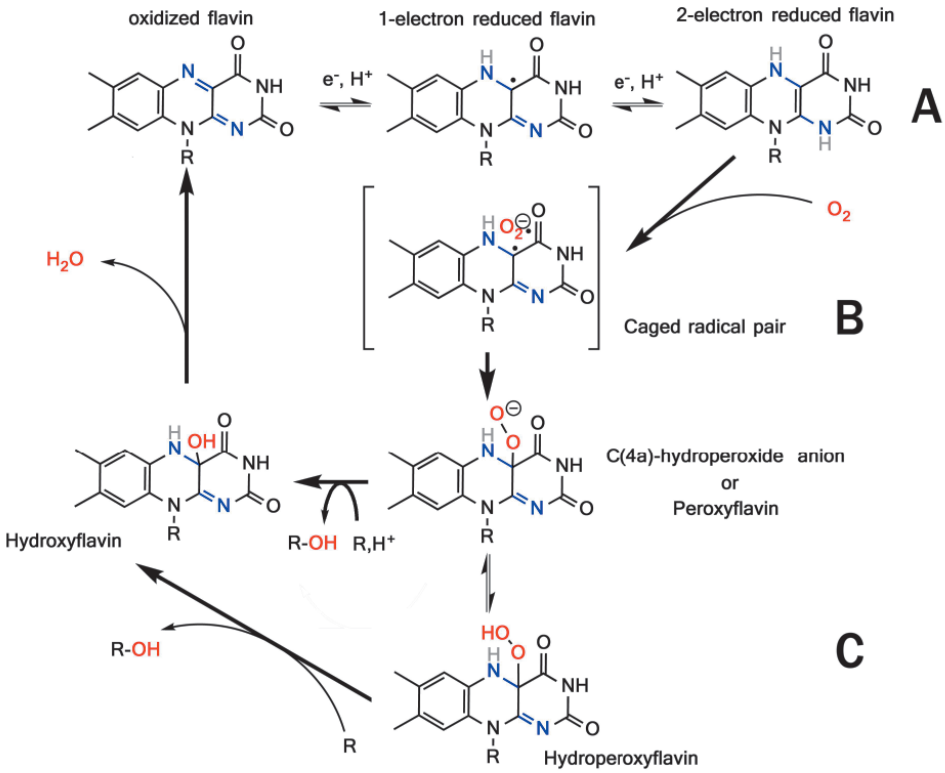

Figure 14: The activation of O_2 by flavins.

A. The three oxidative steps of flavins. Flavin reacts with oxygen only in its fully reduced form.
B. Upon electron transfer from fully reduced flavin to dioxygen, a *caged radical pair* between a superoxide anion radical and a neutral flavin radical occurs.
C. Collapse of the radical pairs results in the spin inversion of molecular oxygen and the formation of peroxyflavin. Upon protonation, neutral hydroperoxyflavin is formed. Both peroxy and hydroperoxyflavin can react with the substrate, resulting in its hydroxylation and hydroxyflavin. Release of water completes the catalytic cycle. (Adapted from Massey, 2000)

1.2.10. Pterin-Dependent Monooxygenases

Another distinct group of monooxygenases is the small group of aromatic amino acid hydroxylases found in both prokaryotes as well as eukaryotes: the pterin-dependent monooxygenases. Examples of pterin-dependent monooxygenases are phenylalanine hydroxylase (PheH), tryptophan hydroxylase (TrpH), and tyrosine hydroxylase (TyrH) (Figure 15). In humans, these enzymes have an important role in the biosynthesis of amino acids and neurotransmitters. PheH, for example, is involved in the conversion of excess phenylalanine to tyrosine in the liver. Deficiency of this enzyme results in phenylketonuria, a genetic disorder resulting in the buildup of phenylalanine in the blood (Strisciuglio and Concolino, 2014). On the other hand, TrpH is involved in the biosynthesis of catechol neurotransmitters (dopamine) synthesized from the precursor L-DOPA, while TyrH is involved in the biosynthesis of, 5-hydroxytryptophan, which is a precursor of the neurotransmitter serotonin.

For activity, PheH, TrpH and TyrH require both a non-heme iron atom as well as the unique cosubstrate tetrahydrobiopterin (BH4). Major differences between prokaryotes and eukaryotes can be seen in all three of these enzymes. In prokaryotes, these enzymes only contain a catalytic domain, whereas in eukaryotes, they also contain an N-terminus regulatory domain and a C-terminus tetramerization domain, leading to allosteric effects (Knappskog *et al.*, 1996; Daubner *et al.*, 1997; Fitzpatrick, 2015).

Despite these differences, the catalytic mechanisms of these enzymes are thought to be identical; molecular oxygen is activated by the electrons from BH_4, and the reaction is mediated by the iron ions (Roberts *et al.*, 2013).

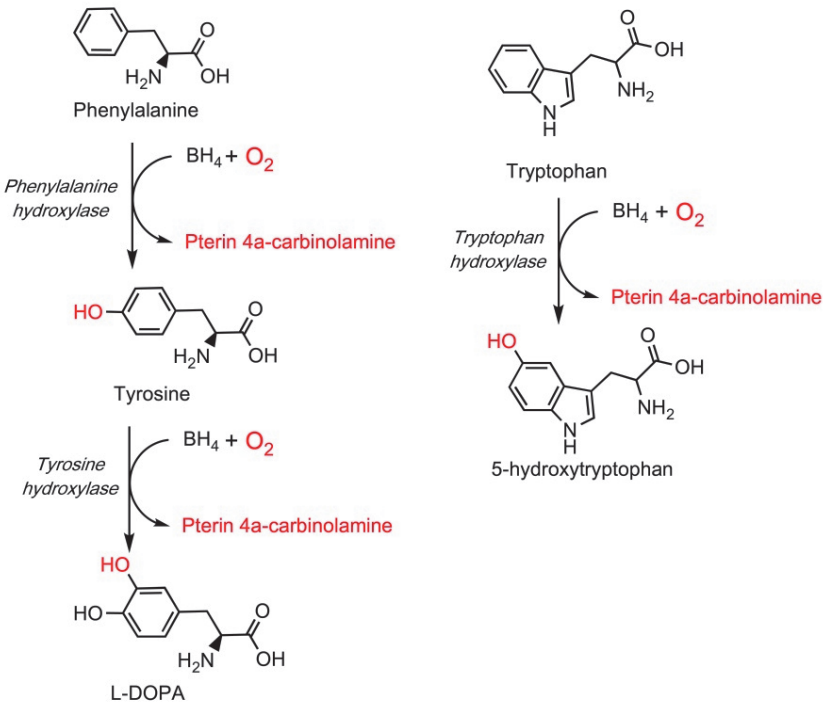

Figure 15: The reactions performed by pterin-dependent hydroxylases (in italics). Phenylalanine, tyrosine and tryptophan hydroxylase all require tetrahydrobiopterin (BH_4) and oxygen for activity. The overall reaction results in the transfer of one oxygen to BH_4 and the incorporation of the other to the substrate (shown in red).

Many similarities can be found between the reaction mechanisms of flavins and BH4. Like flavin, BH4 provides an electron to activate dioxygen for the hydroxylation reaction to occur. Also similarly to flavin, a caged radical pair has been proposed, resulting in BH4 oxidation to pterin 4a-carbinolamine. Once oxidized, two enzymes are required to regenerate BH_4 to its reduced state. The first enzyme dehydrates the 4a-carbinolamine to quinonoid dihydrobiopterin, although spontaneous dehydration to quinonoid dihydrobiopterin does also occur (Roberts, 2013).

The second enzyme, NAD(P)H-dependent dihydropteridine reductase, regenerates the latter back to BH_4 (Figure 16). In the structures of pterin-dependent monooxygenases, the iron atom appears to be coordinated between two histidines (like hemoglobin) and glutamate (Andersen et al., 2003; Roberts et al., 2013). The two histidines and one glutamate motif, also found in α-ketoglutarate-dependent oxygenases (see section 1.2.4.) is responsible for coordinating the iron atom. The role of iron for these enzymes has therefore been thought to be in mediating the incorporation of oxygen into BH4 and the substrate (Roberts et al., 2013).

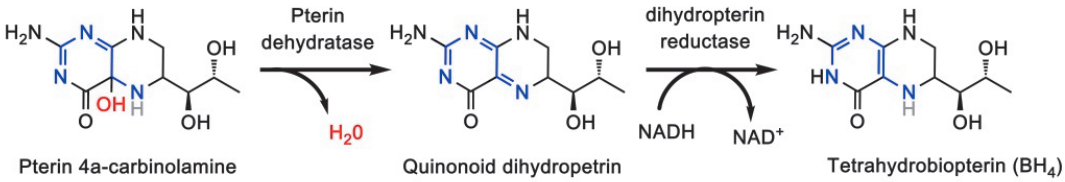

Figure 16: The regeneration of BH_4 is a two-step process requiring dehydration (which has been observed to be spontaneous) and reduction using NADH.

One of the most extensively studied enzymes of the family is the pterin-dependent phenylalanine-hydroxylase (PheH), which was first described more than 40 years ago. Since its discovery, the mechanism of this enzyme has been controversial due to the unusual role the iron atom and historically due to the role of BH_4 and its uncoupled reactions, which lead to the formation of hydrogen peroxide (Kappock & Caradonna, 1996; Chen & Frey, 1998). The uncoupling of the reaction leads to hydrogen peroxide and pterin 4a-carbinolamine. This has been observed with the use of phenylalanine analogues (Hillas & Fitzpatrick, 1996) or with various mutants (Daubner & Fitzpatick, 1999). Similarly, in PheH (from *Chromabacterium violaceum*) without an iron atom, uncoupling is observed despite the presence of phenylalanine (Chen & Frey, 1998). The reaction rates of hydroxylation with iron, phenylalanine and BH_4 are at least one order of magnitude higher than that of hydrogen peroxide formation without iron, suggesting reaction uncoupling. Taken together, the data suggest that the iron atom, although not essential in dioxygen activation, is required for the hydroxylation of phenylalanine. At the beginning and at the end of the catalytic cycle, the iron atoms of these enzymes are found in the ferrous (Fe II) state, although when isolated the enzyme has been found in the ferric state (Fe III).

Below is a hypothetical mechanism for the hydroxylation of phenylalanine by PheH. The reaction can be divided into two parts: firstly, the activation of dioxygen by BH4 and generation of the ferryl oxo intermediate (1-4), and secondly a subsequent reaction of the ferryl oxo intermediate with phenylalanine (5-6) resulting in the hydroxylation (5-6). Upon binding (1, Figure 17), BH_4 is able to transfer an electron to oxygen, resulting in a caged radical (2, Figure 17), which is similar to the oxygen activation with flavins (see section 1.2.9.). The peroxypterin generated then reacts with iron to form a bridged peroxy complex (3, Figure17) which results in a pterin 4a-cabrinolamine and a ferryl oxo intermediate (4, Figure17). This intermediate, observed

spectroscopically (Eser *et al.*, 2007; Panay *et al.*, 2011), is thought to react with phenylalanine in a manner similar to the rebound mechanism of cytochrome P450. The hydroxylation of phenylalanine is also accompanied by a hydride shift of the hydrogen atom (in orange). For this reason, hydroxylation is thought to occur through electrophilic aromatic substitution involving a cationic species (5, Figure 17). Finally, after the hydroxylation reaction, the ferrate iron returns to a ferrous state, unlike in P450 reactions, since a buildup of ferric iron has not been observed (6, Figure 17) (Fitzpatrick, 2003).

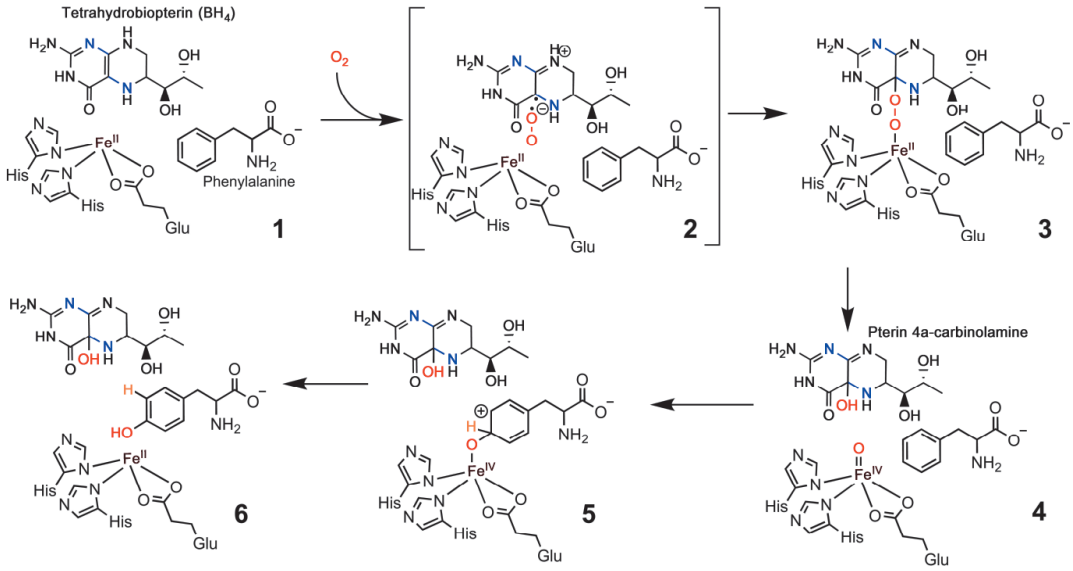

Figure 17: The phenylalanine hydroxylase reaction mechanism with BH_4 and molecular oxygen. The mechanism involves two steps: firstly, the oxidation of BH_4, and secondly, the insertion of an oxygen atom into phenylalanine by a reactive ferric iron. The resulting electrophilic aromatic reaction results in a hydride shift (hydrogen in yellow) (adapted from Roberts *et al.* 2013)

1.2.11. Cofactor-Independent Monooxygenases

Oxygenases were thought to require either metals, cofactors or both to be able to catalyze the incorporation of molecular oxygen into their substrates. Recently, a series of oxygenases have been described to require neither cofactors nor metals for activity (Fetzner, 2002 and 2007; Steiner *et al.*, 2010; Bugg, 2014). One of the first identified cofactor-independent monooxygenases was tetracenomycin F1 monooxygenase (TcmF1) (Shen & Hutchinson, 1993), which is involved in quinone formation in the biosynthesis of aromatic polyketides. Prior to the work on TcmF1, some theories regarding oxygenases without metal ions or cofactors were made, and these were deemed mechanistically possible through protein/solvent protonation to form a stabilized carbanion (Abell and Schloss, 1991). The general consensus, however, was that oxygenases require cofactors or metals to “activate” dioxygen (the Abell paper reaches this conclusion by reiterating the necessity of metals for oxygenase activity).

In the case of TcmF1, various chelating reagents, potential inhibitors and atomic absorption analysis were performed to ensure that the monooxygenase was indeed free of metals and cofactors. Two cofactor-independent 2,4-dioxygenases involved in quinolone ring-cleaving reactions soon followed:

HOD (1 H-3-Hydroxy-4-oxoquinaldine 2,4-dioxygenase) from *Arthobacter* sp. Rü61a and QDO (another 2, 4-dioxygenase) from *Pseudomonas putida* 33/1 (Bauer *et al.*, 1996). Both enzymes were confirmed to use dioxygen by incorporating $^{18}O_2$ into their products but, like TcmF1, neither cofactors nor metals were detected for these enzymes. The first structure of a cofactor-independent enzyme, the monooxygenase ActVA-Orf6 (Sciara *et al.*, 2003), confirmed that neither metals nor cofactors were present in the active site.

Today, a significant series of cofactor-independent oxygenases and oxidases have been reported (Baas *et al.*, 2015; Steiner *et al.*, 2010; Bui *et al.*, 2014; Bugg, 2014). Although the majority of known cofactor-independent monooxygenases are involved in the biosynthesis of polyketide quinone moieties in *Streptomyces* (Shen & Hutchinson, 1993; Sciara *et al.*, 2003; Okamoto *et al.*, 2009; Siitonen *et al.*, 2012), some cofactor-independent monooxygenases have also been found in *E.coli* (Adams & Jin, 2005) and may be present in *M. tuberculosis*, as well (Lemieux *et al.*, 2005).

The obvious question is then how these enzymes are able to "activate" triplet state dioxygen. Since no metal is present and activity is observed in darkness, only two alternative mechanisms for activating triplet state dioxygen are reasonable; coupling with stabilized free radicals or electron transfers (Hamilton, 1990; see section 1.1.5; Fetzner, 2002). The substrates for these oxygenases are usually conjugated aromatic compounds. As such, both radicals and ions could be stabilized. Both possible reaction mechanisms are illustrated in Figure 18 below.

The first mechanism proposed by Shen *et al.* (1993) involved the formation of a substrate/protein radical that would react with oxygen. In the radical mechanism (1A, 2A and 3A in Figure 18), both a phenol radical and an enzyme radical intermediate would need to be generated. Shen *et al.* proposed that the first step in this reaction cycle involves proton abstraction by the enzyme to form a phenol and an enzyme radical (1A to 2A, Figure 18). The formed substrate radical would react with triplet dioxygen in a single electron transfer (2A, Figure 18) to form a peroxo-radical species (3A, Figure 18). Once formed, the peroxo radical species would then abstract an electron from the radical enzyme to form a peroxo-anion (4, Figure 18) which, upon proton transfer, leads to a hydroperoxo intermediate (5, Figure 18). Additional loss of water would result in a hydroxylated product and complete the monooxygenation reaction.

The other mechanism, also called the substrate-assisted mechanism, involves a base-catalyzed deprotonation of the substrate leading to substrate carbanion formation. Once formed, an electron transfer from the substrate carbanion to triplet state dioxygen occurs, thereby resulting in superoxide. The substrate-assisted mechanism (1B-3B, Figure 18) was based on the Bauer dioxygenase papers and reiterated by Fetzner (2002). Upon deprotonation of the substrate (1B, Figure 18) by a base, the substrate is left with a net charge of -1 (2B, Figure 18) stabilized by the conjugated substrate. The base, in this scenario, can be the enzyme, a water molecule or an enzyme-water complex. In the presence of molecular oxygen, a single electron transfer occurs, resulting in a superoxide (3B, Figure 18). Consequentially, a caged radical pair is formed (3B, Figure 18) similarly to the mechanisms of flavin or pterin-dependent enzymes. The outcome would be similar to that of the radical mechanism with the formation of a peroxo-anion (4, Figure 18) and, upon protonation, a hydroperoxo intermediate (5, Figure 18) is formed. In this mechanism a single electron transfer from the substrate to dioxygen drives the reaction.

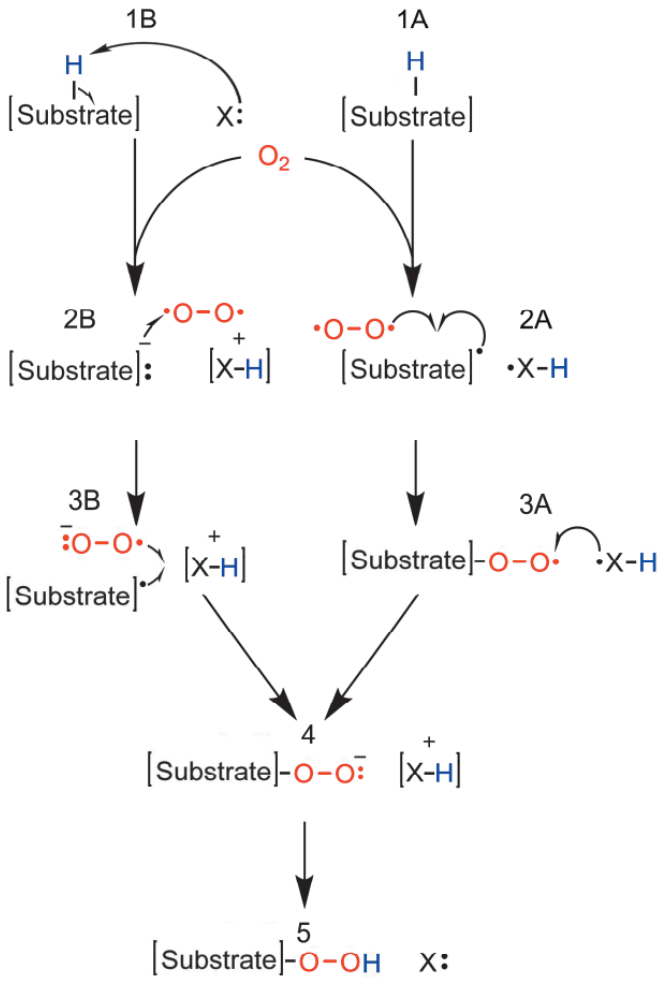

Figure 18: The simplified reaction scheme involving two alternative mechanisms for cofactor-independent monooxygenases. In scenario 1A-3A, the "radical" mechanism, where X represents the enzyme, is shown. Scenario 1B-3B is the "substrate assisted" mechanism, where X represents a base, which can be an enzyme, a solvent, or both. In reactions 1A-3A, the substrate is activated by the enzyme to form a phenol radical intermediate. Upon radical formation, an electron transfer to oxygen occurs, resulting in a superoxide, subsequently forming a peroxo-radical species (3A). Upon additional electron transfer from the enzyme, a peroxo-anion (4) would be formed, leading to a hydroperoxide intermediate with protonation (5). In the "substrate assisted" mechanism, upon deprotonation of the substrate, the charged substrate transfers a single electron to dioxygen, resulting in a superoxide. The superoxide then reacts with the radical substrate to form a peroxo-anion (4), leading to hydroperoxide intermediate with protonation (5).

(Adapted from Fetzner, 2007)

Although no reaction intermediates have been observed for these monooxygenases, recent papers by Thierbach (2014) and Bui (2014), which used cofactor-independent dioxygenases HOD and urate oxidase (UOX), respectively, have provided evidence in support of a caged radical intermediate (3B, Figure 18), suggesting that the "substrate-assisted" activation of oxygen is more likely.

2. AIMS OF THIS STUDY

At the start of this thesis, several types of oxygenases had been described within the biosynthesis of aromatic polyketides. The aim of my research project was to investigate some of these unusual oxygenases and gain further insight into the various mechanisms they employ to activate oxygen.

The first of these enzymes was the cofactor-independent monooxygenase SnoaB, which is involved in the biosynthesis of nogalamycin (papers I and II). One of the underlying questions associated with these enzymes is how, despite the lack of metals or cofactors, these enzymes are able to activate oxygen. Therefore the primary aim for this study was to uncover the catalytic mechanism by which SnoaB is able to activate dioxygen and compare it to other known cofactor-independent monooxygenase enzymes through biochemical and structural studies.

The second part of my thesis concerned the two-component monooxygenase system enzyme pair AlnH and AlnT (paper III). This two-component monooxygenase system was intriguing due to its unusual regiochemistry. Here, we wanted to confirm the function of both of these enzymes and determine if AlnT catalyzes oxygenation at the expected position.

For the final part of my thesis, the methyl transferase DnrK and the closely related hydroxylase RdmB were chosen (paper IV). Using the available crystal structures of both enzymes, this study aimed to identify the regions that would enable a methyltransferase to evolve into a monooxygenase.

In essence, the aim of this thesis was to determine the function and mechanisms of various monooxygenases involved in the biosynthesis of aromatic polyketides and determine if these oxygenases share common characteristics. The results of my thesis are presented in four peer-reviewed articles and further discussed in section 4.

3. MATERIALS AND METHODS

Listed below is a brief overview of all the techniques, materials and methods used during this thesis. A more comprehensive description is presented in the original publications I-IV.

Reagents:
All reagents were purchased from Sigma or TCI Europe, unless stated otherwise. The substrates used for the various enzymes in this study were purchased, derived from bacterial strain cultures, or synthesized from bought reagents through a one-step reduction, as described (paper II).

Bacterial Strains and Culture Conditions:
Only *Escherichia coli* (*E.coli)* strain TOP10 (Invitrogen) was used for cloning purposes and the expression of proteins. The volume of *E.coli* cultures varied depending on the protein of interest. Both Luria-Bertani (LB) or 2 × tryptone yeast (TY) medium were used, supplemented with ampicillin (final concentration 100 µg/mL) for the selection of plasmids.

Streptomyces sp. CM020 and *Streptomyces galilaeus* ATCC 31615 mutant H038 was obtained from Galilaeus Oy (Kaarina, Finland). *Streptomyces albus* strain (Chater & Wilde, 1980) was used as a host for the heterologous expression of both pAoriΔalnH and pAoriΔalnT constructs. *S. albus* was transformed by intergeneric conjugation using E. coli ET12567/pUZ8002 (Kieser *et al.*, 2000). Liquid medium cultures of *S. albus* were made with tryptone soy broth. MS was used as a solid medium for the *Streptomyces* species (Kieser *et al.*, 2000). Production of secondary metabolite was routinely cultivated in 25 mL of E1 medium (Ylihonko *et al.*, 1994) with soy flour instead of Pharmamedia and with no starch added. Cultures were incubated for 5 days at 300 rpm shaking at 30 °C. Amberlite XAD 7HP (Rohm and Haas) was included in the cultures for the adsorption of metabolites (1g/50mL). Apramycin (50µg/mL) and thiostrepton (40 or 50 µg/mL) were used, respectively, for selection in solid and liquid media.

DNA Manipulation Techniques and Cloning of Expression Constructs:
DNA techniques and sequence analysis for both the DNA of *Streptomyces* species and the plasmid DNA used in this study were performed using conventional techniques (Sambrook *et al.*, 1989; Kieser *et al.*, 2000). Commercial DNA isolation kits (Qiagen or Omega Bio-Tek) were used for the recovery of DNA from agarose gels or plasmid purifications in conjunction with restriction endonucleases. Both *alnH* and *alnT* were deleted from the pAlnuori cosmid containing the complete alnumycin biosynthetic cluster (Oja *et al.*, 2008) using the λ Red recombinase system (Datsenko and Wanner, 2000) through a two-step homologous recombination process, which resulted in pAoriΔalnH and pAoriΔalnT cosmids respectively. DNA was amplified using Phusion DNA Polymerase (Finnzymes) for polymerase chain reactions (PCRs) with 3 to 5 % dimethylsulfoxide (DMSO) to amplify GC-rich template sequences. The amplification of *snoaB*, *alnH/alnT*, *dnrK* and *rdmB* was performed using genomic DNA from *Streptomyces nogalater (S. nogalater), Streptomyces sp.* CM020, *Streptomyces peucetius* and *Streptomyces purpurascens* respectively. All SnoaB mutants were made using a conventional 2-step 4-primer PCR method (Higuchi *et al.*, 1988), employing two complementary primers containing the wanted mutation and two primers at the fringe of the wanted sequence to amplify the gene. Some of the DnrK variants were ordered as synthetic genes from GeneArt (Strings DNA fragments). Eurofins MWG Operon was mostly used for DNA sequencing. Only the pBADHisB vector (Invitrogen) or modified versions of this vector (Kallio *et al.*, 2006) were used in protein expression. All polyhistidine-tagged recombinant proteins carried an N-terminal or C-terminal his tag sequence used for purification.

Transformation Methods:
E.coli transformation was carried out by the heat-shock transformation of calcium chloride competent cells (Ausubel *et al.,* 1994). *Streptomyces* protoplasts were prepared and transformed according to standard protocols (Kieser *et al.*, 2000)

Protein Expression, Purification and Analysis:
Diverse culture conditions for each protein were used with varying factors such as volume, temperature, induction amount, and time of cell harvesting after induction (see papers I-IV). The usual protocol involved the inoculation of the main culture from an overnight preculture, the measurement of optical density to determine the appropriate time for induction, induction with L-arabinose (final concentration of 0.02 % (w/v)) to induce the overproduction of the histidine-tagged enzyme, and the collection of cells on a predetermined point of time after the induction. Cell pellets were usually frozen prior to further processing.

The purification of the enzymes involved multiple steps. Cell pellets were initially resuspended in specific buffers. Cells were then lysed using a French Press or ultra sound sonication. After lysis, clarification of the lysis was carried out through centrifugation. The enzyme of interest, contained within the supernatant, was purified by either a single affinity chromatography step involving the histidine-tag or with a combination of several chromatographic steps involving gel filtration or anion exchange through prepack columns (GE healthcare) and ÄKTA FPLC (GE healthcare) chromatographic systems. The purity of all protein samples was verified by SDS electrophoresis. SnoaB was also verified by protein mass spectrometry (TOF MS ES+) to confirm exact mass.

Enzyme Assays and Reaction Product Analysis:
Enzyme reactions conducted *in vitro* were performed in buffer conditions and concentrations optimized for each enzyme. Reactions were monitored either by UV-vis spectrophotometry and/or by quantitative high pressure liquid chromatography (HPLC) analysis of the reaction products. Columns and conditions used during HPLC runs were optimized for each compound or series of compounds. Some of the reaction products were also analyzed by liquid chromatography–mass spectrometry (LC-MS) and nuclear magnetic resonance (NMR).

4. RESULTS AND DISCUSSION

4.1. Introduction – Oxygenases within Polyketide Biosynthesis

Polyketides are a large and distinct class of secondary metabolites produced by bacteria, fungi and plants. One of the most prominent producers of polyketides is a group of gram positive soil bacteria, *Streptomyces*, which are particularly renowned for their ability to produce aromatic polyketide antibiotics. These complex compounds, or their derivatives, are often highly biologically active and have traditionally been used as pharmaceutical drugs (Bentley and Bennett, R. 1999).

Aromatic polyketides may be further classified based on the structure of the initial carbon skeleton assembled by polyketide synthases, but much of the chemical complexity and diversity of polyketides is due to additional modifications made by tailoring enzymes (Hutchinson & Fujii, 1995; Hertweck, 2009). Many different types of tailoring reactions are known, but some of the most ubiquitous are reactions involving oxygenases. Tailoring enzymes utilizing dioxygen that have been identified from these pathways include P450 oxygenases (Li *et al.*, 2012), non-heme iron-dependent oxygenases (Choi *et al.*, 2008), α-ketoglutarate-dependent oxygenases (Eustáquio *et al.*, 2013), many flavin-dependent oxygenases (Koskiniemi *et al.*, 2007, Taguchi *et al.*, 2013, Patrikainen *et al.*, 2014), as well as cofactorless monooxygenases (Fetzner, 2007; Siitonen, 2012; Bugg, 2014). This thesis focuses on oxygenases involved in the biosynthesis of several aromatic polyketides from various Streptomyces species, specifically the cofactor-independent monooxygenase SnoaB, the two-component flavin-dependent hydroxylase system composed of AlnH and AlnT, and the unusual SAM-dependent oxygenase RdmB.

4.2. Cofactor-Independent Monooxygenases (papers I and II)

Cofactor-independent monooxygenases are frequently found to be involved in the biosynthesis of aromatic polyketides, and they are typically responsible for catalyzing quinone formation. Many of these sequences, frequently found in *Streptomyces* species, have been assigned to the antibiotic biosynthetic monooxygenase domain in protein family databases such as Pfam (Finn *et al.*, 2014).

In the biosynthesis of nogalamycin in *S. nogalater* (Ylihonko *et al.*, 1996), SnoaB, a cofactor-independent monooxygenase, catalyzes the oxygenation of carbon atom C-12 of 12-deoxynogalonic acid, yielding a quinone product (Figure 19). Like other known proteins of this family, SnoaB is a small enzyme (118 amino acids at 13.1kDa) that oxidizes a relatively large structure. However, few amino acids are conserved in this enzyme family, making the identification of catalytic residues non-trivial without structural information about the enzyme (paper II, Figure 4). This diversity in amino acid sequences may also point to possible divergent evolution within this enzyme family and hint to a broad substrate tolerance (Sciara *et al.*, 2003). To date, relatively few of these enzymes have been functionally characterized. Prior to 2009 (papers I and II), only three of these enzymes, identified as monooxygenases in aromatic polyketide biosynthesis, were characterized. These include TmcH involved in tetracenomycin biosynthesis (Shen *et al.*, 1993), AknX in aclacinomycin biosynthesis (Chung *et al.*, 2002), and ActVA-Orf6 found in the actinorhodin biosynthetic pathway (Sciara *et al.*, 2003).

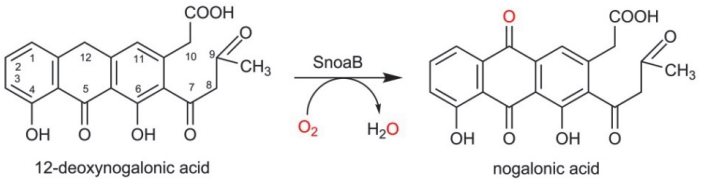

Figure 19: The reaction catalyzed by SnoaB with carbon atom labeling of the tetracyclic ring system of the anthracyclines also shown.

(Taken from paper II, figure 1)

The first mechanistic proposal for these enzymes contained a step where an enzyme/substrate radical intermediate was generated (Shen *et al.*, 1993 and Figure 18). The mechanism was proposed in the absence of any kinetic or structural data, and thus no catalytic amino acids involved in the reaction could be formally identified. Cysteine and histidine residues were identified as potential catalytic amino acids through inactivation experiments by chemical reagents such as p-chloromercuribenzoic acid or N-ethylmaleimide. Almost a decade later, the initial mechanism was questioned through findings obtained by studying AknX (Chung *et al.*, 2002). Analysis of the amino acid sequences of related proteins that were available at the time did not reveal any conserved histidine or cysteine residues. Furthermore, the cysteine or histidine mutants of AknX did not have a significant effect on the catalysis of quinone formation. From these results, the authors proposed that the reaction proceeds via a carbanion intermediate. Sciara *et al.* (2003) who published the first structure of the cofactor-independent monooxygenase ActVA-orf6 (with and without ligands) also adopted this reaction mechanism. Based on their structure, histidine residues present in ActVA-orf6 were regarded as being too far from the active site to be involved in catalysis. From the crystal structure of ActVA-orf6, five key residues were identified as potentially important for binding: Tyr51, Asn62, Trp66, Tyr72, and Arg86 (Figure 20). However, from these only Asn62 and Trp66 appeared to be highly conserved in the enzyme family, while the other residues were more specific to ActVA-orf6 (Figure 20). Based on the structure, the authors concluded that solvent accessibility and the hydrophobic character of the active site cavity were important requirements in substrate binding.

Figure 20: Structure-based amino acid sequence alignment of SnoaB with monooxygenases from the same fold family. The amino acids highlighted in yellow are the key amino acids proposed by Sciara *et al.*

(Taken from paper II, figure 4)

4.2.1. Results from the SnoaB Studies

Despite the low sequence identity between SnoaB and ActVA-orf6 (16 %), many similarities can be observed in both structures including a ferredoxin-like fold, and homodimers formed through an interface of antiparallel β-sheets consisting of hydrophobic interactions, hydrogen bonds, and salt bridges (paper II, Figure3). However, even though the crystal structures and the overall fold of ActVA-orf6 and SnoaB were similar, the identification of residues involved in catalysis was not obvious. Tyr51 Tyr72, and Arg86, identified in ActVA-orf6, were absent from SnoaB.

We were able to confirm SnoaB as a true cofactor-independent enzyme by the addition of metal chelating reagents such as EDTA, which had little effect on the activity of the protein (paper II, Table 4). Additionally, no cofactors typically used by monooxygenases (e.g. flavin) were required for catalysis by the enzyme. Furthermore, no density could be observed in our data for either metal ions or cofactors in the structure. These experiments confirmed that SnoaB was indeed a cofactor-independent monooxygenase.

SnoaB was also observed as having broad substrate specificity, similar to what has been reported with AknX, where quinone formation was observed with various substrates (paper II, Table 2). Furthermore, the monooxygenase function of SnoaB was demonstrated *in vitro* through oxygen 18 isotope experiments, providing evidence that the oxygen atom incorporated into the product was derived from molecular oxygen.

4.2.2. Investigations into the Mechanism of SnoaB

As stated earlier, two mechanisms for cofactor-independent monooxygenases were proposed, based on either a radical or a carbanion intermediate. Due to the small size of the active site and the existence of only few conserved residues between the various members of the enzyme family, not many potential amino acids were available (Figure 21).

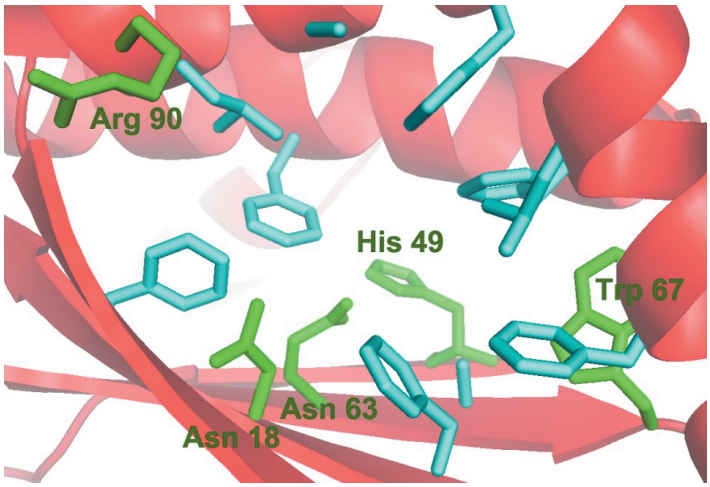

Figure 21: Active site cavity of SnoaB with potential amino acids that may interact with the substrate. The amino acids colored in cyan are hydrophobic (Phe, Leu or Ala) while the only plausible amino acids catalytic residues are colored in green.

Asn18, Asn 63, His 49, Trp 67 and Arg 90 mutant enzymes of SnoaB were generated and their kinetic parameters analyzed along with wild type SnoaB. The results illustrated in Table 1 below (see also table 2, paper II)

Table1: Kinetic parameters of Wild-type SnoaB and Mutant SnoaB

SnoaB variants	V_{max} (µmol min^{-1} mg^{-1})	Relative V_{max} (%)	k_{cat} (s^{-1})	K_M (µM)	k_{cat} / K_M ($M^{-1}s^{-1}$)
SnoaB-N	6.3 +/- 1.1	100	1.5	140 +/- 33	1.5×10^4
Asn 18Ala	0.1 +/- 0.01	1.6	0.03	120 +/- 17	2.2×10^2
His49Ala	1.3 +/- 0.002	20.6	0.3	150 +/- 21	2.2×10^2
Asn63Ala	0.07 +/- 0.004	1.1	0.02	68 +/- 11	2.3×10^2
Trp67Phe	0.06 +/- 0.008	1.0	0.02	220 +/- 45	68
Arg90Gln	1.2 +/- 0.060	19.0	0.3	113 +/- 12	2.5×10^3

Radical based catalytic mechanisms in enzymes rely on tyrosine, tryptophan, cysteine or glycine (Westerlund et al., 2005). Of these amino acids, only Trp67 could potentially form a radical intermediate. Although such intermediates have been observed in many biological reactions, they have typically only been detected in the presence of metals such as iron or manganese (Bleifuss *et al.*, 2001; Pogni, 2005; Bernini *et al.*, 2012). Furthermore, for a radical reaction to occur, a hydrogen atom transfer from the substrate to Trp67 should be required. This would lead to a neutral radical pair resulting in a reduction of Trp67. If the mechanism was based on the formation of a tryptophan radical intermediate, it would be crucial for catalysis. The enzymatic activity was not completely abolished in the Trp67Phe mutant (1 % relative V_{max} compared to wildtype SnoaB; see Table 1). Furthermore, from docking studies of 12-deoxynogalonic acid with SnoaB (figure 5, paper II), and given that no radicals could be detected by EPR, this data suggests that a reaction mechanism based on an enzyme Trp radical / substrate radical is unlikely for SnoaB.

The second mechanism, originally proposed for AknX and ActVA-orf6, involves a carbanion-based intermediate. Yet again, not many conserved residues were identified that could be responsible for the stabilization of the carbanion intermediate. Based on the structure and the architecture of the substrate binding pocket, the most likely residues involved in catalysis were identified as Asn18, Asn63, His49, Trp67 and Arg90. Both Asn18 and Asn63 mutants were found to have an important effect on catalysis (1.6 % and 1.1 % respectively relative to V_{max} compared to wildtype SnoaB; table 1), whereas the effect of His49 and Arg90 appeared to be negligible (both Arg 90Gln and His49Ala mutant had about 20 % relative V_{max} compared to wildtype SnoaB; table 1). Upon further investigation of the SnoaB structure, a water molecule was observed bound between Asn18 and Asn63. Since this triad coordinates the C-12 carbon atom, the water molecule could provide the catalytic base required for the substrate deprotonation of 12-deoxynogalonic acid and the generation of a carbanion. The intermediate formed may be internally stabilized by the ligand itself through charge distribution via the polyaromatic ring system and intramolecular hydrogen bonds. This premise is supported by the observation of considerable differences in reaction rates when alternative substrates were utilized. For instance, with 1-hydroxyanthrone, the rate of catalysis was almost 100-fold lower, and the relative V_{max} was even more affected when anthrone was used as a substrate (Table 2, paper II).

Chemically, the formed carbanion can react with O_2 in a one electron transfer step, which results in a superoxide radical anion evoking the chemistry observed in flavin-dependent monooxygenases. Further protonation, possibly by the same catalytic triad, would eventually lead to the formation of the product and a water molecule. The proposed mechanism utilized by SnoaB is illustrated in paper II in Figure 7.

Even though both ActVA-orf6 and SnoaB rely on substrate activation for catalysis and require no additional external electron sources for activity, the mechanisms of the two enzymes differ

significantly. The mechanism described for ActVA-orf6 involves five key residues, which are distinct from the catalytic triad of Asn18, Asn63 and a coordinated water molecule that were observed to be important for the activity of SnoaB. Since the key residues involved in the reaction of ActVA-orf6 are also absent from many of the other family members, the mechanism of SnoaB might better reflect the mechanism of other cofactor-independent monooxygenases involved in polyketide biosynthesis.

From the experimental data obtained from SnoaB, it seems more likely that this enzyme family relies on the substrate activation of oxygen rather than the generation of a tryptophan-radical intermediate. Recently, work on unrelated cofactor-independent dioxygenases HOD and urate oxidase (UOX) has provided evidence for the existence of a caged radical intermediate during the catalytic cycle, which supports our hypothesis (Figure 18, 3B). From experiments with the dioxygenase HOD and the radical scavenging agent CMH (1-hydroxy-3-methoxycarbonyl-2,2,5,5-tetramethylpyrrolidine), Thierbach *et al.* were able to corroborate the substrate-assisted dioxygen activation mechanism (Figure 18). CMH reacts readily with a superoxide anion peroxide ($O_2\bullet^-$), resulting in a peroxide (O_2^{2-}) / reduced substrate species and a stable nitroxide radical (CM•). The CM• radical could be detected in electron paramagnetic resonance spectroscopy (EPR) with the HOD mutant Trp160Ala. The lower K_m of this enzyme, which enabled the release of the CM• species from the active site, appeared to make the detection of CM• possible. These studies with HOD provided, for the first time, direct experimental evidence for a mechanism relying on a single electron transfer from the substrate to dioxygen, or the substrate assisted mechanism.

In the case of UOX, structures containing a peroxide intermediate have been crystallographically observed and confirmed through quantum mechanical calculations (Biu, 2014). Furthermore, when using low X-ray doses, the carbon peroxide bond could be specifically cleaved, leading to the formation of a uric acid radical that could be detected (Biu, 2014). Since no direct reaction with a uric acid radical and an oxygen residing in the ground state has been observed (Simic, 1989), the presence of uric acid radicals indicates the existence of a carbon peroxide. Thus, since uric acid radicals were detected, the most likely mechanism for UOX involves a single electron transfer to dioxygen, leading to a superoxide radical (Biu, 2014). A substrate radical recombination with superoxide, like in the formation of a caged radical pair in flavin-dependent oxygenases, would lead to the formation of a peroxide intermediate. In light of these two recent papers that provide evidence for a one electron transfer to oxygen, we conclude that a substrate-assisted mechanism seems more likely for SnoaB than a mechanism based on an enzyme-radical intermediate.

4.3. Two-Component Flavin-Dependent Monooxygenases (paper III)

Alnumycin A is another aromatic polyketide that has numerous biological activities, including notable antibiotic properties (Biber, 1998; Björn, 1998, Oja *et al.* 2015). The sequencing of the alnumycin gene cluster from *Streptomyces sp. CM020* led to the identification of two genes, *alnH* and *alnT*. They were recognized as a putative two-component system involved in quinone formation in alnumycin biosynthesis (Oja *et al.*, 2008) by sequence comparison to proteins with established function. AlnH, a protein consisting of 180 amino acids, was identified as a member of the FlaRed enzyme superfamily containing plausible sequences associated with a NADH-dependent flavin reductase domain. The 413 amino acid AlnT sequence was identified as an FMN reductase dependent oxygenase (FMO). To date, similar two component systems have been observed to function on pathways leading to the formation of the benzoisochromanequinone

antibiotics (BIQ) granaticin (Ichinose, 1998), medermycin (Ichinose, 2003), and actinorhodin (Figure 1, paper III). Of these, the ActVA /ActVB system involved in the biosynthesis of actinorhodin from *Streptomyces coelicolor* A3 (2) is the best studied (Valton, 2006; Valton, 2008; Okamoto, 2009; Taguchi, 2012) and has high sequence similarity to AlnT/AlnH: 63 % and 65 %, respectively. The aim of the work described below was to uncover the molecular basis for the generation of the unusual *p*-quinone arrangement found in alnumycin A, which is distinct from the structurally related BIQs. Our work, which consisted of *in vivo* knockout studies and analysis of enzymatic reactions *in vitro*, confirmed that this unique reaction was due to the AlnT/AlnH system.

4.3.1. Discovery of the Functions of AlnT and AlnH

In a two-step homologous recombination process (Datsenko *et al.*, 2000), *alnH* or *alnT* were deleted from the cosmid containing the complete alnumycin biosynthetic cluster (Oja *et al.*, 2008). The resulting strains were cultured, and the produced metabolites were analyzed by HPLC-UV/vis. Both strains had almost identical production profiles with three metabolites not seen in the control cultivation (Figures 2A and 2B, paper III). The first compound, K1115A (Figure 1, paper III), was previously identified as a shunt metabolite from the inactivation of the aldo-ketoreductase *aln4* (Oja, 2008). In order to identify the two remaining compounds, the metabolites were purified and their structures determined by high resolution MS measurements and NMR spectroscopy (Table 1, paper III). Subsequently, one of these was identified as a previously known compound 1,6-dihydroxy-8-propylanthraquinone (DHPA), whereas the other was a novel metabolite that was denoted as thalnumycin A (Figure 1, paper III). The lack of a quinone ring in thalnumycin A corroborated the supposition that the AlnT/AlnH system might be responsible for the formation of the *p*-quinone unit of alnumycin A. Another important observation was that none of the metabolites isolated from the *in vivo* cultures contained correctly cyclized pyran rings, which signified that quinone formation could occur at an early stage in the biosynthesis prior to pyran ring formation.

AlnH and AlnT were both produced as N-terminally histidine-tagged recombinant proteins in *E. coli*. To verify the function of AlnH as a NADH-dependent flavin reductase, the enzyme was incubated together with FMN and an excess of NADH. As expected, conversion of NADH to NAD+ could be observed spectrophotometrically at 340 nm. The enzyme could also reduce FAD and utilize NADPH as a cosubstrate, but based on reaction kinetics, FMN and NADH appeared to be the preferred substrates (Table 2, paper III). A similar preference has been observed for the related flavin reductase ActVB (Filisetti, 2005). The experiments aiming to demonstrate the regiochemistry and specificity of AlnT were complicated by the instability of the putative natural substrate, and henceforth several compounds were screened as alternative substrates. The enzyme appeared to have a relatively strict substrate specificity, since compounds such as dithranol (a substrate for SnoaB) and 1,8-dihydroxynaphthalene were not accepted as substrates, but thalnumycin A was converted to a new reaction product thalnumycin B (Figure 3B, paper III). The structure elucidation of the compound by NMR confirmed the existence of a *p*-hydroquinone structure in thalnumycin B (Figure 1, paper III) and verified the function of AlnT.

A recent comparative study of two-component monooxygenase systems from the medermycin (Med-7), granaticin (Gra-21), actinorhodin (ActVA), and alnumycin (AlnT) pathways revealed further details regarding the substrate specificity of these enzymes (Taguchi, 2013). Both ActVA-orf5 and Gra-orf21 were found to be bifunctional enzymes functioning after pyran ring formation that were responsible for oxidation reactions at both the central and lateral rings of BIQs, whereas Med-7 exclusively catalyzed the hydroxylation of the central ring. The study reinforced

our hypothesis that the timing of *p*-quinone formation in alnumycin biosynthesis is atypical, since AlnT could not convert any of the intermediates from the other related pathways, and it would appear that the natural substrate of AlnT is an earlier bicyclic intermediate (A, Figure 4 paper III).

4.3.2. Mechanism of the Two-Component Monooxygenases

The generally accepted mechanism of FMOs requires two distinct reactions that facilitate the reaction of oxygen with the substrate. In the reductive half-reaction, flavin is reduced in a step that enables the activation of dioxygen, and this is utilized in the oxidative half-reaction where hydroxylation of the substrate is achieved. With single component flavoprotein hydroxylases, this typically requires that the polypeptide adopts two different conformations: one for the reduction of the flavin and the other for the oxygen-dependent reaction. Conversely, the same process is also divided into two in the two-component systems. The NADH flavin reductase catalyzes the reduction of flavin, while the FMO catalyzes the oxygen-dependent reaction. Because of the instability and auto-oxidation of reduced flavin, which would lead to the formation of harmful reactive oxygen species such as superoxide or hydrogen peroxide, the process needs to be efficiently coupled. Indeed, investigations into the two-component system ActVA/ActVB (Valton *et al.*, 2004 and 2006) could not detect significant auto-oxidation of flavin, despite the fact that the enzymes do not appear to form stable complexes in solution.

Several important features of the two-component system were observed in a detailed kinetic study of ActVA and ActVB (Valton *et al.*, 2008), which confirmed that the reaction order is similar to single-component flavoproteins. After the reduction of FMN (FMN_{red}) by ActVB, FMN_{red} gets released and is efficiently transferred to ActVA. Once bound to ActVA, the FMN_{red} reacts with O_2 to form a C(4a)-FMN-OOH intermediate; this reaction is independent of the presence of the substrate (DHK_{red}). However, if the substrate is present, the flavin hydroperoxide is converted to C(4a)-FMNOH and the hydroxylated product DHK_{red}-OH. Finally, dehydration of the flavin results in oxidized FMN and the completion of the reaction cycle. The mechanism of AlnT/AlnH is likely to follow a similar path to the one described above for the ActVA/ ActVB system, even though the regiospecificity and timing of the reaction catalyzed by AlnT differs from the other described FMOs.

One key step in the reaction cycle is the ability of the enzymes to form and stabilize C4a-hydroperoxyflavins. Although structural information on how this is specifically achieved in AlnT is lacking, a multiple sequence alignment with selected sequences (including p-Hydroxyphenylacetate hydroxylase (C_2) (Alfieri, 2007) that is most similar of the enzymes) can provide some insight into the amino acids involved in the catalytic mechanism. In C_2, a solvent-free cavity is created through the precise fitting of both hydrophobic and hydrophilic amino acid side chains with $FMNH^-$ (highlighted in green in Figure 22) and the aromatic substrate *p*-hydroxyphenylacetate (blue stars in Figure 22). The local environment created within this cavity stabilizes, through solvent exclusion, the C4a intermediate and enables a precise orientation of bound *p*-hydroxyphenylacetate with FMN_{red} favoring hydroxyl transfer. Some of these amino acids are in proximity to both FMNH- and *p*-hydroxyphenylacetate and are the key amino acids relevant to the hydroxylation reaction (illustrated in Figure 22 with a circled star).

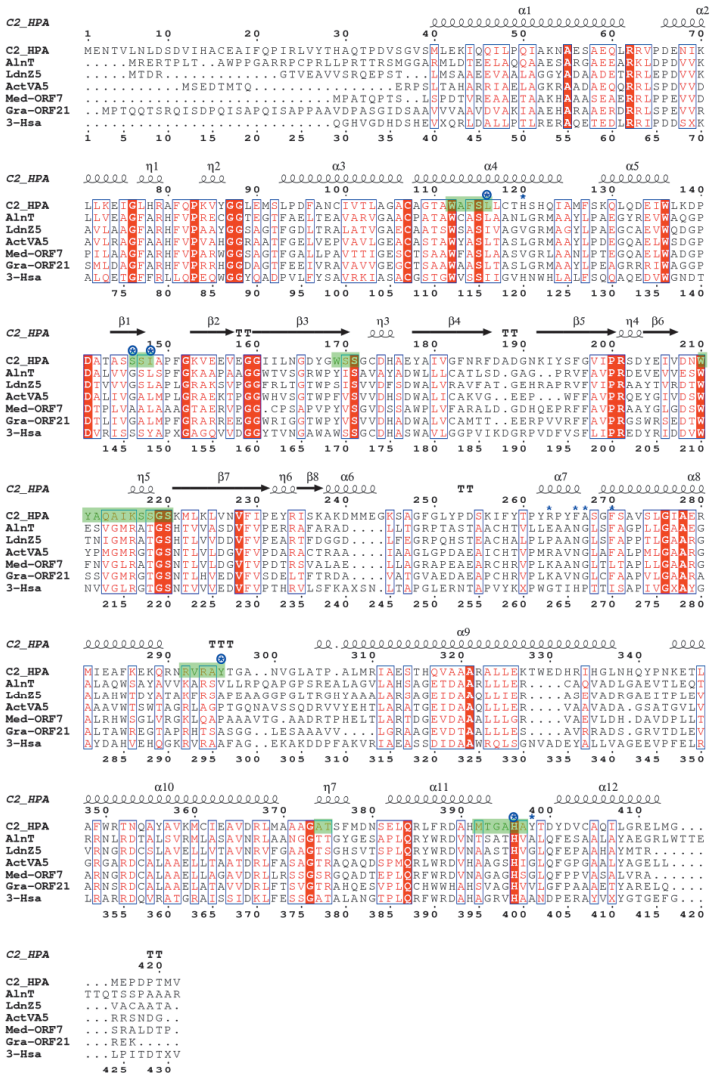

Figure 22: Multiple sequence alignment of the AlnT hydroxylase from *Streptomyces sp. CM020* with selected homologous proteins. Two of the closest structures to AlnT, 3-Has (PDB: 2RFQ) and C_2 HPA (PDB: 2JBT) are provided. Only C_2 HPA contained a bound substrate and cofactor. Other sequences include: LndZ5, *Streptomyces globisporus* (GenBank: AAR16420); actVA5, *Streptomyces coelicolor* A3 (2) (GenBank: CAA41641); Med-ORF7, *Streptomyces sp. AM-7161* (GenBank: BAC79043) and Gra-ORF21, *Streptomyces violaceoruber* (GenBank: CAA09642). The secondary structure of C 2 HPA is determined from the structure and illustrated with turns, α- helices and β- sheets. In many flavoenzymes, the flavin is held in its position through hydrophobic interactions and hydrogen bond networks. Of the highly conserved amino acids (highlighted in red), many are associated with flavin binding (highlighted in green), notably S171, which is involved in hydrogen bonding, and H396, which is thought to play a role in catalysis as a proton donor. Amino acids involved in *p*-hydroxyphenylacetate binding (blue stars) are not as conserved, reflecting differences in the substrates. Some amino acids involved in binding both $FMNH^-$ and the substrate (circled blue star), are conserved in C_2 and AlnT, reflecting the shared ancestry of the enzymes.

Many of the hydrophobic amino acids that bind FMN_{red} are conserved in both C_2 and AlnT. These include several stretches of hydrophobic amino acids (Figure 22) as well as Ser171 (Ser164 in

AlnT), which is a key amino acids that binds FMN_{red} through two hydrogen bonds. Furthermore, mechanistic similarities based on the stabilization of the C4a-FMN-OOH intermediate and solvent exclusion for flavoenzymes of this folding topology (Alfieri, 2007) are reflected in the conservation of His396 (His381 in AlnT), which is likely to be in proximity to the reduced flavin and substrate of AlnT. Differences related to substrate binding are more striking. The substrate of C_2 is considerably smaller than that of AlnT, and because the substrate binding pocket of AlnT is likely to be larger, many of the amino acids involved in binding *p*-hydroxyphenylacetate are not relevant in AlnT. Although some of these amino acids are conserved, it is difficult to pinpoint the amino acids involved in determining the regiospecificity of the oxygenation reaction without the crystal structure of the enzyme.

4.4. Atypical SAM Dependent Monooxygenase (paper IV)

4.4.1. S-Adenosyl-L-Methionine (SAM) as a Cosubstrate

S-adenosyl-L-methionine (SAM) (Figure 23, A) is a cosubstrate that is used in many enzymatic reactions, and it is principally utilized as a universal methyl group donor. Methyl transfer reactions based on SAM are widely present in many metabolic pathways, including the interconversion of cysteine and homocysteine, sulphur-metabolism, gene expression and regulation, protein modification, lipid modifications, and secondary metabolism (Wang & Breaker, 2008, Price *et al.*, 2014; Moussaieff *et al.*, 2014; Mandaviya *et al.*, 2014).

The utility of SAM resides in the presence of a reactive methyl group that is readily transferred to the substrate, while the cosubstrate is simultaneously converted to S-adenosyl-L-homocysteine (SAH) in the process (Figure 23, B). These enzymes are typically categorized based on the recipients of the methyl groups, and consequently O-, N- and C-methyltransferases have been observed. Enzymes that utilize SAM have also been observed to catalyze methyl transfer reactions on halide ions, thiols as well as double bonded fatty acids (Roje, 2006).

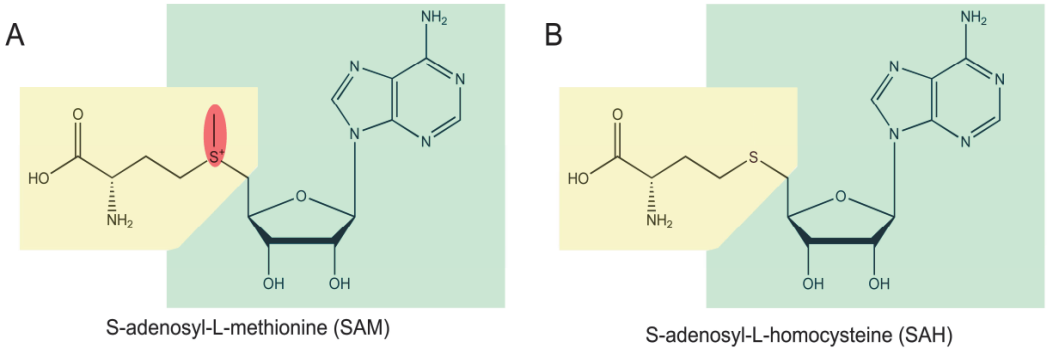

Figure 23: The chemical structure of S-adenosyl-L-methionine (SAM) in A and S-adenosyl-L-homocysteine (SAH) in B. The positively charged sulphur, in red, is prone to lose the methyl group to nucleophiles. The methionine is highlighted in yellow and the nucleotide in green.

Various enzyme-catalyzed methyl transfer reactions have been observed. The three major families of methyltransferases include *O*-, *N*- and *C*-methyltransferases are named according to the reactions they perform. Enzyme-catalyzed methyl transfer reactions with SAM have also been observed on halide ions, thiols as well as double bonded fatty acids (Roje, 2006).

Interestingly, the role of SAM is not limited to the transfer of methyl groups, and the cosubstrate has received particular attention in the context of radical SAM enzymes. First classified as a superfamily in 2001, this family is readily identified from a conserved CX3CX2C motif, and it currently comprises of more than 48000 members (Broderick *et al.*, 2014). Most radical SAM enzymes initiate a set of radical reactions with the help of a [4Fe − 4S] cluster and SAM to generate a 5 ′ -deoxyadenosyl radical (dAdo •) intermediate, which is used to catalyze various oxidative transformations.

4.4.2. Comparison of Methyltransferase Homologs Involved in Aromatic Polyketide Biosynthesis

Genes encoding methyltransferases appear to be widely spread on the biosynthetic pathways of anthracycline anticancer agents. Based on sequence alignment, DnrK from the daunorubicin pathway in *S. peucetius* and RdmB from the rhodomycin pathway in S. purpurascens are classified as SAM-dependent methyltransferases (Figure 1, paper IV). They both possess a glycine rich fingerprint, E/DXGXGXG, responsible for shaping the SAM binding cavity (Figure 24), but neither possess the CX3CX2C motif typical to radical SAM enzymes. Indeed, DnrK is a true O-methyltransferase, which catalyzes the methylation of position C4 of anthracyclines (Jansson *et al.*, 2004). It has also been noted to possess surprisingly relaxed substrate specificity and to even be able to methylate various flavonoids (Kim *et al.*, 2007). The crystal structure of DnrK in complex with SAM and the substrate 4-methoxy-ϵ-rhodomycin T revealed that the enzyme is likely to function via an S_N2-type reaction mechanism, where the electrophilic SAM reacts with a nucleophilic substrate (Jansson *et al.*, 2004). In general, the mechanism is typical for methyl transferases, although DnrK appears to rely strongly on proximity and orientation effects in catalysis (Figure 1, paper IV).

The high sequence identity between RdmB and DnrK (52 %) is also reflected in the structures of the enzymes, which have a root-mean square deviation of 1.14 Å for 335 equivalent Cα atoms. However, the possible functions of RdmB are put to question immediately upon the discovery of the rhodomycin gene cluster (Wang *et al.*, 2000), since these anthracycline polyketides do not contain 4-O-methyl groups. The role of RdmB as a hydroxylase was subsequently confirmed *in vitro* when it was demonstrated that the enzyme could hydroxylate 15-demethoxyaclacinomycin T at position C-10 (Figure 1, paper IV). This reaction required SAM, molecular oxygen and a reducing agent (DTT/GSH) for activity. Since this initial observation, other differences in RdmB and DnrK have been observed, including the use of monoglycosylated and triglycosylated anthracyclines substrates. Where RdmB is able to use both, DnrK can only methylate monoglycosylated substrates.

Furthermore, DnrK and RdmB differ in the timing of the biosynthetic step they catalyze. RdmB only works strictly in conjunction with RdmC, which is a methylesterase involved in removing the C15 methyl group of anthracyclines, since RdmB requires a compound with a free carboxy group at C15 as a substrate. The reaction order of DnrK and DnrP (the methylesterase homologous to RdmC) in the daunomycin pathway is more relaxed, and DnrK can methylate various substrates (Dickens *et al.*, 1997), which include both the substrate and product of DnrP. The RdmC and RdmB reactions are, therefore, more stringently controlled that the DnrK and DnrP reactions, since they require the RdmC reaction to occur prior to the one catalyzed by RdmB.

4.4.3. Engineering a Methyltransferase into a Hydroxylase

In order to understand how a methyltransferase has evolved to catalyze a hydroxylation reaction, we opted to generate chimeric enzymes, where distinct segments of DnrK and RdmB were

interchanged. The first generated chimera contained the dimerization domain of DnrK, which was fused with the catalytic domain of RdmB (Figure 24). The created enzyme variant (RdmB-CT) had similar activity to the native recombinant RdmB enzyme, when the activity was tested in conjunction with RdmC; the enzyme catalyzed the C-10 hydroxylation of an anthracycline substrate (Compound 11, paper IV). This initial experiment confirmed the boundaries of the catalytic domain and demonstrated that regions outside of the binding area of the cosubstrate SAM and the anthracycline substrate did not influence the hydroxylation reaction. Next, a detailed analysis of the crystal structures and the sequence alignment of RdmB and DnrK (Figure 24) were used to identify regions, denoted as R1, R2 and R3, that could potentially contribute to the notable differences between the two enzymes. R1, the first region identified, consisted of a loop region near the C-10 position of the substrate. Distinct differences could be observed in both structures related to the proximity of the loop near the substrate; the RdmB loop region was found to be closer to the substrate than the equivalent region in DnrK. Other perceptible differences included the R2 region, a loop region in the proximity to the substrate, which could affect the orientation and geometry of ligand binding. Finally R3, the third region, was associated with the binding of the carbohydrate unit of the substrate.

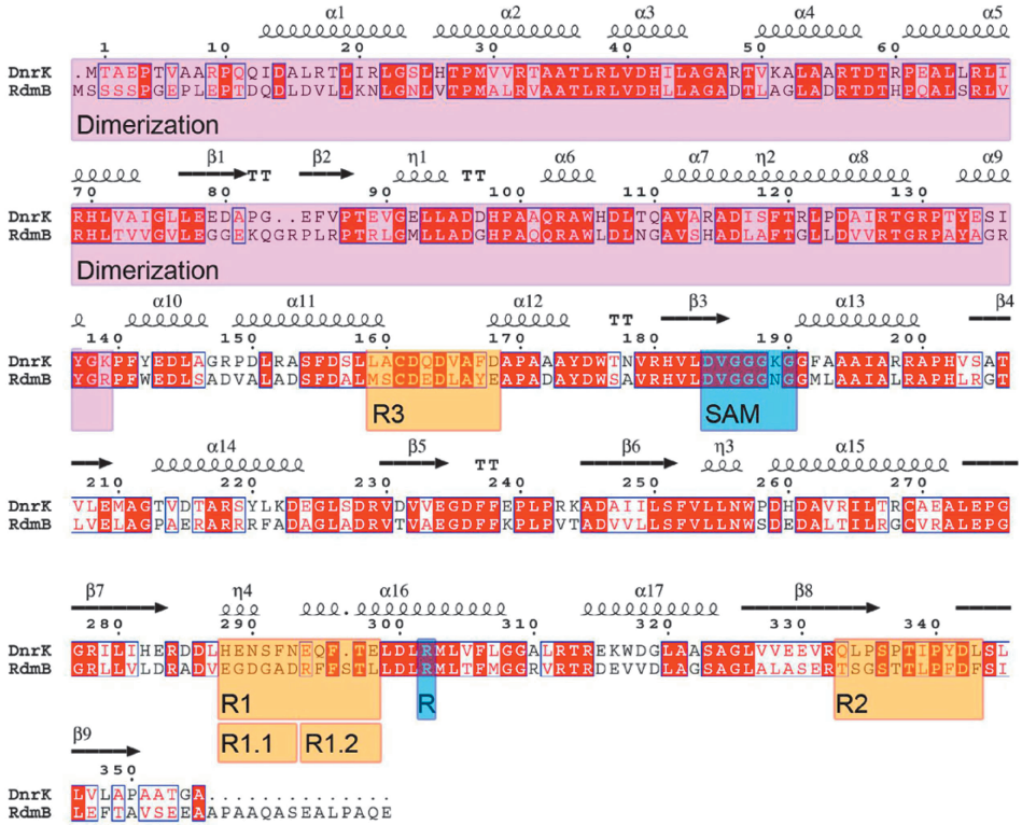

Figure 24: Structure –based alignment of DnrK and RdmB. Highlighted in blue is the characteristic E/DXGXGXG SAM binding cavity and residues involved in catalysis. Shown in pink is the dimerization domain. Highlighted in orange (R1, R2, R3, R1.1 and R1.2) are the regions selected for chimeragenesis. (Taken from paper IV, figure S1)

Of the three tested regions, R2 and R3 had no effect on switching the reaction specificity of DnrK (Figure 2D, paper IV), but they appeared to be important for substrate binding and, in part,

provided an explanation for the difference in substrate specificity in RdmB and DnrK. R1 chimeras, on the other hand, were consistently observed to produce a small amount of the RdmB reaction product (Compound 11; Figure 2, paper IV). Many of the R1 reactions also contained an additional compound not found in either the DnrK or RdmB reactions alone. This product, identified later as Compound 12 (Figure 2, paper IV), was also produced if both RdmB and DnrK were incubated together, which indicated that the compound resulted from both C-10 hydroxylation and C-4 O-methylation. Based on these results, it became clear that the R1 region was responsible for the shift in catalytic activity. To further pinpoint the residues involved in the change in activity, the R1 region was subdivided into two parts denoted as R1.1 and R1.2 (figure 24). Hydroxylated products could be observed solely from reactions conducted with the R1.2 mutant, whereas the R1.1 mutant appeared to behave similarly to native DnrK in the activity assays (Figure 2, paper IV). Upon examination of the sequence of the R1.2 region, an additional serine residue was found in RdmB, which was absent in DnrK. The insertion of this single amino acid was sufficient for the introduction of the 10-hydroxylase activity into the DnrK scaffold (Figure 2, paper IV).

Next, the structure of this serine mutant, DnrK-ser, was solved, which yielded important insight into the catalytic domain of the enzyme. Only slight differences could be observed in the overall structures of native DnrK and the DnrK-ser mutant with an r.m.s.d. of 0.90 Å over 327 residues. The main differences were observed in the R1 region due to the serine insertion. By introducing the serine, the secondary structure of α16 was not disrupted but resulted in a shift of all residues upstream of the serine. Due to this shift, the residue preceding the inserted serine, Phe296, was found to point towards the ligand near the site of monooxygenation at position C-10 of the ligand (Fig. 3, paper IV). Conversely, Gln295, which is found in the equivalent structural position in the native enzyme, had shifted away from the active site. An important consequence of this shift was that the bulky hydrophobic phenylalanine blocks the access of solvent molecules to the active site in a manner similar to what is found in RdmB, whereas in native DnrK a channel is open to the surface of the protein. Further structure/function studies indicated that the rise of the hydroxylation activity appears not to be due to the insertion of the serine residue itself but rather is caused by a shift of the phenylalanine residue towards the active site.

In addition to the findings mentioned above, two additional important observations were made during analysis of the coupled reactions with the chimeric enzymes and RdmC. Firstly, we noted that the RdmC reaction product (Compound 15 in paper IV) is unstable and will spontaneously decarboxylate if exposed to light but remains stable if kept in the dark. Secondly, we could unambiguously demonstrate that DnrK is able to catalyze this same decarboxylation reaction upon testing the activity of the enzymes in the dark (see Fig S3). In our view, the discovery of this moonlighting activity for DnrK has important implications for the proposed mechanism of C10 hydroxylation and provides an explanation for how the atypical monooxygenation activity has emerged during enzyme evolution.

4.4.4. The Divergence of RdmB and DnrK Reaction Mechanisms

Our proposed mechanism for DnrK/RdmB (illustrated in Figure 4, paper IV) dictates that it is likely that the initial step is decarboxylation at C10 and that it is catalyzed by both enzymes. If we stipulate that both enzymes catalyze decarboxylation at the C-10 position, then it is logical to assume that the mechanism for decarboxylation should be alike and be reflected in the structures of the proteins. Indeed, both enzymes contain a conserved arginine residue (R302 and R307 in DnrK and RdmB respectively), which we believe plays a role in this reaction. In agreement with this hypothesis, DnrK R1.2 R303Q and R1.2 R303K mutants both lost much of their activity. These

results may suggest that arginine plays a common role in the decarboxylation reactions, although in the absence of kinetic data it cannot be excluded that the residues have a critical role in substrate binding.

Our mechanistic model suggests that, after the decarboxylation step, access of solvent ions to the active site cavity determines if a hydroxylation reaction may occur. If solvent ions have free entry to the active site like in DnrK, hydroxylation is prohibited by facile protonation of the carbanion at C-10 by H_2O. On the other hand, this step is prevented in RdmB, where the solvent ions are blocked from the active site. We suggest that the carbanion intermediate is further stabilized by the nature of the substrate (polyphenolic ring system) and the positive charges (in this case provided by the SAM) in the active site, which enables the carbanion to react with O_2 in a one electron transfer step. The resulting superoxide radical anion intermediate is reminiscent of substrate assisted reactions with cofactorless monooxygenases and the mechanism of the reaction of flavin with dioxygen at the C4a position. Once formed, the 10- peroxyanthracycline is reduced, possibly outside the active-site cavity, by a reducing agent to form the final hydroxylated end-product of the reaction.

The consequence of our mechanistic proposal is that it implies that the hydroxylation at the C-10 position must occur prior to or in conjunction with the methyl transfer at the C-4 position. This might explain why the yields of the observed double reaction product (Compound 12, paper IV) and the methylated product (Compound 10, paper IV) are consistently higher than the hydroxylated product (Compound 11, paper IV) in reactions with the mutant enzymes. The exception to this would be the R1.2 S297F mutant, where the serine is replaced with a bulky phenylalanine. While this enzyme is able to perform both reactions, this replacement seems to favor hydroxylation, as the percentage of only hydroxylated product (Compound 11, paper IV) is higher than that of the double reaction product (Compound 12, paper IV), which may be caused by reduced methyl transfer activity due to changes in the orientation of the C4 oxygen atom of the ligand in respect to the cosubstrate SAM.

5. CONCLUDING REMARKS

The experimental work in this thesis focused on four enzymes and the mechanisms they likely employ for activating molecular oxygen. One of these enzymes included the cofactorless monooxygenase SnoaB, whose function was confirmed with the use of O_2^{18} isotopes. Sequence comparison provided few clues as to the mechanism employed by this enzyme. Using kinetic data and X-ray structures a reaction mechanism was proposed for SnoaB (A, Figure 25). Based on our data, the most likely mechanism employed by SnoaB relies on the deprotonation of the substrate by a catalytic triad composed of Asn 18, Asn 63, and a water molecule, resulting in a carbanion. The carbanion formed would, through a single electron transfer, reduce oxygen, resulting in a caged radical pair consistent with the substrate assisted mechanism. Since it is the substrate that "drives" the reaction, only transient stabilization of the carbanion is required for reaction with O_2. This may explain why large amino acid sequence variation is observed in this group of enzymes with only few key residues being conserved.

From the studies with the two-component system AlnT and AlnH, the functions of both the NADH-dependent flavin reductase, AlnH, and the reduced flavin dependent monooxygenase, AlnT were confirmed based on product analysis. The unusual regiochemistry proposed for AlnT was confirmed based identification of the reaction products. The mechanism of AlnT, as with other flavin-dependent monooxygenases, is likely to involve a caged radical pair consisting of a superoxide anion and a neutral flavin radical formed from a carbanion intermediate (B, Figure 25). Subsequently, the formed neutral flavin-hydroperoxide leads to the hydroxylation of the substrate. Insufficient data are currently available to determine which amino acids are required for the unusual regiospecifity of AlnT. Further work, including a crystal structure and mutational studies, is needed to pinpoint these amino acids.

With the studies concerning RdmB, DnrK and DnrK variants, our data suggest that an initial decarboxylation of the substrate is catalyzed by all these enzymes, forming a carbanion intermediate. A single electron transfer to O_2 from the formed carbanion would result in a caged radical pair consistent with the substrate assisted mechanism (C, Figure 25). Furthermore, the insertion of a single amino acid in DnrK (S297) was sufficient for gaining a hydroxylation function. This insertion leads to restriction in solvent accessibility of the active site, hence stabilization the carbanion intermediate. Like with SnoaB, the mechanism for hydroxylation in RdmB/DnrK variants is likely to be a substrate-assisted mechanism facilitated by the positive cofactor SAM.

Despite the many mechanisms for dioxygen activation by oxygenases explored in this thesis, with the enzymes in my studies, the activation of oxygen relies on carbanion intermediates found in flavins or substrates (circled in red, Figure 25). The activation of triplet oxygen is achieved through a single electron transfer to one of the oxygen atoms (a monovalent reduction), leading to a caged radical pair. Although this mechanism is not utilized in metal-dependent oxygenases mentioned here, it is more common in reactions involving flavins and cofactorless oxygenases. This type of mechanism seems to be more prevalent in aromatic polyketide biosynthesis and may reflect the propensity of these compounds to form a stable anion through hydrogen bonding and delocalized π-electrons.

Furthermore, another conclusion that can be drawn from these studies is that function prediction, based on sequence identity or structure alone, can be misleading. Biochemical characterizations of enzymes are required for correct function determination. With DnrK and RdmB despite having 52 % sequence identity and almost identical structures, both enzymes catalyze two different reactions. The insertion of a single serine residue is sufficient for the

introduction of the monooxygenation activity into DnrK. Without biochemical characterization, prediction of this result would be impossible based on sequence or structure analysis alone.

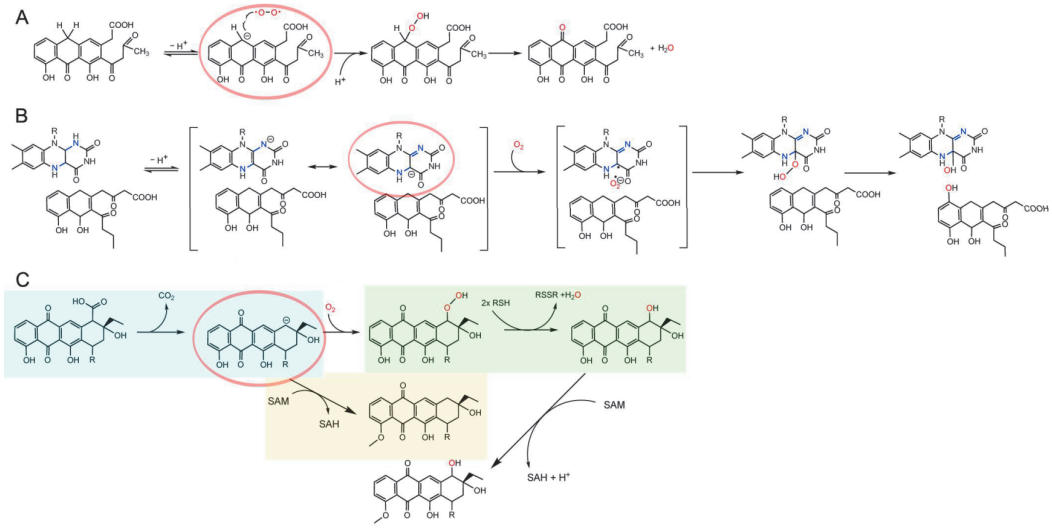

Figure 25: Model for the monooxygenation reactions for SnoaB (A), AlnT (B) and RdmB or DnrK variants (C). The activation of oxygen for all these enzymes relies on carbanion intermediates (circled in red). A hydroperoxide is then produced and subsequently reduced to a hydroxylated product and water. Both the oxygen in the hydroxylated product and in the water molecule are derived from molecular oxygen (in red). For SnoaB (A), only the substrate and O_2 are required for hydroxylation to occur. For AlnT (B), the activation of oxygen involves the presence of a flavin to form a caged radical pair and, upon reduction, hydroxylation. For the hydroxylation reactions with RdmB/DnrK variants (C), decarboxylation must first occur (in Blue). Depending on solvent access, either methylation (in yellow), as with the DnrK reaction, or hydroxylation occurs (in green) in reducing conditions with RdmB or certain DnrK variants. Subsequent methylation can then occur with certain DnrK variants, leading to a "double" reaction product.

Additionally, parallels between the investigated oxygenases can be made. This includes the importance of the environment around the substrate and of water, which are the key factors in oxygenation reactions. For example in CYP, the iron in the heme prosthetic group is coordinated by a cysteine axial ligand. Although it does not participate in the reaction directly, if the axial ligand is coordinated by another amino acid, such as histidine, the enzyme's ability to hydroxylate the substrate is compromised. Likewise, subtle differences in residues surrounding the substrate-binding pocket greatly affect the ability of oxygenases to perform their reactions such as the monooxygenase ability of Ty vs the oxidase ability of Co. This is also echoed in the experimental work involving RdmB/DnrK variants or the AlnT reactions where, through steric hindrance, active site accessibility to solvents is restricted, which is likely to result in transient carbanion stabilization and oxygen activation.

Finally, it is noteworthy that water and solvent access also play an important role in oxygenase reactions. Water is a key ligand in many of the metal-dependent oxygenases such as CYP, αKG oxygenase or MMOH and part of the proposed catalytic triad in SnoaB.

Hopefully, the mechanisms suggested here can provide further insight into the oxygen activation of tailoring enzymes in the biosynthesis of polyketides and aid future research concerning oxygenases.

6. ACKNOWLEDGEMENTS

The studies for this thesis were carried out during 2005-2015 at the Department of Biochemistry, University of Turku, Finland within the Antibiotic Biosynthetic Enzyme research group. I would first like to thank my supervisors PhD Jarmo Niemi, Professor Emeritus Pekka Mäntsälä, and PhD Mikko Metsä-Ketelä for giving me the opportunity to work and learn in your lab for which I will always be grateful. You gave me the chance to choose interesting and challenging projects as well as nurture my curiosity. I would like to thank Jarmo Niemi in particular for being present throughout my studies and for being a continual part of this thesis. I would especially like to thank Mikko Metsä-Ketelä, who was instrumental in the latter half of my studies, for steering me towards the completion of this thesis.

Furthermore, I wish to thank Professor Jyrki Heino and Professor Reijo Lahti for providing the excellent research facilities to do research as well as for advice and encouragement. I would also like to thank the administrative staff, particularly Satu Jasu. In addition, big thanks to the technical staff, especially Jani Sointusalo for your friendship, help and support. Also thank you to Anssi Malinen, my work “psychiatrist” and friend. In addition, thank you Georgiy Belogurov for giving me the opportunity to work in your lab with Matti Turtola when funding was difficult. Moreover, I would also like to thank all the colleagues at our department that have helped me during my time here.

Professor Mark Johnson and The National Doctoral Program in Informational and Structural Biology (ISB) are also acknowledged for providing support for this thesis project. In addition, I would like to thank, on behalf of our research group, The Academy of Finland for long-term financing of our research. I would also like to thank the UTUGS graduate school for their financial contribution towards finalizing my PhD.

I especially want to thank our collaborators Professor Gunther Schneider and former member Hanna Koskiniemi from Karolinska Institutet, Stockholm. I am grateful to Professor Gunther Schneider who was always kind, friendly and consistently provided insightful knowledge to any discussion. Also, thank you to Hanna Koskiniemi for your work and your encouragement regarding the SnoaB project!

I would also like to thank all current and former lab members of the ABE group. Terhi, I am grateful to have had the opportunity to work with you and thank you for your friendship. Pedro and Laila thank you as well for all your contributions. Thank you, Pauli, for showing me the ropes. Also thanks goes to Pekka, Vilja and Kaisa for being part of our lab. Thank you as well to Bastian and all other former lab members listed here who have contributed to the ABE group.

Finally, I want to thank my friends and family for their support and understanding. A big thank you to my parents and my sister who have always been supportive of whatever I have undertaken. Thank you as well to Marjo, Hannu and Riina for making me feel at home here and Finland and helping so much with the day to day and with Remy and Alexander. I would also like to thank you Remy and Alexander for being who you are and leading me into this wonderful journey of fatherhood. Finally, I would like to thank my wife Tiina who is in a category of her own. You are my rock. Without your love, support and understanding I would not be here today. Thank you!

REFERENCES

Abell, L. M., & Schloss, J. V. (1991). Oxygenase side reactions of acetolactate synthase and other carbanion-forming enzymes. *Biochemistry*, *30*(32), 7883–7887.

Adams, M. A., & Jia, Z. (2005). Structural and biochemical evidence for an enzymatic quinone redox cycle in Escherichia coli: Identification of a novel quinol monooxygenase. *J. Biol. Chem.*, *280*(9), 8358–8363.

Aitken, J. B., Thomas, S. E., Stocker, R., Thomas, S. R., Takikawa, O., Armstrong, R. S., & Lay, P. A. (2004). Determination of the Nature of the Heme Environment in Nitrosyl Indoleamine 2,3-Dioxygenase Using Multiple-Scattering Analyses of X-ray Absorption Fine Structure. *Biochemistry*, *43*(17), 4892–4898.

Alexeev, I., Sultana, A., Mäntsälä, P., Niemi, J., & Schneider, G. (2007). Aclacinomycin oxidoreductase (AknOx) from the biosynthetic pathway of the antibiotic aclacinomycin is an unusual flavoenzyme with a dual active site. *Proc. Natl. Acad. Sci. U.S.A*, *104*(15), 6170-6175.

Alfieri, A., Fersini, F., Ruangchan, N., Prongjit, M., Chaiyen, P., & Mattevi, A. (2007). Structure of the monooxygenase component of a two-component flavoprotein monooxygenase. *Proc. Natl. Acad. Sci. U.S.A*, *104*(4), 1177–1182.

Andersen, O.A., Stokka, A.J., Flatmark, T., & Hough E.(2003) 2.0A resolution crystal structures of the ternary complexes of human phenylalanine hydroxylase catalytic domain with tetrahydrobiopterin and 3-(2-thienyl)-L-alanine or L-norleucine: substrate specificity and molecular motions related to substrate binding. *J. Mo.l Biol., 333*(4),747-57.

Ausubel, F.M., Brent, R., Kinston, R.E., Moore, D.D., Seidman, J.G., Smith, J.A.& Struhl, K. (1994). C*urrent protocols in molecular biology*. John Wiley & Sons Inc./USA

Baas, B.-J., Poddar, H., Geertsema, E. M., Rozeboom, H. J., de Vries, M. P., Permentier, H. P.,Thunnissen, A-M.W.H. & Poelarends, G. J. (2015). Functional and Structural Characterization of an Unusual Cofactor-Independent Oxygenase. Biochemistry, 54(5), 1219–1232.Bacher, A., Eberhardt, S., Fischer, M., Kis, K., & Richter, G. (2000). Biosynthesis of vitamin B2 (Riboflavin). *Annu. Rev. Nutr.*, *20*, 153–167.

Banerjee, R., Meier, K.K., Münck, E., Lipscomb, J.D.(2013) Intermediate P* from soluble methane monooxygenase contains a diferrous cluster. *Biochemistry.,52*(25):4331-42.

Banerjee, R., Proshlyakov, Y., Lipscomb, J. D., & Proshlyakov, D. a. (2015). Structure of the key species in the enzymatic oxidation of methane to methanol. *Nature*, *518*(7539), 431–434.

Bauer, I., Max, N., Fetzner, S.& Lingens, F. (1996). 2,4-dioxygenases catalyzing N-heterocyclic-ring cleavage and formation of carbon monoxide. Purification and some properties of 1H-3-hydroxy-4-oxoquinaldine 2,4-dioxygenase from Arthrobacter sp. Rü61a and comparison with 1H-3-hydroxy-4-oxoquinoline 2,4-dioxygenase from Pseudomonas putida 33/1. *Eur. J. Biochem.*, *240*(3), 576–583.

Bentley, R. & Bennett, J.W.(1999) Constructing polyketides: from collie to combinatorial biosynthesis. *Annu. Rev. Microbiol.* 53, 411-46.

Bernini C., Pogni, R., Basosi, R., & Sinicropi, A. (2012). The nature of tryptophan radicals involved in the long-range electron transfer of lignin peroxidase and lignin peroxidase-like systems: Insights from quantum mechanical/molecular mechanics simulations. *Proteins: Struct. Funct. Bioinf.*, *80*(5), 1476–1483.

Björn B.& Jörg N. (1998). Alnumycin useful as antibiotic. German patent DE19745914.

Bleifuss, G., Kolberg, M., Pötsch, S., Hofbauer, W., Bittl, R., Lubitz, W., Gräslund, A., Lassmann, G., & Lendzian, F. (2001). Tryptophan and tyrosine radicals in ribonucleotide reductase: A comparative high-field EPR study at 94 GHz. *Biochemistry*, *40*(50), 15362–15368.

Bogdan, C. (2007). Oxidative burst without phagocytes: the role of respiratory proteins. *Nat. Immunol.*, *8*(10), 1029–1031.

Brazeau, B. J., Austin, R. N., Tarr, C., Groves, J. T., & Lipscomb, J. D. (2001). Intermediate Q from soluble methane monooxygenase hydroxylates the mechanistic substrate probe norcarane: Evidence for a stepwise reaction. *J. Am. Chem. Soc.*, *123*(48), 11831–11837. doi:10.1021/ja016376+

Broderick, J. B., Du, B. R., Duschene, K. S., & Shepard, E. M. (2014). Radical S-Adenosylmethionine Enzymes. *Chem. Rev.*, *114*(8), 4229–4317.

Brosi, R., Bittl, R. & Engelhard, C., (2014). EPR on Flavoproteins. *Methods Mol. Biol.*, *1146*(06 Mar), 341–60.

Brown, C. K., Vetting, M. W., Earhart, C. A, & Ohlendorf, D. H. (2004). Biophysical analyses of designed and selected mutants of protocatechuate 3,4-dioxygenase1. A*nnu. Rev. Microbiol.*, *58*, 555–585. doi:10.1146/ annurev.micro.57.030502.090927

Büch, K., Stransky, H. & Hager, A., (1995). FAD is a further essential cofactor of the NAD(P)H and O2-dependent zeaxanthin-epoxidase. *FEBS Lett.* , *376*(1-2), 45–48.

Bugg, T. D. H. (2003). Dioxygenase enzymes: Catalytic mechanisms and chemical models. *Tetrahedron*, *59*(36), 7075–7101.

Bugg, T. D. H. (2014). How to break the rules of dioxygen activation. *Chem. Biol.*, *21*(2), 168–169.

Bui, S.,Von Stetten, D., Jambrina, P.G., Prangé, T., Colloc'h, N., de Sanctis, D., Royant, A., Rosta,E. & Steiner, R.A. (2014). Direct Evidence for a Peroxide Intermediate and a Reactive Enzyme-Substrate-Dioxygen Configuration in a Cofactor-free Oxidase. *Angew. Chem. Int. Ed. Engl.*, *53*(50), 13710–13714.

Buongiorno, D., & Straganz, G. D. (2013). Structure and function of atypically coordinated enzymatic mononuclear non-heme-Fe(II) centers. *Coord. Chem. Rev.*, *257*(2), 541–563.

Burmester, T. (2001). Molecular evolution of the arthropod hemocyanin superfamily. *Mol. Biol. Evol.*, *18*(2), 184–195.

Canfield, D.E., Ngombi-Pemba, L., Hammarlund, E.U., Bengtson, S., Chaussidon, M.,Gauthier-Lafaye, F., Meunier, A., Riboulleau, A., Rollion-Bard, C., Rouxel, O., Asael, D., Pierson-Wickmann, A-C. & El Albani, A. (2013). Oxygen dynamics in the aftermath of the Great Oxidation of Earth's atmosphere. *Proc. Natl. Acad. Sci. U.S.A*, *110*(42), 16736–41.

Casey T.M., Grzyska P.K., Hausinger R.P. & McCracken, J., (2013). NIH Public Access. *J. Phys. Chem. B.*, *117*(36), 10384–94.

Chater, K.F. & Wilde, L.C. (1980). Streptomyces albus G mutants defective in the SalGI restriction-modification system. *J. Gen. Microbiol.*, *116*(2), 323–34.

Chen, D., & Frey, P. A. (1998). Phenylalanine Hydroxylase from Chromobacterium violaceum. *J. Biol. Chem.*, *273*(40), 25594–25601.

Chen, D., & Solomon,E.I.(2004). Oxygen activation by the noncoupled binuclear copper site in peptidylglycine alpha-hydroxylating monooxygenase. Reaction mechanism and role of the noncoupled nature of the active site. *J. Am. Chem. Soc. 126*(15),4991-5000.

Cheng, A. X., Han, X. J., Wu, Y. F., & Lou, H. X. (2014). The function and catalysis of 2-oxoglutarate-dependent oxygenases involved in plant flavonoid biosynthesis. *Int. J. Mol. Sci.*, *15*(1), 1080–1095.

Choi, Y. S., Zhang, H., Brunzelle, J. S., Nair, S. K., & Zhao, H. (2008). In vitro reconstitution and crystal structure of p-aminobenzoate N-oxygenase (AurF) involved in aureothin biosynthesis. *Proc. Natl. Acad. Sci. U.S.A*, *105*(19), 6858–6863.

Chung, J. Y., Fujii, I., Harada, S., Sankawa, U., & Ebizuka, Y. (2002). Expression, purification, and characterization of AknX anthrone oxygenase, which is involved in aklavinone biosynthesis in Streptomyces galilaeus. *J. Bacteriol.*, *184*(22), 6115–6122.

Clennan, E. L., & Pace, A. (2005). Advances in singlet oxygen chemistry. *Tetrahedron*, *61*(28), 6665–6691.

Cochrane, R. V. K., & Vederas, J. C. (2014). Highly Selective but Multifunctional Oxygenases in Secondary Metabolism. *Acc . Chem. Res.*, *47*, 3148–3161.

Conner, K. P., Cruce, A. A, Krzyaniak, M. D., Schimpf, A. M., Frank, D. J., Ortiz de Montellano, P., Atkins, W.M. & Bowman, M.K. (2015). Drug Modulation of Water-Heme Interactions in Low-Spin P450 Complexes of CYP2C9d and CYP125A1. *Biochemistry*.

Coon, M. J. (2005). Cytochrome P450: nature's most versatile biological catalyst. *Ann. Rev. Pharmacol. Toxicol*, *45*, 1–25.

Costas, M., Mehn, M. P., Jensen, M. P., & Que, L. (2004). Dioxygen Activation at Mononuclear Nonheme Iron Active Sites: Enzymes, Models, and Intermediates. *Chem. Rev.*, *104*(2), 939–986.

Crowe, S. A, Døssing, L. N., Beukes, N. J., Bau, M., Kruger, S. J., Frei, R., & Canfield, D. E. (2013). Atmospheric oxygenation three billion years ago. *Nature*, *501*(7468), 535–8.

Culpepper, M. A, Scott, E. E., & Limburg, J. (2011). NIH Public Access. *Structure*, *49*(1), 124–133.

Dann, C. E., Bruick, R. K., & Deisenhofer, J. (2002). Structure of factor-inhibiting hypoxia-inducible factor 1: An asparaginyl hydroxylase involved in the hypoxic response pathway. *Proc. Natl. Acad. Sci. U.S.A*, *99*(24), 15351–15356.

Datsenko, K. A, & Wanner, B. L. (2000). One-step inactivation of chromosomal genes in Escherichia coli K-12 using PCR products. *Proc. Natl. Acad. Sci. U.S.A*, *97*(12), 6640–6645.

Davydov, R., Perera, R., Jin, S., Yang, T.C., Bryson, T.A., Sono, M., Dawson, J.H., & Hoffman, B.M. (2005). Substrate modulation of the properties and reactivity of the oxy-ferrous and hydroperoxo-ferric intermediates of cytochrome P450cam as shown by cryoreduction-EPR/ENDOR spectroscopy. *J. Am. Chem. Soc.,127*(5):1403-13

De Colibus, L., & Mattevi, A. (2006). New frontiers in structural flavoenzymology. *Curr. Opin. Struct. Biol.*, *16*(6), 722–728.

Decker, H., Schweikardt, T., & Tuczek, F. (2006). The first crystal structure of tyrosinase: All questions answered? *Angew. Chem. Int. Ed. Engl.*, *45*(28), 4546–4550.

Dickens, M. L., Priestley, N. D., & Strohl, W. R. (1997). In vivo and in vitro bioconversion of epsilon- rhodomycinone glycoside to doxorubicin: Functions of DauP, DauK, and DoxA. *J. Bacterriol.*, *179*(8), 2641–2650.

Daubner, S.C., Hillas, P.J., & Fitzpatrick, P.F.(1997) Characterization of chimeric pterin-dependent hydroxylases: contributions of the regulatory domains of tyrosine and phenylalanine hydroxylase to substrate specificity. *Biochemistry. ,36*(39),11574-82.

Daubner, S.C., Fitzpatrick, P.F.(1999) Site-directed mutants of charged residues in the active site of tyrosine hydroxylase. *Biochemistry. 38*(14),4448-54

Eaton, P. E., & Yip, Y. C. (1991). The Preparation and Fate of Cubylcarbinyl Radicals. *J. Am. Chem. Soc.*, *113*, 7692–7697.

Eleftherianos, I., & Revenis, C., (2011). Role and importance of phenoloxidase in insect hemostasis. *J. Innate. Immun., 3*(1),28-33.

Emerson, J. P., Kovaleva, E. G., Farquhar, E. R., Lipscomb, J. D., & Que, L. (2008). Swapping metals in Fe- and Mn-dependent dioxygenases: evidence for oxygen activation without a change in metal redox state. *Proc. Natl. Acad. Sci. U.S.A*, *105*(21), 7347–7352.

Ener, M.E., Lee, Y.T., Winkler, J.R., Gray, H.B., & Cheruzel, L. (2010). Photooxidation of cytochrome P450-BM3. *Proc. Natl. Acad. Sci. U.S.A, 107*(44),18783-6.

Eser, B.E., Barr, E.W., Frantom, P.A., Saleh, L., Bollinger, J.M. Jr., Krebs, C., Fitzpatrick, P.F.(2007) Direct spectroscopic evidence for a high-spin Fe(IV) intermediate in tyrosine hydroxylase. *J. Am. Chem. Soc.*, *129*(37),11334-5

Evans, J.P., Ahn, K. & Klinman, J.P. (2003). Evidence that dioxygen and substrate activation are tightly coupled in dopamine beta-monooxygenase. Implications for the reactive oxygen species. *J. Biol. Chem.*, *278*(50), 49691–8.

Fenchel, T., & Finlay, B. (2008). Oxygen and the spatial structure of microbial communities. *Biol. Rev.*, *83*(4), 553–569.

Fetzner, S. (2003). Oxygenases without requirement for cofactors or metal ions. *App. Microbiol. Biot.*, *60*(3), 243–257.

Fetzner, S. (2007). Cofactor-independent oxygenases go it alone. *Nat. Chem. Biol.*, *3*(7), 374–375.

Frey, P.A., & Hegeman A.D. (2007) Enzymatic Reaction Mechanisms (1st Edition) Oxford University press Inc./ New York U.S.A

Filisetti, L., Valton, J., Fontecave, M., & Nivière, V. (2005). The flavin reductase ActVB from Streptomyces coelicolor: Characterization of the electron transferase activity of the flavoprotein form. *FEBS Lett.* , *579*(13), 2817–2820.

Fitzpatrick, P.F.(2015) Structural insights into the regulation of aromatic amino acid hydroxylation. *Curr. Opin. Struct. Biol. 35*, 1-6.

Fujimoto, K., Okino, N., Kawabata, S., Iwanaga, S., & Ohnishi, E. (1995). Nucleotide sequence of the cDNA encoding the proenzyme of phenol oxidase A1 of Drosophila melanogaster. *Proc. Natl. Acad. Sci. U.S.A*, *92*(17), 7769–7773.

Fujisawa, H., Hayaishi, O. (1968). Protocatechuate 3,4-dioxygenase. I. Crystallization and characterization. *J Biol Chem.*, *243*(10), 2673–81.

Fujisawa, H., Hiromi, K., Uyeda, M., Okuno, S., Nozaki, M., Hayaishi, O. (1972). Protocatechuate 3,4-dioxygenase. 3. An oxygenated form of enzyme as reaction intermediate. *J Biol Chem.*, *247*(13), 4422–4428.

Goldfeder, M., Kanteev, M., Isaschar-Ovdat, S., Adir, N., & Fishman, A.(2014). Determination of tyrosinase substrate-binding modes reveals mechanistic differences between type-3 copper proteins. *Nat. Commun. 30*(5),4505.

Gray, E. E., Small, S. N., & McGuirl, M.A. (2006). Expression and characterization of recombinant tyramine epsilon-monooxygenase from Drosophila: A monomeric copper-containing hydroxylase. *Protein Expres. Purif.*, *47*(1), 162–170.

Grzyska, P. K., Appelman, E. H., Hausinger, R. P., & Proshlyakov, D. a. (2010). Insight into the mechanism of an iron dioxygenase by resolution of steps following the FeIV=HO species. *Proc. Natl. Acad. Sci. U.S.A*, *107*(9), 3982–3987.

Hakulinen, N., Gasparetti, C., Kaljunen, H., Kruus, K.,& Rouvinen, J. (2013. The crystal structure of an extracellular catechol oxidase from the ascomycete fungus Aspergillus oryzae. *J. Biol. Inorg. Chem. 18*(8), 917-29.

Halaouli, S., Asther, M., Sigoillot, J. C., Hamdi, M., & Lomascolo, A. (2006). Fungal tyrosinases: New prospects in molecular characteristics, bioengineering and biotechnological applications. *Journal of Applied Microbiol.*, *100*(2), 219–232.

Hamdane, D., Zhang, H., Hollenberg, P. (2008). Oxygen Activation by Cytochrome P450 Monooxygenase. *Photosynth. Res.*, *98*(1-3), 657–666.

Hamilton, G.A.(1990). Mechanisms of biological oxidation reactions involving oxygen and reduced oxygen derivatives, in *Biological Oxidation Systems (Volume I)*. Academic Press/ New York, U.S.A

Hanauske-Abel, H. M., & Günzler, V. (1982). A stereochemical concept for the catalytic mechanism of prolylhydroxylase: applicability to classification and design of inhibitors. *J. Theor. Biol.*, *94*(2), 421–455.

Hausinger, R. P. (2004). FeII/alpha-ketoglutarate-dependent hydroxylases and related enzymes. *Crit. Rev. Biochem.Mol.,* 39(1), 21-68

Hayaishi, O. (1974). *Molecular Mechanisms Of Oxygen Activation*. Academic press Inc. New York/ U.S.A.

Hayaishi, O., Katagiri, M., & Rothberg, S. (1955). Mechanism of the pyrocatechase reaction. *J. Am. Chem. Soc.*, *77*(20), 5450–5451.

Hemsworth, G. R., Davies, G. J., & Walton, P. H. (2013). Recent insights into copper-containing lytic polysaccharide mono-oxygenases. *Curr. Opin. Struc. Biol.*, *23*(5), 660–668.

Hertweck, C. (2009). The biosynthetic logic of polyketide diversity. *Angew. Chem. Int. Ed. Engl.*, *48*(26), 4688–4716.

Hess, C. R., Wu, Z., Ng, A., Gray, E. E., McGuirl, M. A., & Klinman, J. P. (2008). Hydroxylase activity of Met471Cys tyramine β-monooxygenase. *J. Am. Chem. Soc.*, *130*(36), 11939–11944.

Higuchi, R., Krummel, B., Saiki, R.K. (1988). A general method of in vitro preparation and specific mutagenesis of DNA fragments: study of protein and DNA interactions. *Nucleic Acids Res.*, *16*(15), 7351–67.

Holland, H. D. (2006). The Oxygenation of the aAtmosphere and Oceans. *Philos. T. Roy. Soc.B*, *361*(1470), 903–915.

Holland, H. D. (2009). Why the atmosphere became oxygenated: A proposal. *Geochim. Cosmochim. Ac.*, *73*(18), 5241–5255.

Holm, R. H., Kennepohl, P., & Solomon, E. I. (1996). Structural and functional aspects of metal sites in biology. *Chem. Rev.*, *96*(7), 2239–2314.

Horsman, G.P., Jirasek, A., Vaillancourt, F.H., Barbosa, C.J., Jarzecki, A.A., Xu, C., Mekmouche, Y., Spiro, T.G., Lipscomb, J.D., Blades, M.W., Turner, R.F. & Eltis L.D. (2005). Spectroscopic Studies of the Anaerobic Enzyme - Substrate Complex of Catechol 1 , 2-Dioxygenase, *J. Am. Chem. Soc.*, 127(48),16882–16891.

Huijbers, M. M. E., Montersino, S., Westphal, A. H., Tischler, D., & Van Berkel, W. J. H. (2014). Flavin dependent monooxygenases. *Arch. Biochem. Biophys.*, *544*, 2–17.

Hutchinson, C. R., & Fujii, I. (1995). Polyketide synthase gene manipulation: a structure-function approach in engineering novel antibiotics. *Annu. Rev. Microbiol.*, *49*, 201–238.

Hüttermann, A., Mai. C., & Kharazipour, A. (2001). Modification of lignin for the production of new compounded materials. *Appl. Microbiol. Biotechnol. 55*(4), 387-94.

Ichinose, K., Bedford, D. J., Tornus, D., Bechthold, A., Bibb, M. J., Revill, W. P., Floss, H.G., Hopwood, D.A. (1998). The granaticin biosynthetic gene cluster of Streptomyces violaceoruber Tü22: sequence analysis and expression in a heterologous host. *Chemistry & Biology*, *5*(11), 647–659.

Ichinose, K., Ozawa, M., Itou, K., Kunieda, K., & Ebizuka, Y. (2003). Cloning, sequencing and heterologous expression of the medermycin biosynthetic gene cluster of Streptomyces sp. AM-7161: Towards comparative analysis of the benzoisochromanequinone gene clusters. *Microbiology*, *149*(7), 1633–1645.

Jansson, A., Koskiniemi, H., Mäntsälä, P., Niemi, J., & Schneider, G.(2004) . Crystal structure of a ternary complex of DnrK, a methyltransferase in daunorubicin biosynthesis, with bound products. *J. Biol. Chem., 279*(39), 41149-56

Jensen, C. N., Cartwright, J., Ward, J., Hart, S., Turkenburg, J. P., Ali, S. T., Allen, M.J., Grogan, G. (2012). A Flavoprotein Monooxygenase that Catalyses a Baeyer-Villiger Reaction and Thioether Oxidation Using NADH as the Nicotinamide Cofactor. *Chembiochem*, *13*, 872–878.

Johnston, D. T., Wing, B. a, Farquhar, J., Kaufman, A. J., Strauss, H., Lyons, T. W., Kah, L.C. & Canfield, D. E. (2005). Active microbial sulfur disproportionation in the Mesoproterozoic. *Science*, *310*(5753), 1477–1479.

Joosten, V., & van Berkel, W. J. (2007). Flavoenzymes. *Current Opinion in Chemical Biology*, *11*(2), 195–202.

Kallio, P., Patrikainen, P., Belogurov, G. a., Mäntsälä, P., Yang, K., Niemi, J., & Metsä-Ketelä, M. (2013). Tracing the evolution of angucyclinone monooxygenases: Structural determinants for C-12b hydroxylation and substrate inhibition in PgaE. *Biochemistry*, *52*, 4507–4516.

Kallio, P., Sultana, A., Niemi, J., Mäntsälä, P., & Schneider, G. (2006). Crystal structure of the polyketide cyclase AknH with bound substrate and product analogue: Implications for catalytic mechanism and product stereoselectivity. *J. Mol. Biol.*, *357*(1), 210–220.

Kappock, T.J. & Caradonna, J.P. (1996). Pterin-Dependent Amino Acid Hydroxylases. *Chem. Rev.*, *96*(7), 2659–2756.

Kautsky, H., & de Bruijn, H. (1931) Die Aufklärung der Photolumineszenztilgung fluorescierender Systeme durch Sauerstoff: Die Bildung aktiver, diffusionsfähiger Sauerstoffmoleküle durch Sensibilisierung. Naturwiss., 19, 1043.

Kieser, T., Bibb, M.J., Buttner, M.J., Chater, K. F. (2000). *Practical Streptomyces genetics.* The John Innes Foundation / Norwich, England.

Kim, N.Y., Kim, J.H., Lee, Y.H., Lee, E.J., Kim, J., Lim, Y., & Chong Y, A. J. (2007). O-Methylation of flavonoids using DnrK based on molecular docking. *J. Microbiol. Biotechnol.*, *17*(12), 1991–1995.

Klabunde, T., Eicken, C., Sacchettini, J.C.,& Krebs, B. (1995) Crystal structure of a plant catechol oxidase containing a dicopper center. *Nat. Struct. Biol. 5*(12),1084-90.

Klinman, J. P. (2006). The copper-enzyme family of dopamine β-monooxygenase and peptidylglycine α-hydroxylating monooxygenase: Resolving the chemical pathway for substrate hydroxylation. *J. Biol. Chem.*, *281*(6), 3013–3016.

Knappskog, P.M., Flatmark, T., Aarden, J.M., Haavik, J.,& Martínez, A.(1996) Structure/function relationships in human phenylalanine hydroxylase. Effect of terminal deletions on the oligomerization, activation and cooperativity of substrate binding to the enzyme. *Eur. J. Biochem., 242*(3):813-21.

Knoot, C. J., Purpero, V. M., & Lipscomb, J. D. (2015). Crystal structures of alkylperoxo and anhydride intermediates in an intradiol ring-cleaving dioxygenase. *Proc. Natl. Acad. Sc.i U.S.A.*, *112*(2), 388–393.

Koskiniemi, H., Metsä-Ketelä, M., Dobritzsch, D., Kallio, P., Korhonen, H., Mäntsälä, P., Schneider, G. & Niemi, J. (2007). Crystal Structures of Two Aromatic Hydroxylases Involved in the Early Tailoring Steps of Angucycline Biosynthesis. *J. Mol. Biol.*, *372*(3), 633–648.

Krest, C. M., Onderko, E. L., Yosca, T. H., Calixto, J. C., Karp, R. F., Livada, J., Rittle, J. & Green, M. T. (2013). Reactive intermediates in cytochrome p450 catalysis. *J. Biol. Chem.*, *288*(24), 17074–81.

Kumar, D., de Visser, S. P., Sharma, P. K., Cohen, S., & Shaik, S. (2004). Radical clock substrates, their C-H hydroxylation mechanism by cytochrome P450, and other reactivity patterns: what does theory reveal about the clocks' behavior? *J. Am. Chem. Soc.*, *126*(6), 1907–1920.

Lange, S.J. & Que, L. Jr. (1998). Oxygen activating nonheme iron enzymes. *Curr. Opin. Chem. Biol., 2(2)*, 159–172.

Lee, S.K. & Lipscomb, J.D.(1999). Oxygen activation catalyzed by methane monooxygenase hydroxylase component: proton delivery during the O-O bond cleavage steps. *Biochemistry. 1999 38*(14), 4423-32

Lemieux, M. J., Ference, C., Cherney, M. M., Wang, M., Garen, C., & James, M. N. G. (2005). The crystal structure of Rv0793, a hypothetical monooxygenase from M. tuberculosis. *Journal of Structural and Functional Genomics*, *6*(4), 245–257.

Lewis, E. A., & Tolman, W. B. (2004). Reactivity of Dioxygen − Copper Systems. *Chem. Rev.*, *104*, 1047–1076.

Li, L., Liu, X., Yang, W., Xu, F., Wang, W., Feng, L., Bartlam, M., Wang, L. & Rao, Z. (2008). Crystal Structure of Long-Chain Alkane Monooxygenase (LadA) in Complex with Coenzyme FMN: Unveiling the Long-Chain Alkane Hydroxylase. *J. Mol. Biol.*, *376*, 453–465.

Li, S., Tietz, D. R., Rutaganira, F. U., Kells, P. M., Anzai, Y., Kato, F., Pochapsky, T.C., Sherman, D.H. & Podust, L. M. (2012). Substrate recognition by the multifunctional cytochrome P450 MycG in mycinamicin hydroxylation and epoxidation reactions. *J. Biol. Chem.*, *287*(45), 37880–37890.

Li, Y., Wang, Y., Jiang, H., & Deng, J. (2009). Crystal structure of Manduca sexta prophenoloxidase provides insights into the mechanism of type 3 copper enzymes. *Proc. Natl. Acad. Sci. U.S.A*, *106*(40), 17002–17006.

Lin, Y.-W., & Wang, J. (2013). Structure and function of heme proteins in non-native states: a mini-review. *J. Inorg. Biochem.*, *129*, 162–71.

Lindqvist, Y., Koskiniemi, H., Jansson, A., Sandalova, T., Schnell, R., Liu, Z., Mäntsälä, P., Niemi, J., Schneider, G. (2009). Structural Basis for Substrate Recognition and Specificity in Aklavinone-11-Hydroxylase from Rhodomycin Biosynthesis. *J. Mol. Biol.*, *393*(4), 966–977.

Liu, K. E., Johnson, C. C., Newcomb, M., & Lippard, S. J. (1993). Radical clock substrate probes and kinetic isotope effect studies of the hydroxylation of hydrocarbons by methane monooxygenase. *J. Am. Chem. Soc.*, *115*(3), 939–947.

Loenarz, C., & Schofield, C. J. (2011). Physiological and biochemical aspects of hydroxylations and demethylations catalyzed by human 2-oxoglutarate oxygenases. *Trends Biochem. Sci.*, *36*(1), 7–18. doi:10.1016/j.tibs.2010.07.002

Malmström, B. G. (1982). Enzymology of oxygen. *Annu. Rev. Biochem.*, *51*, 21–59.

Mandaviya, P. R., Stolk, L., & Heil, S. G. (2014). Homocysteine and DNA methylation: A review of animal and human literature. *Mol. Genet. Metab.*, *113*(4), 243–252.

Markolovic, S., Wilkins, S. E., & Schofield, C. J. (2015). Protein Hydroxylation Catalyzed by 2-Oxoglutarate-Dependent Oxygenases. *J. Biol. Chem.*, 290(34),20712-22.

Mason, H.S., Fowlks, W.L., Peterson, E. (1955). Oxygen transfer and electron transport by the phenolase complex. *J. Am. Chem. Soc.*, *77*(10), 2914–2915.

Massey, V. (1995). Introduction: Flavoprotein Structure and mechanism. *FASEB J.*, *9*, 473–475.

Massey, V. (2000). The chemical and biological versatility of riboflavin. *Biochem. Soc. T.*, *28*(4), 283–296.

Matoba, Y., Kumagai, T., Yamamoto, A., Yoshitsu, H., & Sugiyama, M. (2006). Crystallographic evidence that the dinuclear copper center of tyrosinase is flexible during catalysis. *J. Biol. Chem.* ,281(13),8981-90.

Mattevi, A., Vanoni, M.A., Curti, B. (1997). Structure of D-amino acid oxidase: new insights from an old enzyme. *Curr. Opin. Struc. Biol.*, *7*(6), 804–810.

Mayfield, J.A., Carolyn, A.D. & DuBois, J.L. (2011). Recent advances in bacterial heme protein biochemistry. *Curr Opin Chem Biol.*, *15*(2), 260–266.

McDonough, M. A., Loenarz, C., Chowdhury, R., Clifton, I. J., & Schofield, C. J. (2010). Structural studies on human 2-oxoglutarate dependent oxygenases. *Curr. Opin. Struc. Biol.*, *20*(6), 659–672.

Merkx, M., Kopp, D. A., Sazinsky, M. H., Blazyk, J. L., Muanẗller, J., & Lippard, S. J. (2001). Dioxygen activation and methane hydroxylation by soluble methane monooxygenase: A tale of two irons and three proteins. *Angew. Chem. Int. Ed. Engl.*, *40*(15), 2782–2807.

Meliá, C., Ferrer, S., Řezáč, J., Parisel, O., Reinaud, O., Moliner, V., & de la Lande, A. (2013). Investigation of the hydroxylation mechanism of noncoupled copper oxygenases by ab initio molecular dynamics simulations. *Chemistry.*,*19*(51),17328-37.

Moan, J., & Kaalhus, O. (1974). Ultraviolet and x-ray induced radicals in frozen polar solutions of L-tryptophan. *J. Chem. Phys.*, *61*(9), 3556–3566.

Morgan, J. W., & Anders, E. (1980). Chemical composition of Earth, Venus, and Mercury. *Proc. Nati. Acad. Sci.*, *77*(12), 6973–6977.

Moussaieff, A., Kogan, N.M., & Aberdam, D. (2015). Concise Review : Energy Metabolites : Key Mediators of the Epigenetic State of Pluripotency. *Stem Cells*, *33*(8), 2374–2380.

Müller I, Stückl C, Wakeley J, Kertesz M, & Usón, I. (2005). Succinate Complex Crystal Structures of the α-Ketoglutarate-dependent Dioxygenase AtsK, *J. Biol. Chem.*, *280*(7), 5716–5723.

Nelson, D.R., Oymans, L.K., Amataki, T.K., Tegeman, J.J.S., Feyereisen, R., Waxman, D.J.,Waterman, M.R., Gotoh, O., Coon, M.J., Estabrook, R.W., Gunsalus, I.C., & Nebert D.W. (1996). P450 superfamily: update on new sequences, gene mapping, accession numbers and nomenclature. *Pharmacogenetics.*, *6(1)*, 1–42.

Nelson, D.R. (2004). Methods In Molecular Biology, vol. 320: Cytochrome P450 protocols: Second edition.Humana Press /Totowa, NJ

Newcomb, M., & Chandrasena, R.E. (2005). Highly reactive electrophilic oxidants in cytochrome P450 catalysis. *Biochem. Biophys. Res. Commun. 338*(1), 394-403.

Newcomb, M., Hollenberg, P. F., & Coon, M. J. (2003). Multiple mechanisms and multiple oxidants in P450-catalyzed hydroxylations. *Arch. Biochem. Biophys*, *409*(1), 72–79.

Newcomb, M., & Toy, P. H. (2000). Hypersensitive Radical Probes and the Mechanisms of Cytochrome P450 - Catalyzed Hydroxylation Reactions. *Acc . Chem. Res.*, *33*(7), 449–455.

Nishikimi, M. (1975). Oxidation of ascorbic acid with superoxide anion generated by the xanthine-xanthine oxidase system. *Biochem. Biophys. Res. Commun.*, *63*(2),463-8.

Oetting, W. S. (2000). The tyrosinase gene and oculocutaneous albinism type 1 (OCA1): A model for understanding the molecular biology of melanin formation. *Pigm. Cell Res.*, *13*(5), 320–325.

Ohlendorf, D. H., Lipscomb, J. D. & Weber P. C. (1988). Structure and assembly of protocatechuate 3,4-dioxygenase. *Nature*, *336*, 403–405.

Oja, T., Palmu, K., Lehmussola, H., Leppäranta, O., Hännikäinen, K., Niemi, J., Mäntsälä, P., & Metsä-Ketelä, M. (2008). Characterization of the Alnumycin Gene Cluster Reveals Unusual Gene Products for Pyran Ring Formation and Dioxan Biosynthesis. *Chem. Biol.*, *15*(10), 1046–1057.

Oja, T., San Martin Galindo, P., Taguchi, T., Manner, S., Vuorela, P.M., Ichinose, K., Metsä-Ketelä, M.,& Fallarero, A. (2015). Effective Antibiofilm Polyketides against Staphylococcus aureus from the Pyranonaphthoquinone Biosynthetic Pathways of Streptomyces Species. *Antimicrob. Agents Chemother. 59*(10),6046-52.

Okamoto, S., Taguchi, T., Ochi, K., & Ichinose, K. (2009). Biosynthesis of Actinorhodin and Related Antibiotics: Discovery of Alternative Routes for Quinone Formation Encoded in the act Gene Cluster. *Chem. Biol.*, *16*(2), 226–236.

Ortiz de Montellano, P. R. (2013). Cytochrome P450-activated prodrugs. *Future Med. Chem.*, *5*(2), 213–228.

Osborne, R.L., Zhu, H., Iavarone, A.T., Blackburn, N.J.,& Klinman, J.P. (2013) Interdomain long-range electron transfer becomes rate-limiting in the Y216A variant of tyramine β-monooxygenase. *Biochemistry*. *52*(7),1179-91.

Panieri, E., & Santoro, M. M. (2015). ROS signaling and redox biology in endothelial cells. *Cell. Mol. Life Sci.*

Panay, A.J., Lee, M., Krebs, C., Bollinger, J.M., & Fitzpatrick, P.F.(2011)Evidence for a high-spin Fe(IV) species in the catalytic cycle of a bacterial phenylalanine hydroxylase. *Biochemistry.*, *50*(11),1928-33.

Patrikainen, P., Niiranen, L., Thapa, K., Paananen, P., Tähtinen, P., Mäntsälä, P., Niemi, J., & Metsä-Ketelä, M. (2014). Structure-Based Engineering of Angucyclinone 6-Ketoreductases. *Chem. Biol.*, *21*(10), 1381–1391.

Pattison, D.I.,& Davies, M.J.(2006) Actions of ultraviolet light on cellular structures. *EXS. 96*, 131-57.Pau, M. Y. M., Lipscomb, J. D., & Solomon, E. I. (2007). Substrate activation for O2 reactions by oxidized metal centers in biology. *Proc. Natl. Acad. Sci. U.S.A*, *104*(47), 18355–18362.

Prigge, S.T., Kolhekar, A.S., Eipper, B.A., Mains, R.E., & Amzel, L.M. (1997) Amidation of bioactive peptides: the structure of peptidylglycine alpha-hydroxylating monooxygenase., *Science., 278*(5341),1300-5

Pogni, R., Baratto, M. C., Giansanti, S., Teutloff, C., Verdin, J., Valderrama, B., Lendzian, F., Lubitz, W., Vazquez-Duhalt, R., & Basosi, R. (2005). Tryptophan-based radical in the catalytic mechanism of versatile peroxidase from Bjerkandera adusta. *Biochemistry*, *44*(11), 4267–4274.

Priestley, N. D., Floss, H. G. , Froland, W. A., Lipscomb, J. D., Williams, P. G., & Morimoto, H. (1992). Cryptic stereospecificity of methane monooxygenase. *J. Am. Chem. Soc.*, *114*(19), 7561–7562.

Price, I. R., Grigg, J. C., & Ke, A. (2014). Common themes and differences in SAM recognition among SAM riboswitches. *Biochim. Biophys. Acta.*, *1839*(10), 931–938.

Proshlyakov, D. a., Henshaw, T. F., Monterosso, G. R., Ryle, M. J., & Hausinger, R. P. (2004). Direct Detection of Oxygen Intermediates in the Non-Heme Fe Enzyme Taurine/alpha-Ketoglutarate Dioxygenase. *J. Am. Chem. Soc.*, *126*(4), 1022–1023.

Pulsinelli, P.D., Perutz, M.F.,& Nagel, RL. (1973). Structure of Hemoglobin M Boston, a variant with a Five-Coordinated Ferric Heme. *Proc. Natl. Acad. Sci. U S A. 70(12),* 3870-4

Qin, H. M., Miyakawa, T., Jia, M. Z., Nakamura, A., Ohtsuka, J., Xue, Y. L., Kawashima, T., Kasahara, T., Hibi, M., Ogawa, J.,& Tanokura, M. (2013). Crystal Structure of a Novel N-Substituted L-Amino Acid Dioxygenase from Burkholderia ambifaria AMMD. *PLoS ONE*, *8*(5), 1–9.

R.D. Finn, A. Bateman, J. Clements, P. Coggill, R.Y. Eberhardt, S.R. Eddy, A. Heger, K. Hetherington, L. Holm, J. Mistry, E.L.L. Sonnhammer, J. Tate, M. P. (2014). The Pfam protein families database. *Nucleic Acids Res.*, *(Database issue):D364-73*.

Rittle, J., & Green, M. T. (2010). Cytochrome P450 Compound I: Capture, Characterization, and C-H Bond Activation Kinetics. *Science*, *330*, 933–938.

Roach, P. L., Clifton, I. J., Fülöp, V., Harlos, K., Barton, G. J., Hajdu, J., Andersson, I., Schofield, C.J., Baldwin, J. E. (1995). Crystal structure of isopenicillin N synthase is the first from a new structural family of enzymes. *Nature*, *375*(6533), 700–704.

Roberts, K.M., Pavon, J.A. & Fitzpatrick, P.F. (2013). The Kinetic Mechanism of Phenylalanine Hydroxylase: Intrinsic Binding and Rate Constants from Single Turnover Experiments. *Biochemistry*, *52*(6), 1062–1073

Rolff, M., Schottenheim, J., Decker, H., & Tuczek, F. (2011). Copper-O2 reactivity of tyrosinase models towards external monophenolic substrates: molecular mechanism and comparison with the enzyme. *Chem. Soc. Rev.*, *40*, 4077–4098.

Rosenzweig, A. C., Frederick, C. A., Lippard, S. J., & Nordlund, F. (1993). Crystal structure of a bacterial non-haem iron hydroxylase that catalyses the biological oxidation of methane. *Nature*, *366*(6455), 537–543.

Rosenzweig, A. C., & Sazinsky, M. H. (2006). Structural insights into dioxygen-activating copper enzymes. *Curr. Opin. Struc. Biol.*, *16*(6), 729-35.

Ruzicka,F., Huang D-S., Donnelly,M.I. & Frey P. A. (1990). Methane monooxygenase catalyzed oxygenation of 1,1-dimethylcyclopropane. Evidence for radical and carbocationic intermediates, 29 (7), 1696–1700

Ryle, M. J., Padmakumar, R., & Hausinger, R. P. (1999). Stopped-flow kinetic analysis of Escherichia coli taurine/alpha-ketoglutarate dioxygenase: interactions with alpha-ketoglutarate, taurine, and oxygen. *Biochemistry*, *38*(46), 15278–15286.

Salminen, A., Kauppinen, A., & Kaarniranta, K. (2015). 2-Oxoglutarate-dependent dioxygenases are sensors of energy metabolism, oxygen availability, and iron homeostasis: potential role in the regulation of aging process. *Cell. Mol. Life Sci. 72*(20)*,* 3897-3914.

Sambrook J., Fritsch E.F., Maniatis T. (1989). *Molecular cloning: A laboratory manual (2nd edition)* Cold spring Harbour Laboratory Press/ Cold Spring Harbor, New York, U.S.A.

Sawyer, D.T.(1991). *Oxygen Chemistry. International Series of Monographs on Chemistry*. Oxford University Press, Inc./ New York, U.S.A.

Sciara, G., Kendrew, S. G., Miele, A. E., Marsh, N. G., Federici, L., Malatesta, F., Schimperna, G., Savino, C., Vallone, B. (2003). The structure of ActVA-Orf6, a novel type of monooxygenase involved in actinorhodin biosynthesis. *EMBO J.*, *22*(2), 205–215.

Senda, T., Senda, M., Kimura, S., & Ishida, T. (2009). Redox control of protein conformation in flavoproteins. *Antioxid. Redox Signal.*, *11*(7), 1741–1766.

Sendovski, M., Kanteev, M., Ben-Yosef, V.S., Adir, N., & Fishman, A. (2011) First structures of an active bacterial tyrosinase reveal copper plasticity. *J. Mol. Biol., 405*(1):227-37.

Shen, B., & Hutchinson, C. R. (1993). Tetracenomycin F1 monooxygenase: oxidation of a naphthacenone to a naphthacenequinone in the biosynthesis of tetracenomycin C in Streptomyces glaucescens. *Biochemistry*, *32*(26), 6656–6663.

Siitonen, V., Blauenburg, B., Kallio, P., Mäntsälä, P., & Metsä-Ketelä, M. (2012). Discovery of a two-component monooxygenase SnoaW/SnoaL2 involved in nogalamycin biosynthesis. *Chem. Biol.*, *19*(5), 638–646.

Simic, M. G., & Jovanovic, S. V. (1989). Antioxidation mechanisms of uric acid. *J. Am. Chem. Soc.*, *111*(14), 5778–5782.

Solomon, E. I., Brunold, T. C., Davis, M. I., Kemsley, J. N., Lee, S. K., Lehnert, N., Neese, F., Skulan, A.J., Yang, Y.S. Zhou, J. (2000). Geometric and electronic structure/function correlations in non-heme iron enzymes. *Chem. Rev.*, *100*(1), 235–350.

Solomon, E. I., Heppner, D. E., Johnston, E. M., Ginsbach, J. W., Cirera, J., Qayyum, M., Kieber-Emmons, M.T., Kjaergaard, C.H., Hadt, R.G., Tian, L. (2014). Copper active sites in biology. *Chem. rev.*, *114*(7), 3659–3853.

Solomon, E. I., Sundaram, U. M., & Machonkin, T. E. (1996). Multicopper Oxidases and Oxygenases. *Chem. Rev.*, *96*(7), 2563-2606.

Srnec, M., Wong, S. D., & Solomon, E. I. (2014). Excited state potential energy surfaces and their interactions in Fe IV =O active sites. *Dalton Trans.*, *43*(47), 17567–17577.

Steiner, R. A., Janssen, H. J., Roversi, P., Oakley, A. J., & Fetzner, S. (2010). Structural basis for cofactor-independent dioxygenation of N-heteroaromatic compounds at the alpha/beta-hydrolase fold. *Proc. Natl. Acad. Sci. U.S.A*, *107*(2), 657–662.

Strisciuglio, P., & Concolino, D. (2014). New Strategies for the Treatment of Phenylketonuria (PKU). *Metabolites*, *4*, 1007–1017.

Taguchi, T., Yabe, M., Odaki, H., Shinozaki, M., Metsä-Ketelä, M., Arai, T., Okamoto, S., & Ichinose, K. (2013). Biosynthetic conclusions from the functional dissection of oxygenases for biosynthesis of actinorhodin and related streptomyces antibiotics. *Chem. Biol.*, *20*(4), 510–520.

Tarhonskaya, H., Szöllössi, A., Leung, I. K. H., Bush, J. T., Henry, L., Chowdhury, R., Iqbal, A., Claridge, T.D., Schofield, C.J., & Flashman, E. (2014). Studies on deacetoxycephalosporin C synthase support a consensus mechanism for 2-oxoglutarate dependent oxygenases. *Biochemistry*, *53*(15), 2483–2493.

Thierbach, S., Bui, N., Zapp, J., Chhabra, S.R., Kappl, R., & Fetzner, S.(2014). Substrate-assisted O2 activation in a cofactor-independent dioxygenase. *Chem Biol*. *21*(2), 217-25.

Tinberg, C. E., & Lippard, S. J. (2009). Revisiting the mechanism of dioxygen activation in soluble methane monooxygenase from M. capsulatus (Bath): evidence for a multi-step, proton-dependent reaction pathway. *Biochemistry,48*(51),12145-58.

Tinberg, C. E., & Lippard, S. J. (2011). Dioxygen Activation in Soluble Methane Monooxygenase. *Acc. Chem. Res.*, *44*(4), 280–288.

Torres Pazmiño, D. E., Winkler, M., Glieder, a., & Fraaije, M. W. (2010). Monooxygenases as biocatalysts: Classification, mechanistic aspects and biotechnological applications. *Journal of Biotechnology*, *146*(1-2),

Valegård, K., van Scheltinga, A.C., Lloyd, M.D., Hara, T., Ramaswamy, S., Perrakis, A., Thompson, A., Lee, H.J., Baldwin, J.E., Schofield, C.J., Hajdu, J. & Andersson I. (1998). Structure of a cephalosporin synthase. *Nature*, *394* (6695), 805–809.

Valegård, K., Terwisscha van Scheltinga, A. C., Dubus, A., Ranghino, G., Oster, L. M., Hajdu, J., & Andersson, I. (2004). The structural basis of cephalosporin formation in a mononuclear ferrous enzyme. *Nat. Struct. Mol. Biol.*, *11*(1), 95–101.

Valentine, A. M., LeTadic-Biadatti, M. H., Toy, P. H., Newcomb, M., & Lippard, S. J. (1999). Oxidation of ultrafast radical clock substrate probes by the soluble methane monooxygenase from Methylococcus capsulatus (Bath). *J. Biol. Chem.*, *274*(16), 10771–10776.

Valton, J., Fontecave, M., Douki, T., Kendrew, S. G., & Nivière, V. (2006). An aromatic hydroxylation reaction catalyzed by a two-component FMN-dependent monooxygenase: The ActVA-ActVB system from Streptomyces coelicolor. *J. Biol. Chem.*, *281*(1), 27–35.

Valton, J., Mathevon, C., Fontecave, M., Nivière, V., & Ballou, D. P. (2008). Mechanism and regulation of the two-component FMN-dependent monooxygenase ActVA-ActVB from Streptomyces coelicolor. *J. Biol. Chem.*, *283*(16), 10287–10296.

Van Pée, K. H. (2012). Enzymatic chlorination and bromination. *Methods Enzymol. 516*(1),237-57

Vetting, M. W., D'Argenio, D. A., Ornston, L. N., & Ohlendorf, D. H. (2000). Structure of Acinetobacter strain ADP1 protocatechuate 3,4- dioxygenase at 2.2 Å resolution: Implications for the mechanism of an intradiol dioxygenase. *Biochemistry*, *39*(27), 7943–7955.

Vetting, M., Wackett, L., Que, L., Lipscomb, J. D., & Ohlendorf, D. H. (2004). Crystallographic comparison of manganese- and iron-dependent homoprotocatechuate 2, 3-dioxygenases. *J. Bacterriol.*, *186*(7), 1945–1958.

Wang JX, B. R. (2008). Riboswitches that sense S-adenosylmethionine and S-adenosylhomocysteine. *Biochem Cell Biol.*, *86*(2), 157–68.

Wang, Y., Niemi, J., Airas, K., Ylihonko, K., Hakala, J., & Mäntsälä, P. (2000). Modifications of aclacinomycin T by aclacinomycin methyl esterase (RdmC) and aclacinomycin-10-hydroxylase (RdmB) from Streptomyces purpurascens. *Biochimica et Biophysica Acta - Protein Structure and Molecular Enzymology*, *1480*(1-2), 191–200.

Westerlund, K., Berry, B.W., Privett, H.,K., & Tommos, C.(2005) Exploring amino-acid radical chemistry: protein engineering and de novo design. *Biochim. Biophys. Acta.*, *1707*(1),103-16.

Wong, S.D., Srnec, M., Matthews, M.L., Liu, L.V., Kwak, Y., Park, K., Bell, C.B. 3rd, Alp, E.E., Zhao, J., Yoda, Y., Kitao, S., Seto, M., Krebs, C., Bollinger, J.M. Jr, & Solomon EI. (2013). *Nature*, *499*(7458), 320–323.

Yamamoto, S. (2006). The 50th anniversary of the discovery of oxygenases. *IUBMB Life*, *58*(5-6), 248–250.

Yamazaki, S., & Itoh, S.(2003) Kinetic evaluation of phenolase activity of tyrosinase using simplified catalytic reaction system. *J. Am. Chem. Soc. 125*(43),13034-5.

Ylihonko, K., Hakala, J., Niemi, J., Lundell, J., & Mantsala, P. (1994). Isolation and characterization of aclacinomycin A-non-producing Streptomyces galilaeus (ATCC 31615) mutants. *Microbiology*, *140*(6),

Ylihonko, K., Tuikkanen, J., Jussila, S., Cong, L. & Mäntsälä, P. (1996). A gene cluster involved in nogalamycin biosynthesis from Streptomyces nogalater: sequence analysis and complementation of early-block mutations in the anthracycline pathway. *Mol. Gen. Genet.*, *251*(2), 113–20.

Ylihonko, K., Hakala, J., Kunnari, T. & Mäntsälä, P. (1996). Production of hybrid anthracycline antibiotics by heterologous expression of Streptomyces nogalater nogalamycin biosynthesis genes. *Microbiology*, *142*(Pt8), 1965–1972.

Zhang, R. U. I., & Newcomb, M. (2008). Laser Flash Photolysis Generation of High-Valent Transition Metal - Oxo Species : Insights from. *Acc . Chem. Res.*, *41*(3), 468–477.

Zhang, Z., Ren, J., Stammers, D. K., Baldwin, J. E., Harlos, K., & Schofield, C. J. (2000). Structural origins of the selectivity ofthe trifunctional oxygenase clavaminic acid synthase. *Nat. Struct. Biol.*, *7*(2), 127–133.

Zhao, C., Gao, Q., Roberts, A.G., Shaffer, S.A., Doneanu, C.E., Xue, S., Goodlett, D.R., Nelson, S.D., & Atkins, W.M. (2012). Cross-linking Mass Spectrometry and Mutagenesis Confirm the Functional Importance of Surface Interactions between CYP3A4 and Holo/Apo Cytochrome b5. *Biochemistry*, *51*(47), 9488–9500.

Zhou, J., Kelly, W. L., Bachmann, B. O., Gunsior, M., Townsend, C. A., & Solomon, E. I. (2001). Spectroscopic studies of substrate interactionswith clavaminate synthase 2, a multifunctional alpha-KG-dependent non-heme iron enzyme: Correlation with mechanisms and reactivities. *J. Am. Chem. Soc.*, *123*(30), 7388–7398.

Zhu, H., Sommerhalter, M., Nguy, A.K., & Klinman, J.P. (2015). Solvent and Temperature Probes of the Long-Range Electron-Transfer Step in Tyramine β-Monooxygenase: Demonstration of a Long-Range Proton-Coupled Electron-Transfer Mechanism. *J. Am. Chem. Soc. 137*(17),5720-9.